Radiation Pressure and the AMD

Agata Różańska

Tek P. Adhikari, Krzysztof Hryniewicz

Bożena Czerny, Anne-Marie Dumont

AGN Driven Winds in Haifa, Israel May 25th 2017

EU FP7-SPACE research project 312789 2013 - 2017

STRONGGRAVITY

POLISH ACADEMY OF SCIENCES
N. COPERNICUS ASTRONOMICAL CENTER

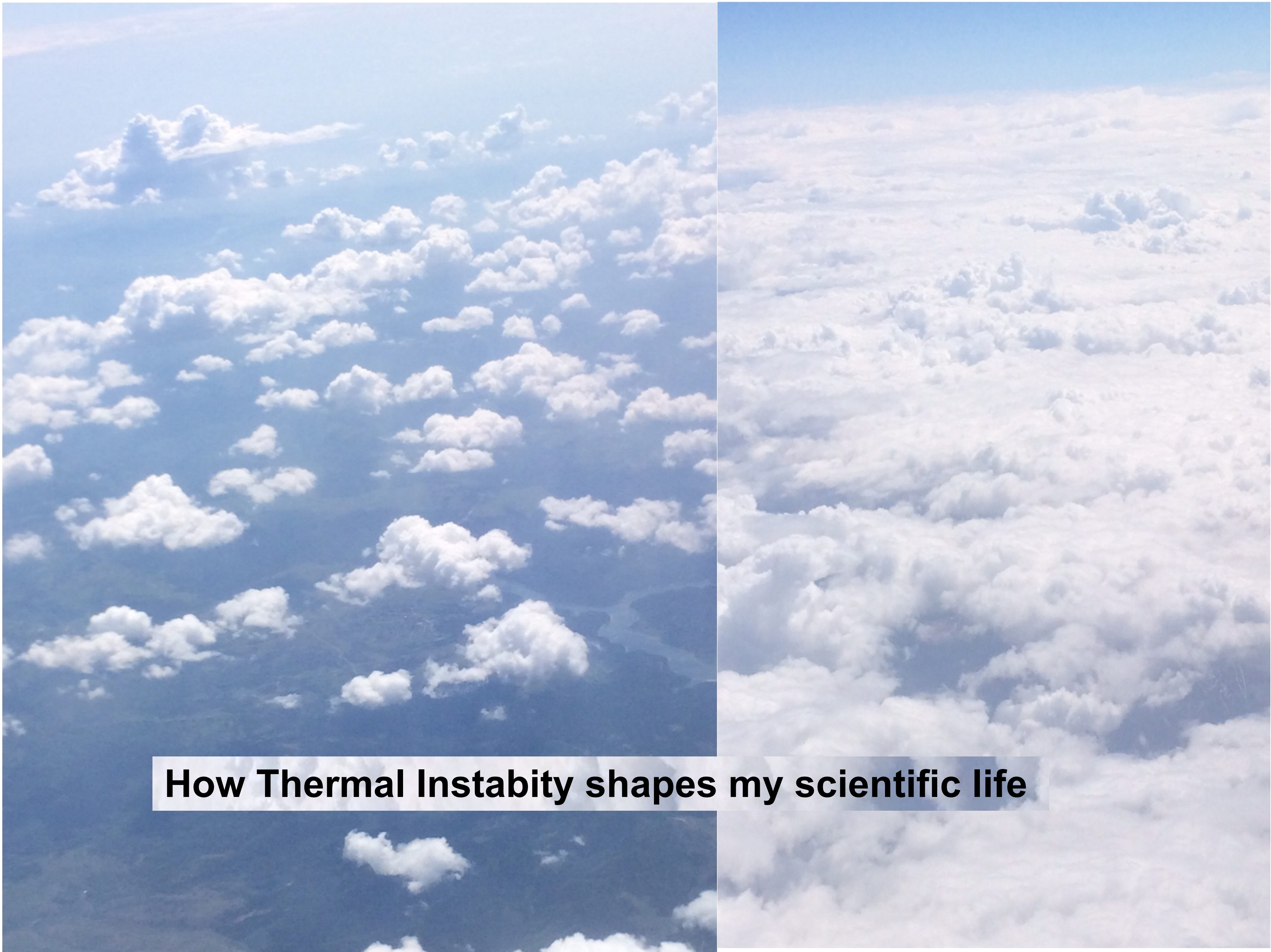
How Thermal Instabity shapes my scientific life

Conclusion first

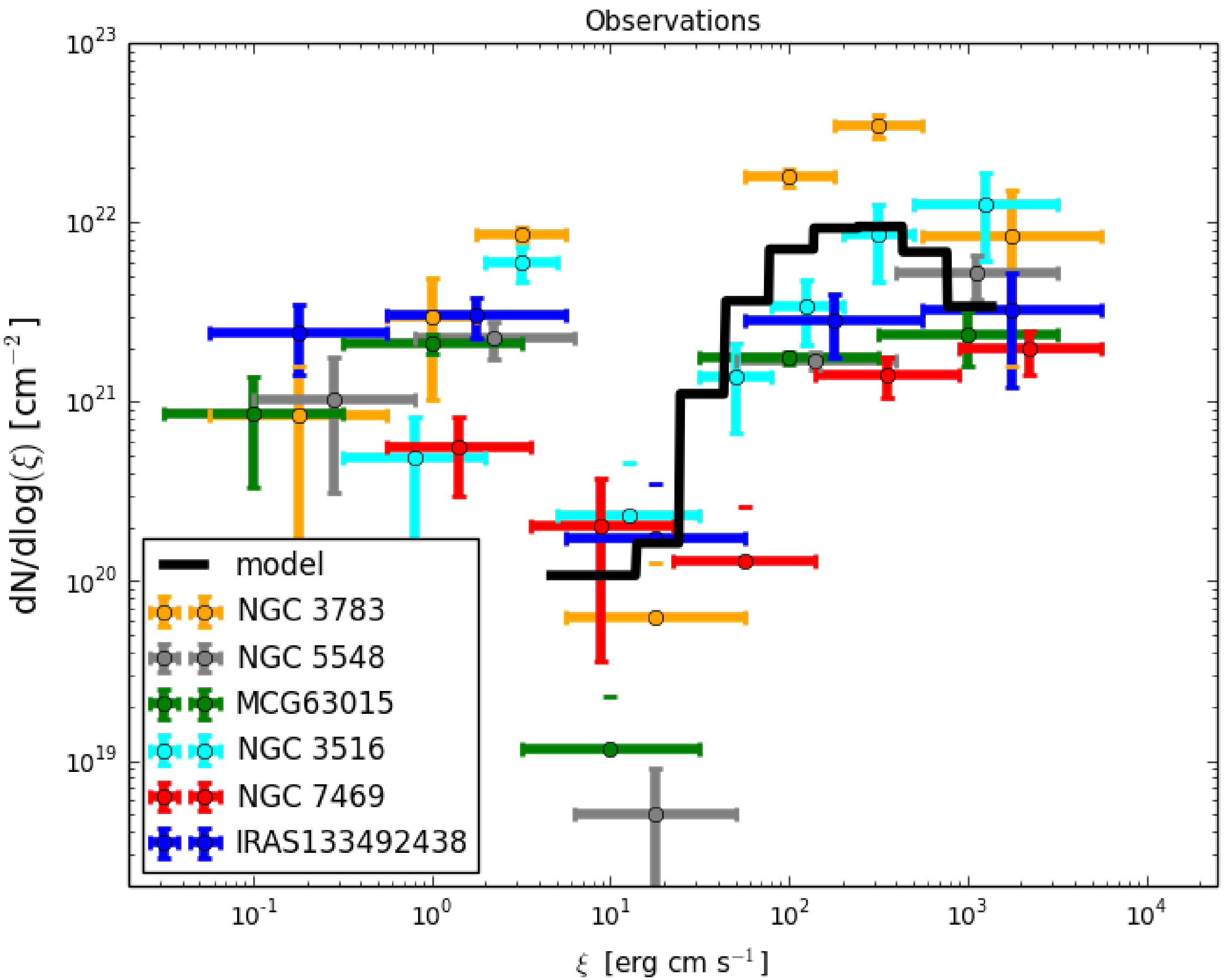

AMD data provided by Ehud Behar
Model computed with TITAN (Anne-Marie Dumont)

Conclusion first

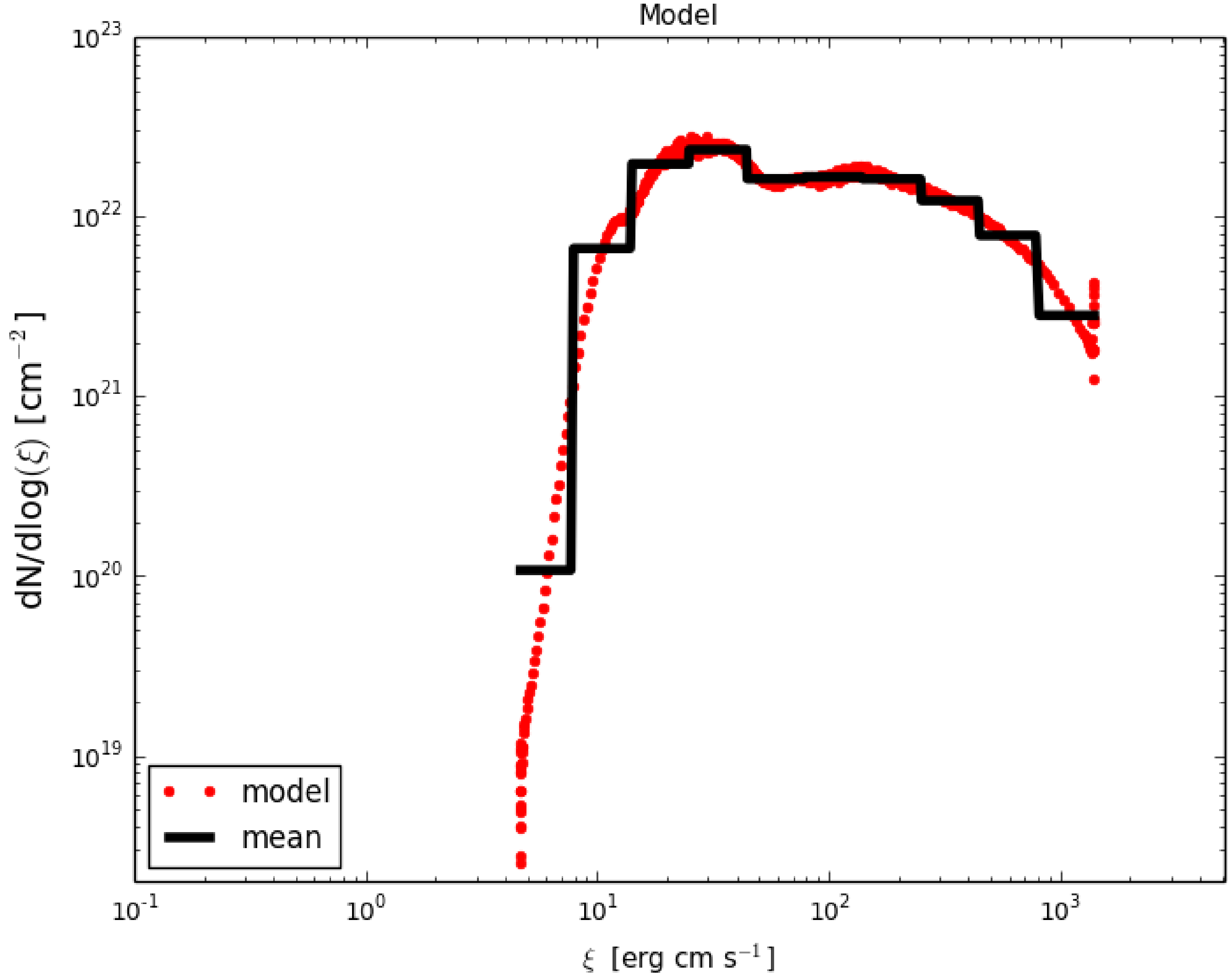

Our first AMD paper

Adhikari +15, single TITAN model for Mrk 509

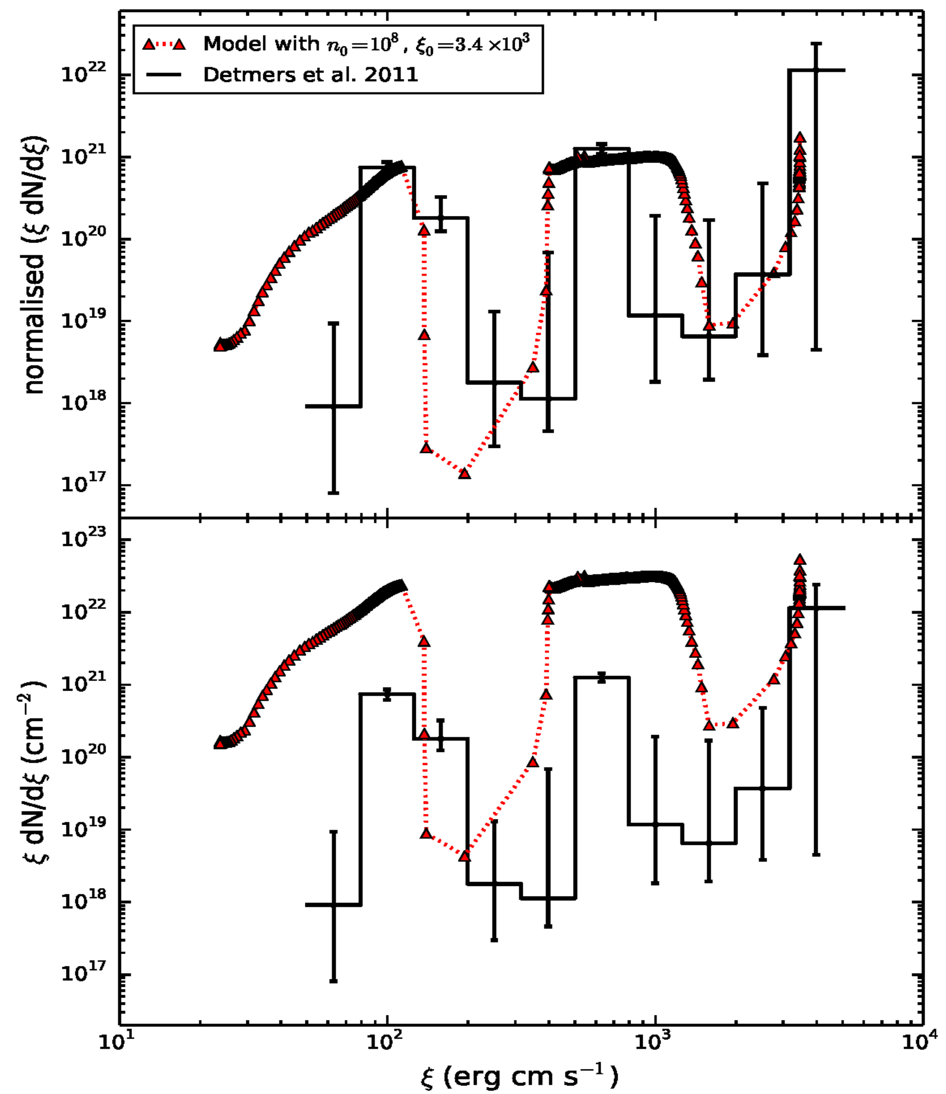

Our first AMD paper

Adhikari +15, normalization of AMD - wrong

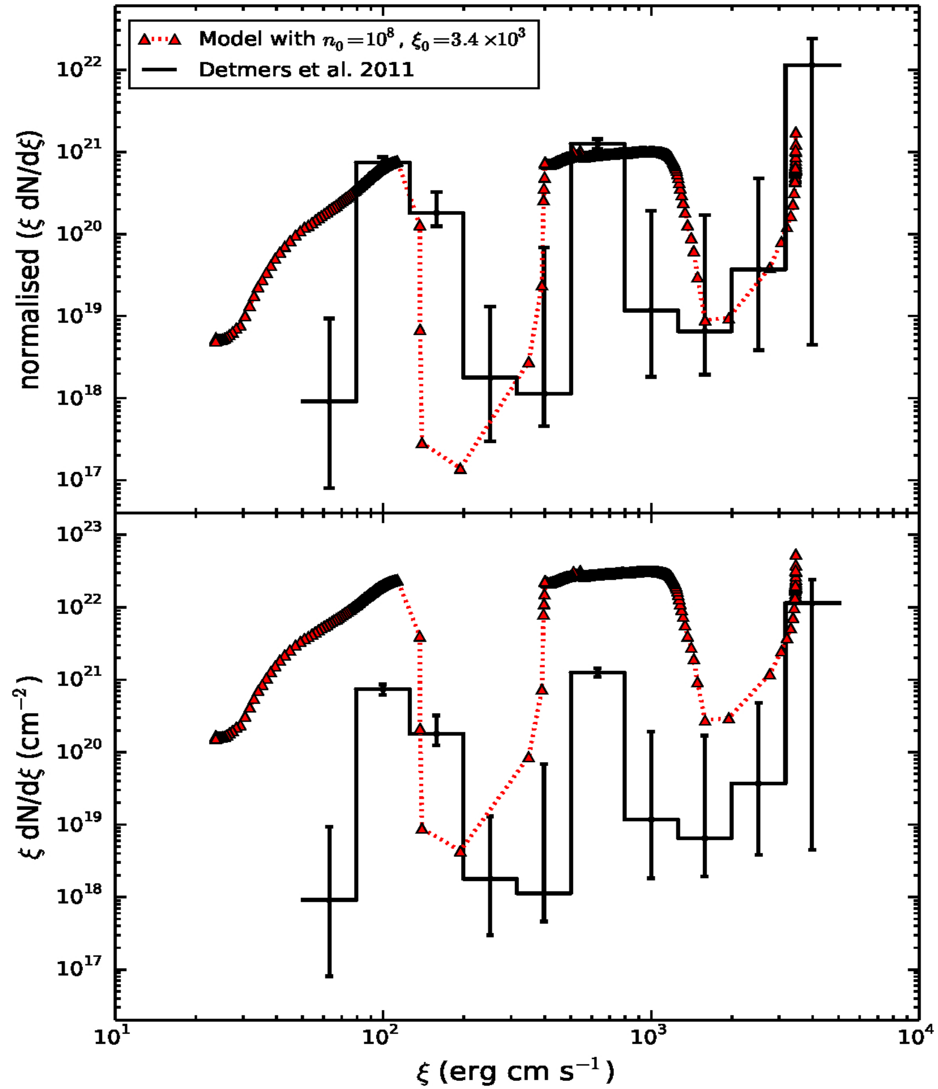

Conclusion first

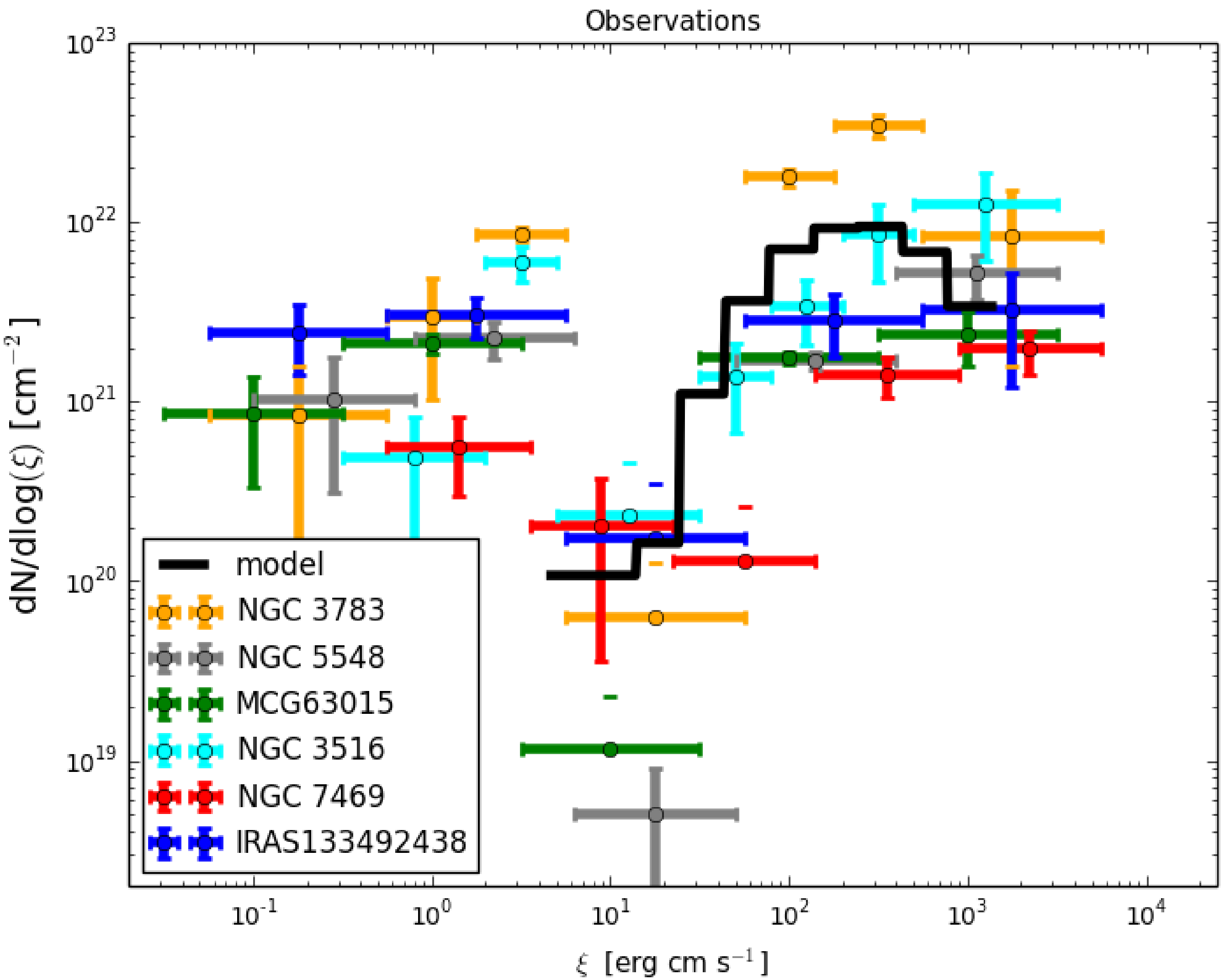

Normalization and the position of the drop agrees

Spectral analysis

Detmers +11, **Mrk 509**,
XMM=Newton, RGS 600 ksec

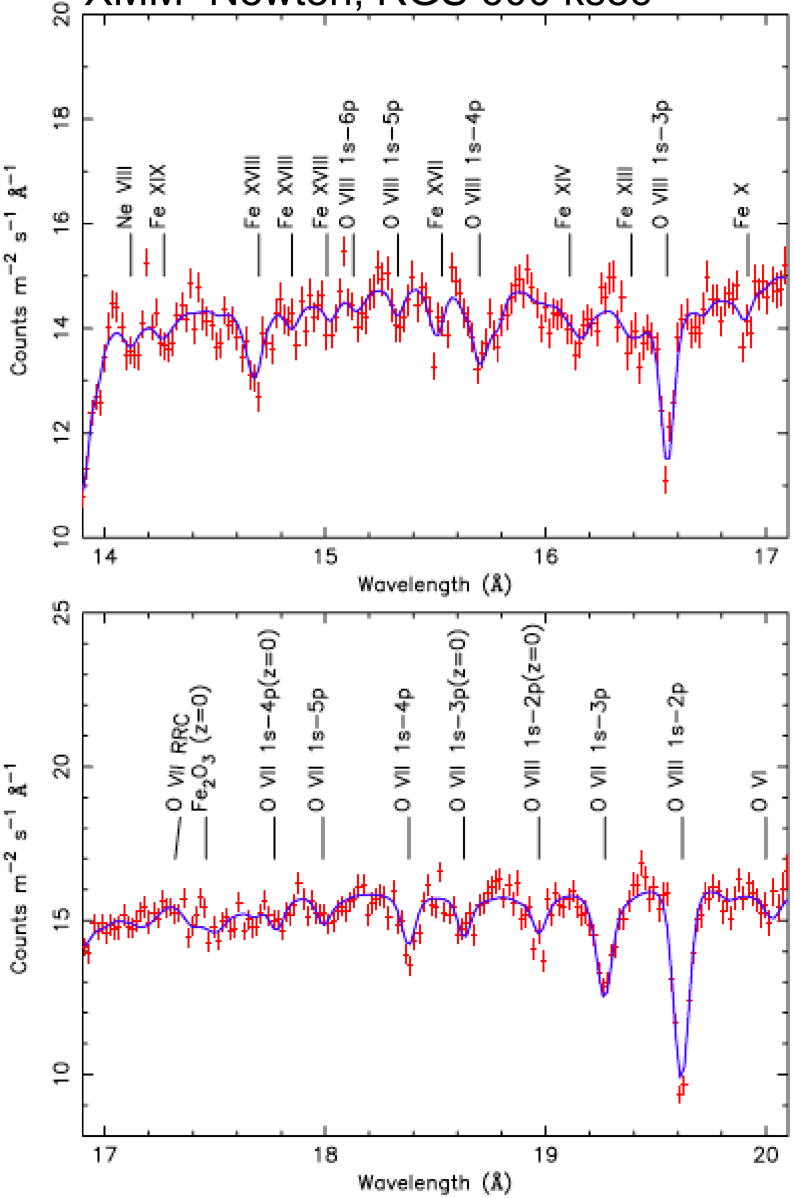

- Each line fitted with Gaussian profile, energy shift gives v_i

Spectral analysis

Detmers +11, Mrk 509,
XMM=Newton, RGS 600 ksec

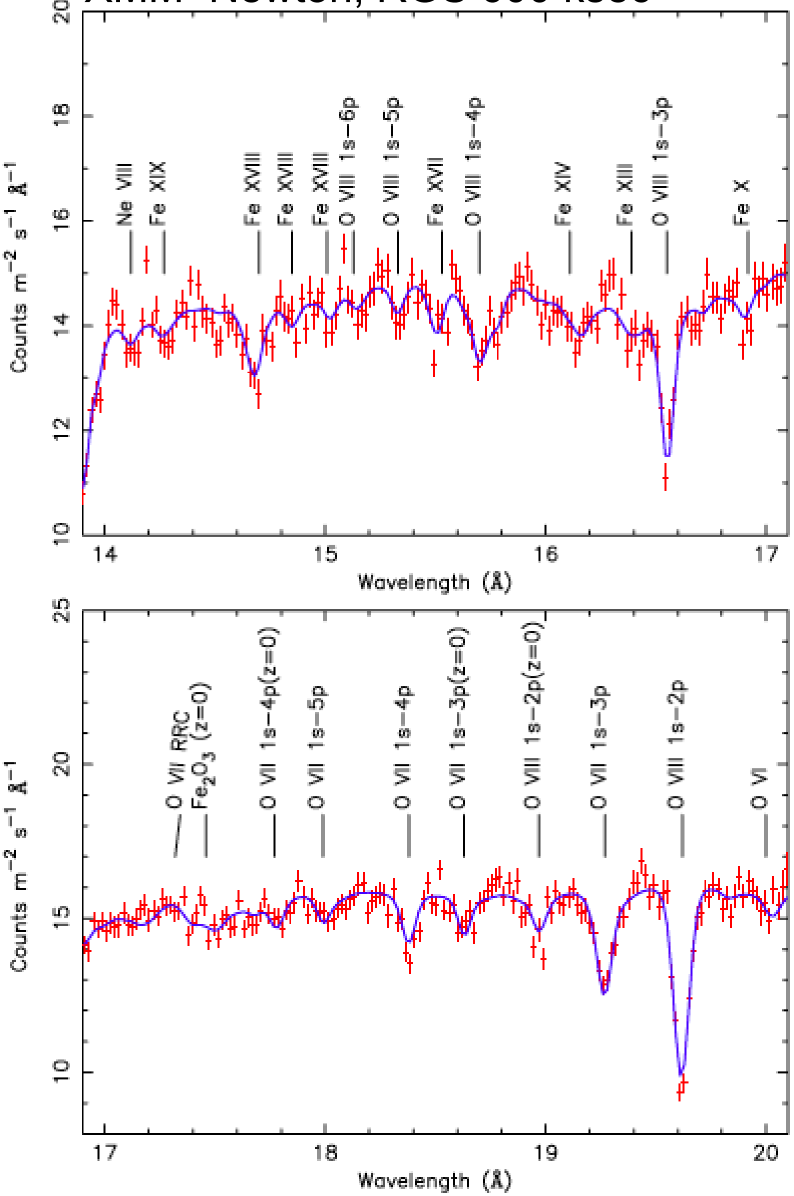

- Each line fitted with Gaussian profile, energy shift gives v_i
- EW – standard XSPEC command

Spectral analysis

Detmers +11, Mrk 509,
XMM=Newton, RGS 600 ksec

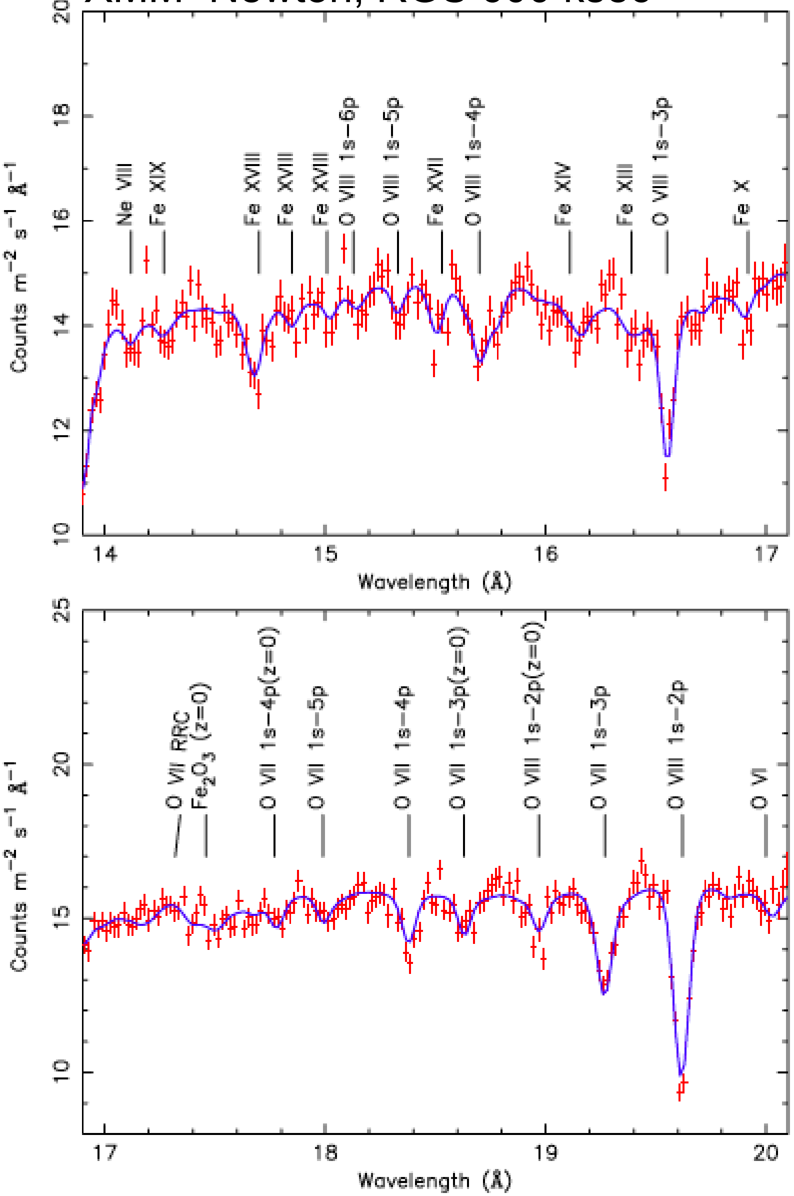

- Each line fitted with Gaussian profile, energy shift gives v_i
- EW – standard XSPEC command
- Ionic column densities integrated over the model:

$$N_i = \frac{m_e c}{\pi e^2 f_i \lambda_i} \int \tau(\nu) d\nu$$

Spectral analysis

Detmers +11, Mrk 509,
XMM=Newton, RGS 600 ksec

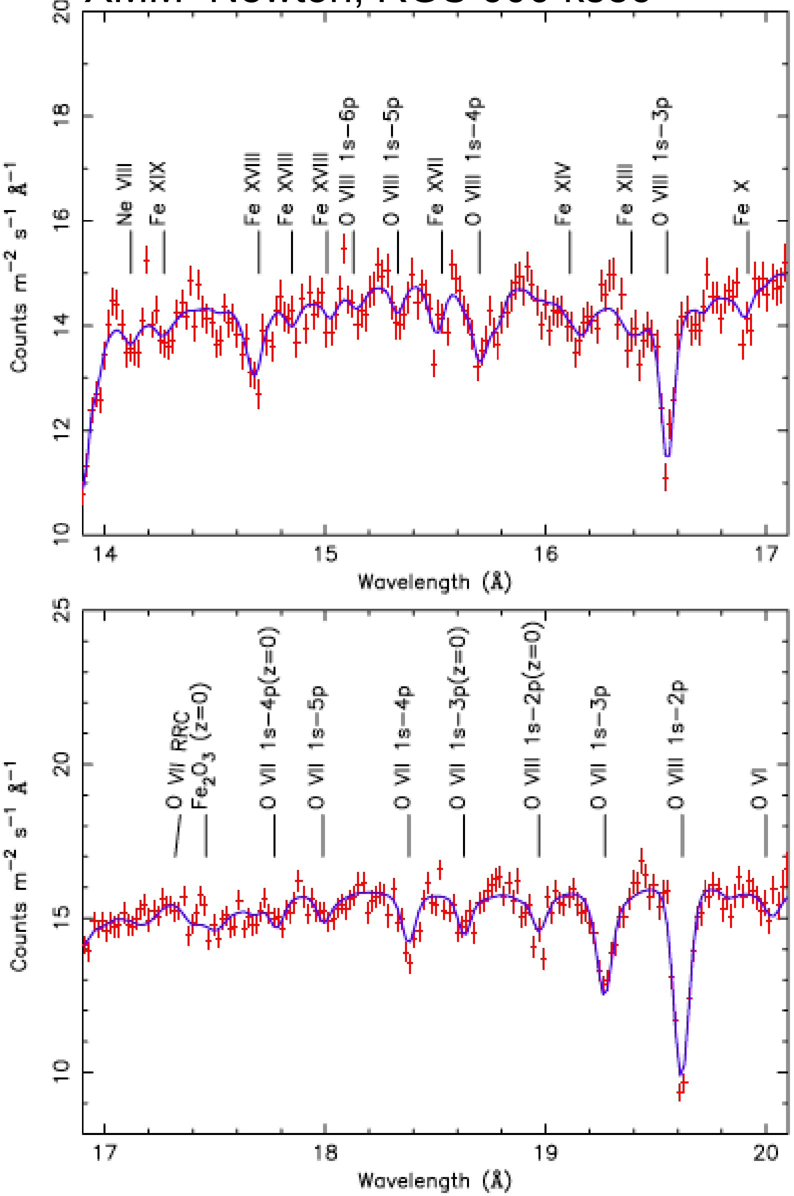

- Each line fitted with Gaussian profile, energy shift gives v_i
- EW – standard XSPEC command
- Ionic column densities integrated over the model:

$$N_i = \frac{m_e c}{\pi e^2 f_i \lambda_i} \int \tau(\nu) d\nu$$

- With Solar :) abundances photoionization calculations

Spectral analysis

Detmers +11, Mrk 509,
XMM=Newton, RGS 600 ksec

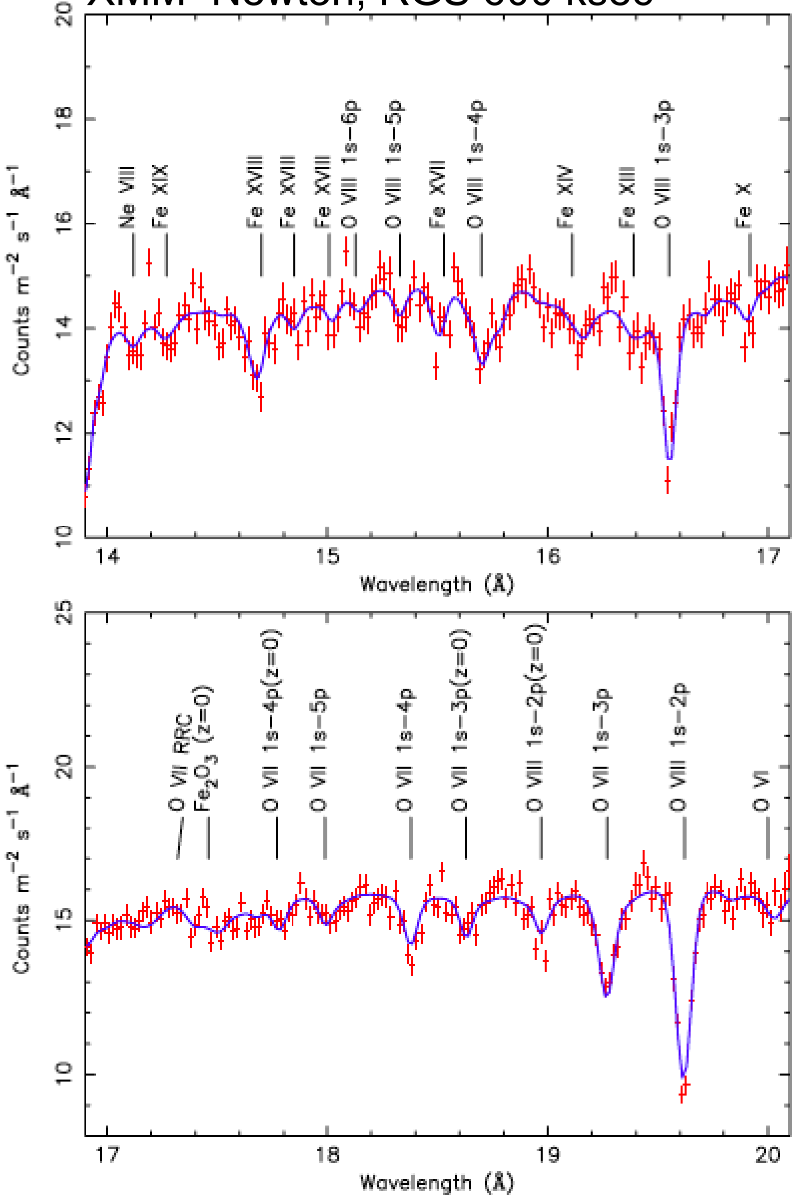

- Each line fitted with Gaussian profile, energy shift gives v_i
- EW – standard XSPEC command
- Ionic column densities integrated over the model:

$$N_i = \frac{m_e c}{\pi e^2 f_i \lambda_i} \int \tau(\nu) d\nu$$

- With Solar :) abundances photoionization calculations
- Connects N_i with N_H and N_{tot} column density of the absorber **AMD – broad**

Curve of growth

Linear dependence of EW (named W here) on ionic column density is valid only if lines are unsaturated

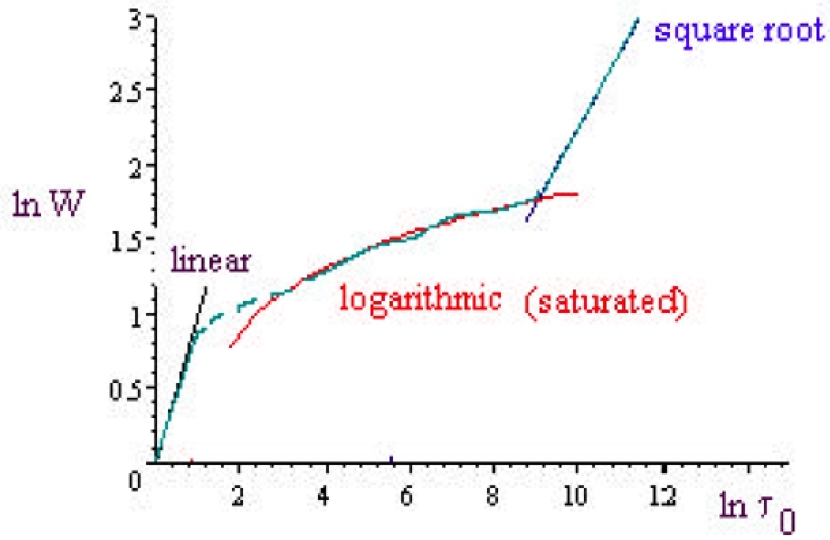

For saturated lines velocity matters

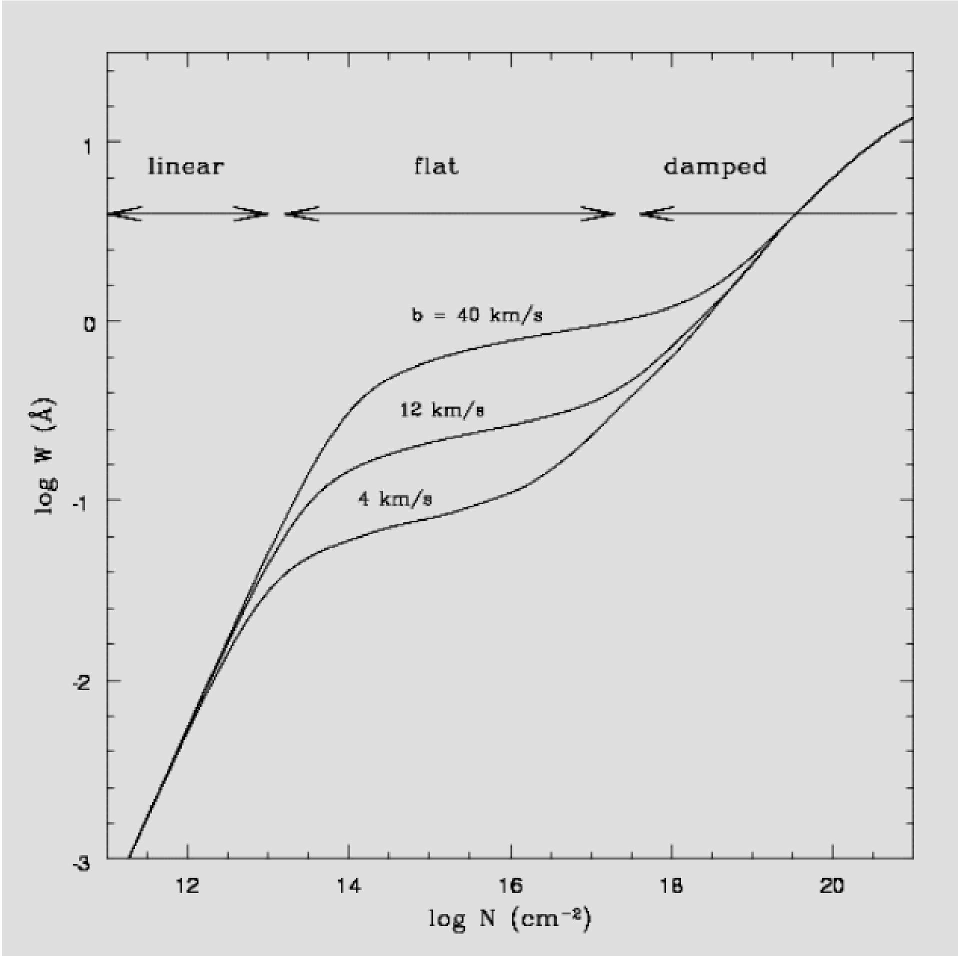

Curve of growth from TITAN model

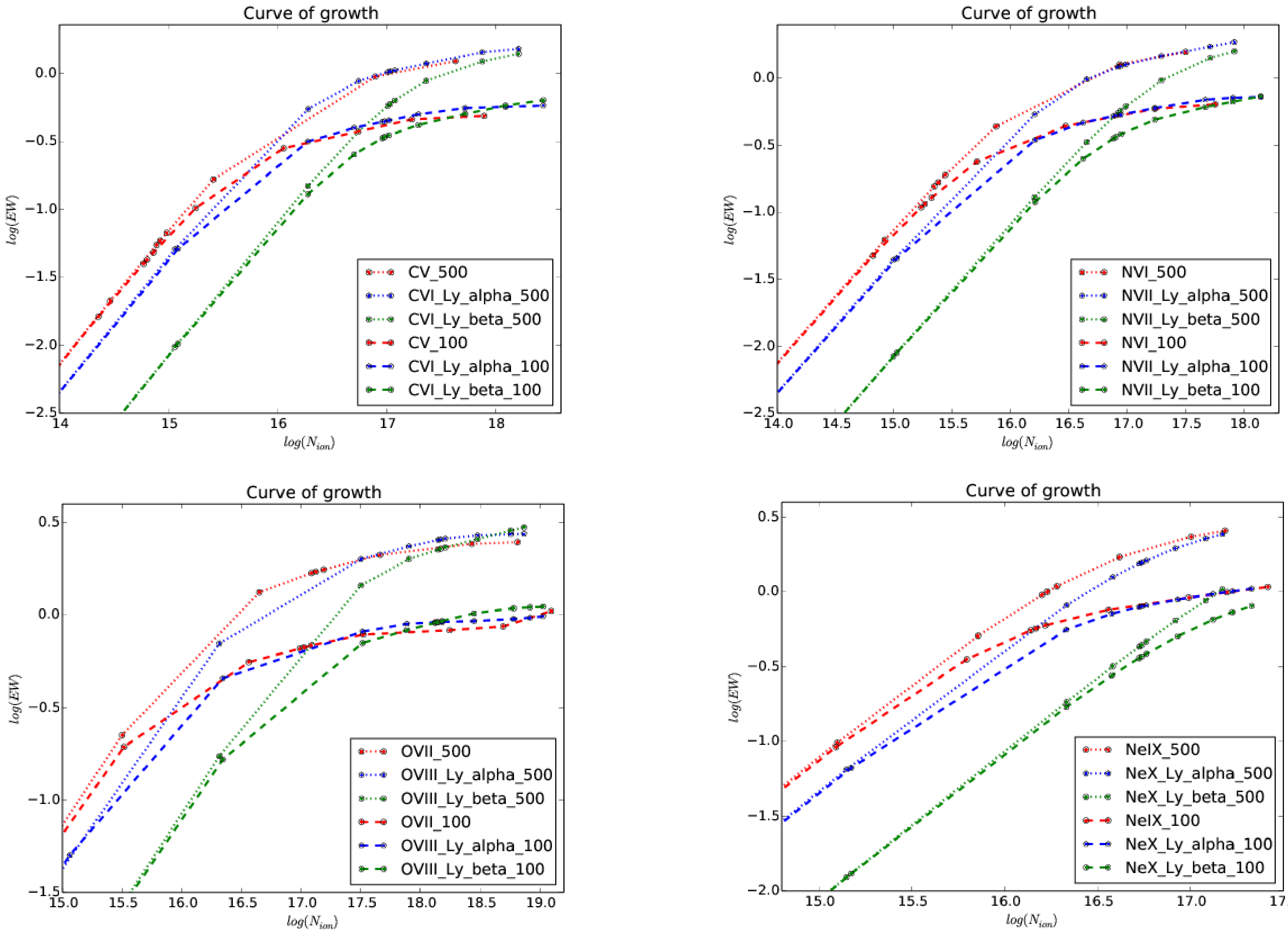

Questions to the audience

- Do we observe saturated lines in X-ray domain?

UV lines in AGN

Dunn +10, **SDSS J0318-0600**, VLT, z=1.96

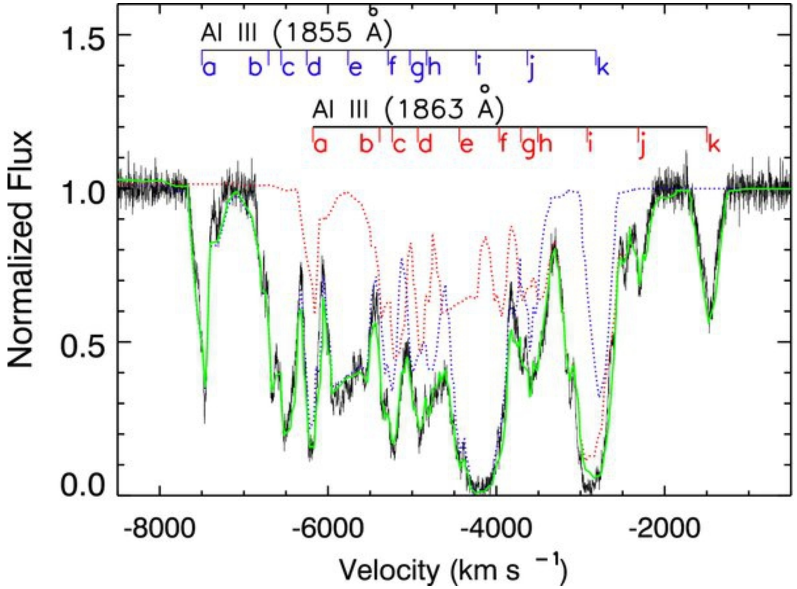

Holczer +05, **NGC 3783**, HETG

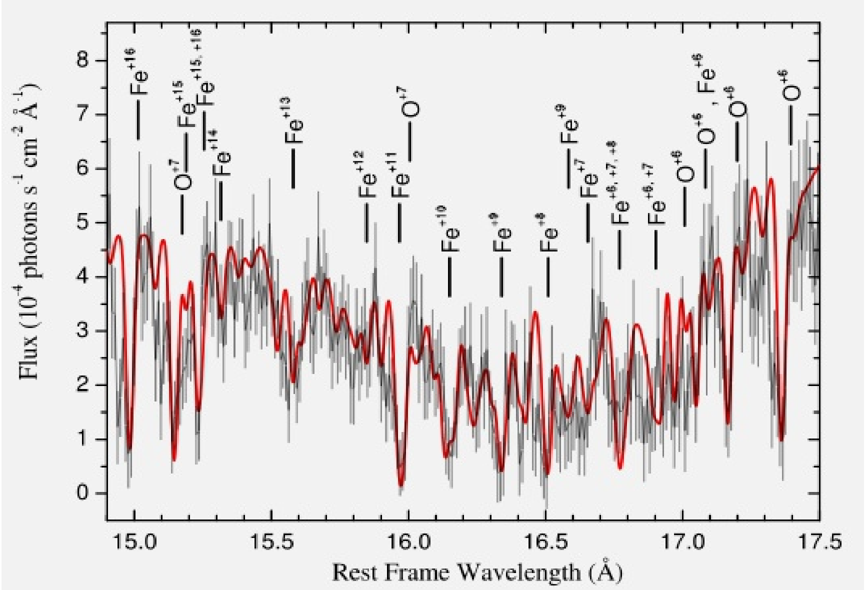

- Velocity components clearly seen

UV lines in AGN

Dunn +10, **SDSS J0318-0600**, VLT, z=1.96

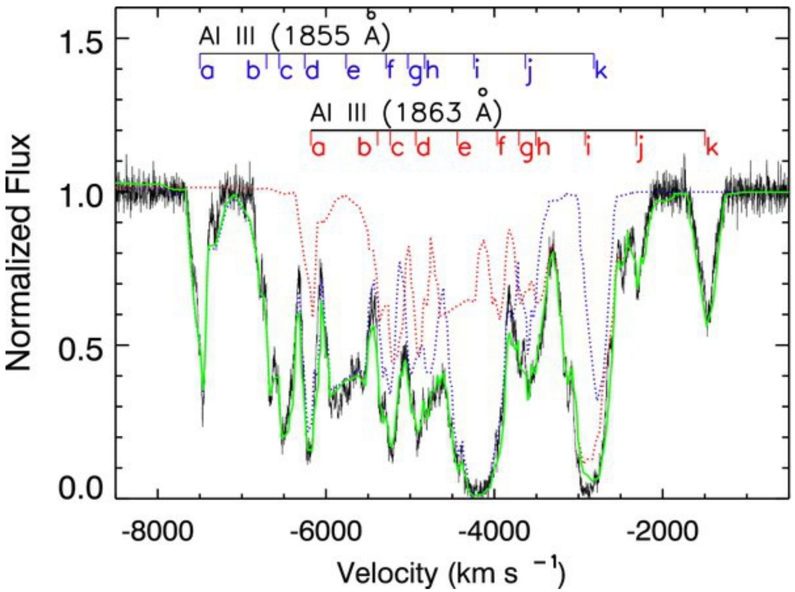

Holczer +05, **NGC 3783**, HETG

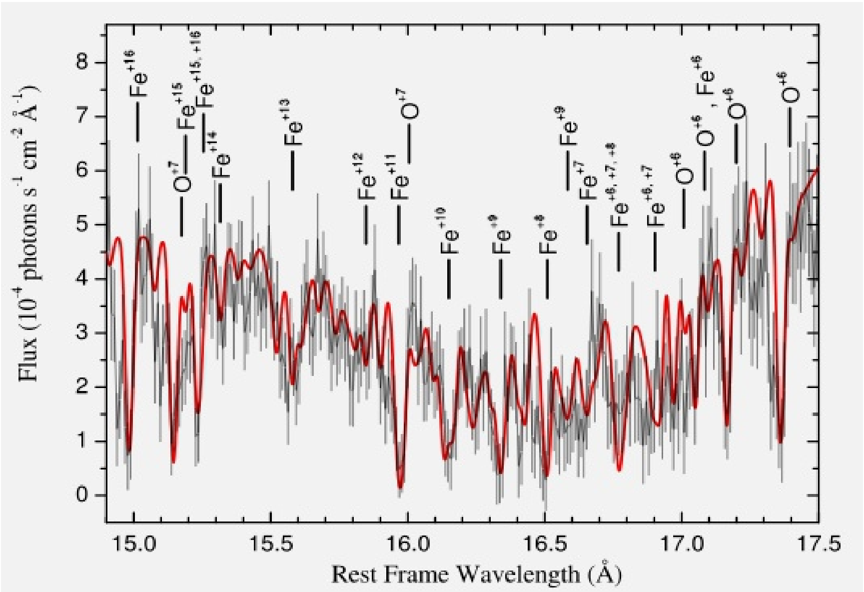

- Velocity components clearly seen
- Different absorbers

UV lines in AGN

Dunn +10, **SDSS J0318-0600**, VLT, z=1.96

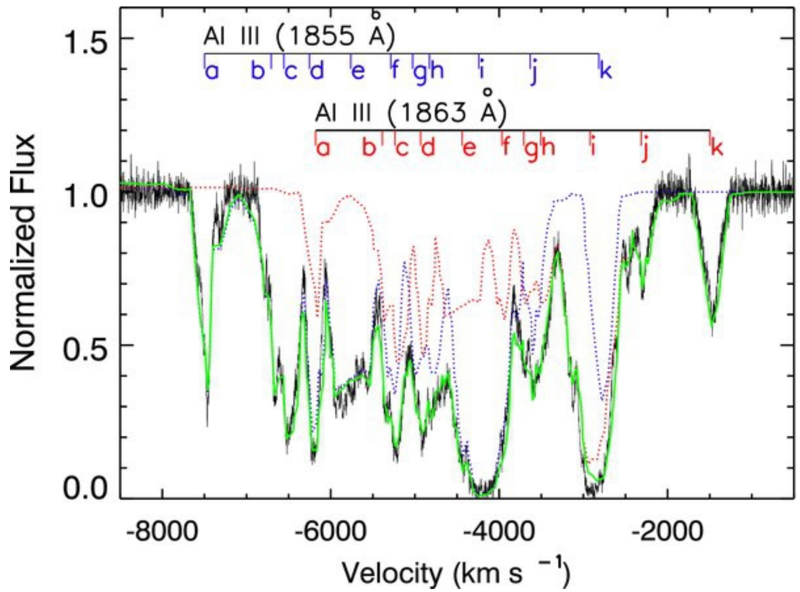

Holczer +05, **NGC 3783**, HETG

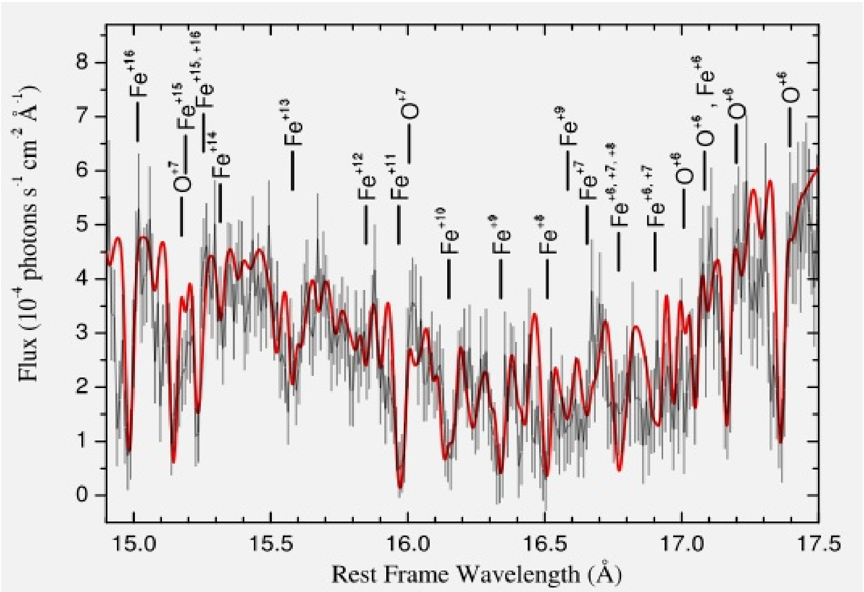

- Velocity components clearly seen
- Different absorbers
- Ionic column densities by integration over data

$$N_i = \frac{m_e c}{\pi e^2 f_i \lambda_i} \int \tau(\nu) d\nu$$

UV lines in AGN

Dunn +10, **SDSS J0318-0600**, VLT, z=1.96

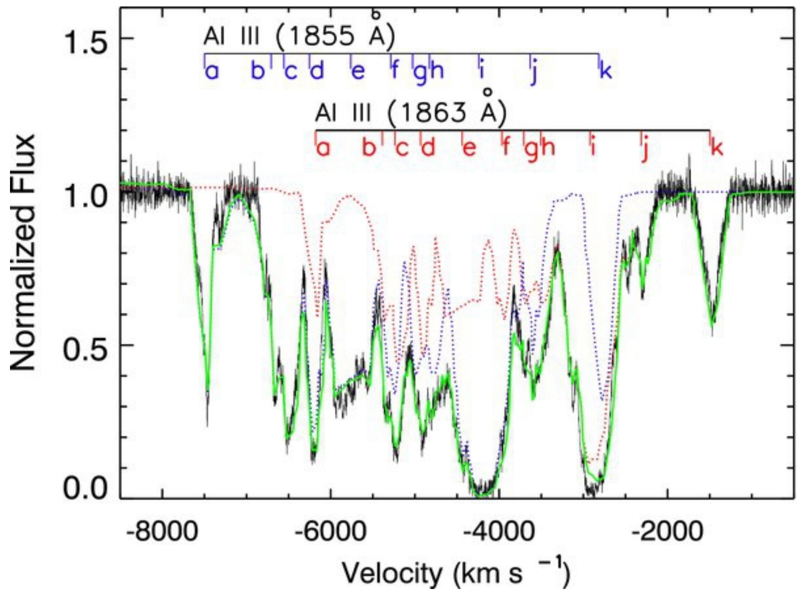

Holczer +05, **NGC 3783**, HETG

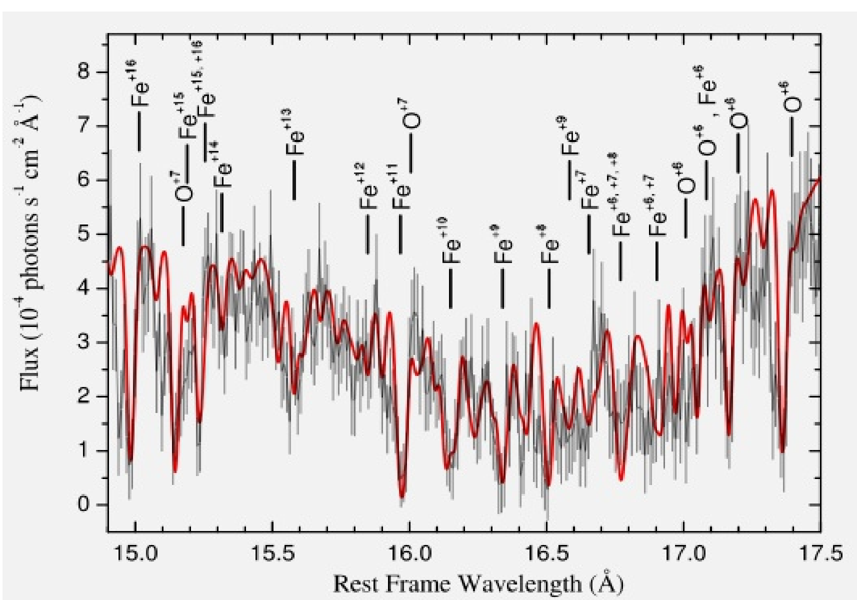

- Velocity components clearly seen
- Different absorbers
- Ionic column densities by integration over data

$$N_i = \frac{m_e c}{\pi e^2 f_i \lambda_i} \int \tau(\nu) d\nu$$

- Covering factors possible

$$\tau_\nu = -ln\left(\frac{I_\nu - 1 - C_f}{C_f}\right)$$

- Photoionization calculations, **AMD**?

Questions to the audience

- Do we observe saturated lines in X-ray domain?
- Do we derive AMD for UV absorbers?

Photoionization calculations

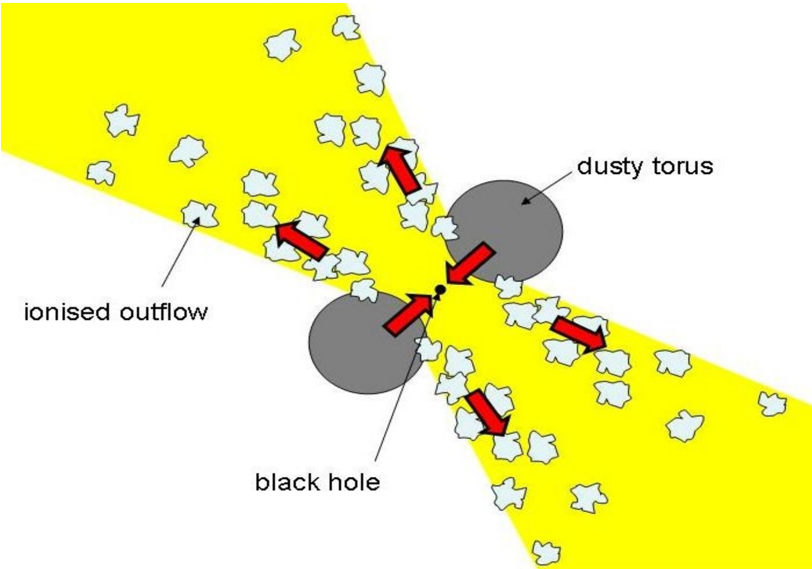

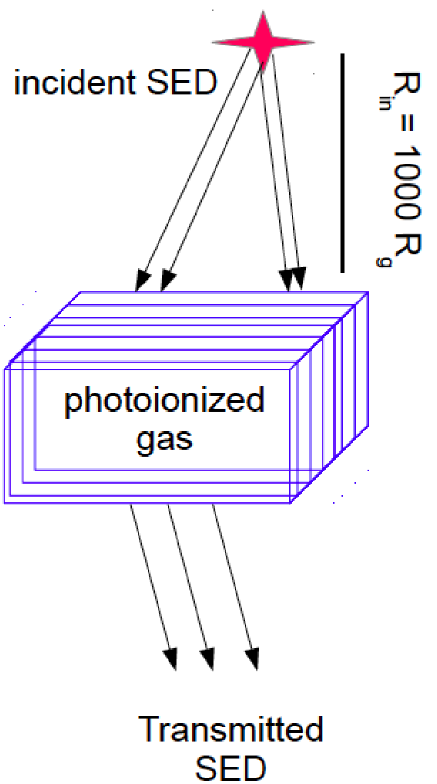

- Parameters: A_i – Solar :), R, n_0, N_{tot}, L_{ion}, SED, C_f=1

Photoionization calculations

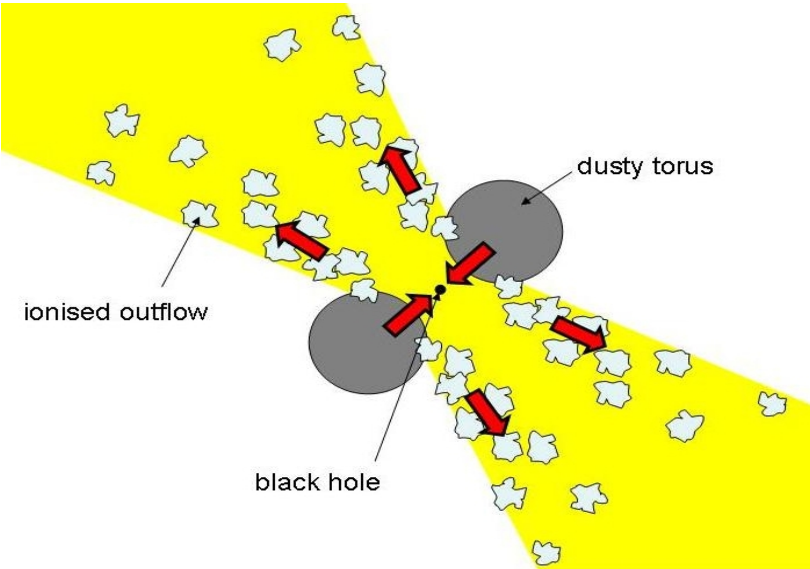

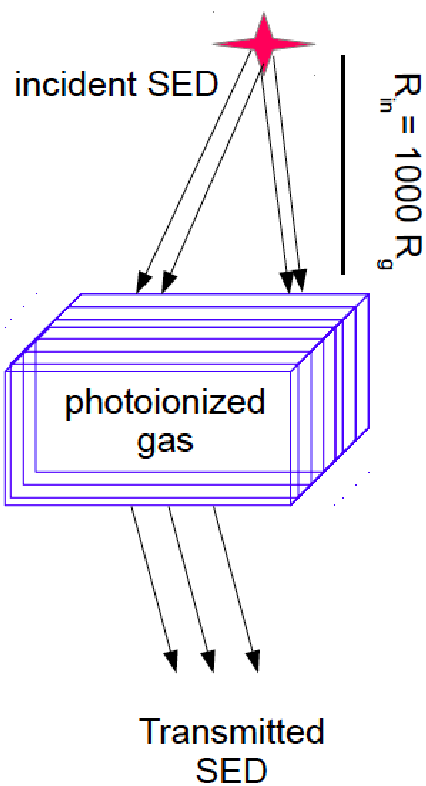

- Parameters: A_i – Solar :), R, n_0, N_{tot}, L_{ion}, SED, $C_f=1$
- 1D non-LTE radiative transfer with ionization and thermal eq.: CLOUDY, XSTAR, TITAN, PHASE, PION, SPEX, XABS, SLAB

Photoionization calculations

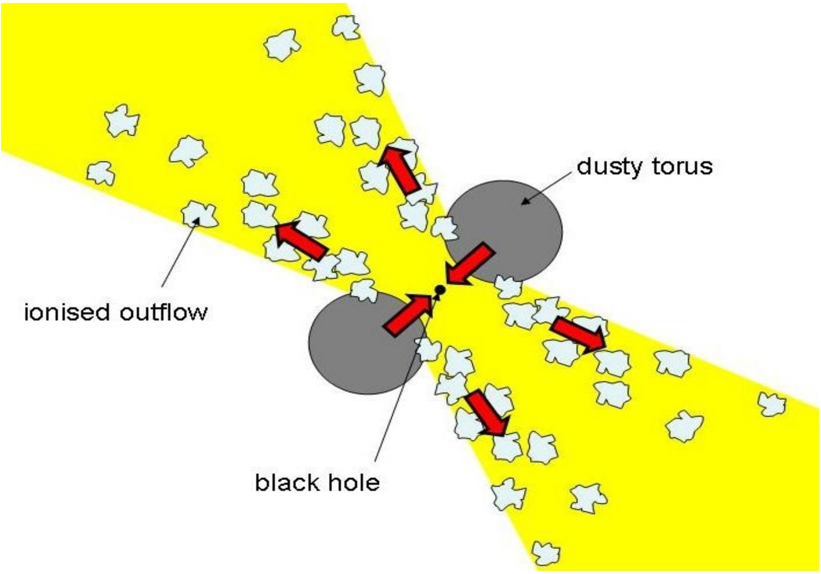

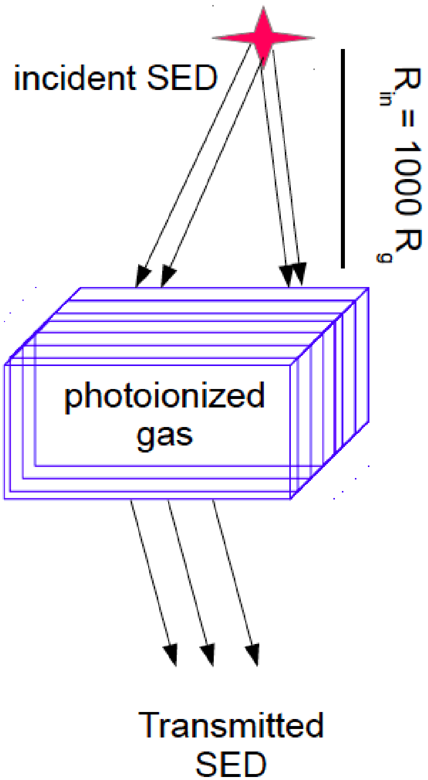

- Parameters: A_i – Solar :), R, n_0, N_{tot}, L_{ion}, SED, $C_f=1$
- 1D non-LTE radiative transfer with ionization and thermal eq.: CLOUDY, XSTAR, TITAN, PHASE, PION, SPEX, XABS, SLAB
- Ionization parameter

$$\xi_0 = \frac{L_{ion}}{n_0 R^2}$$

Photoionization calculations

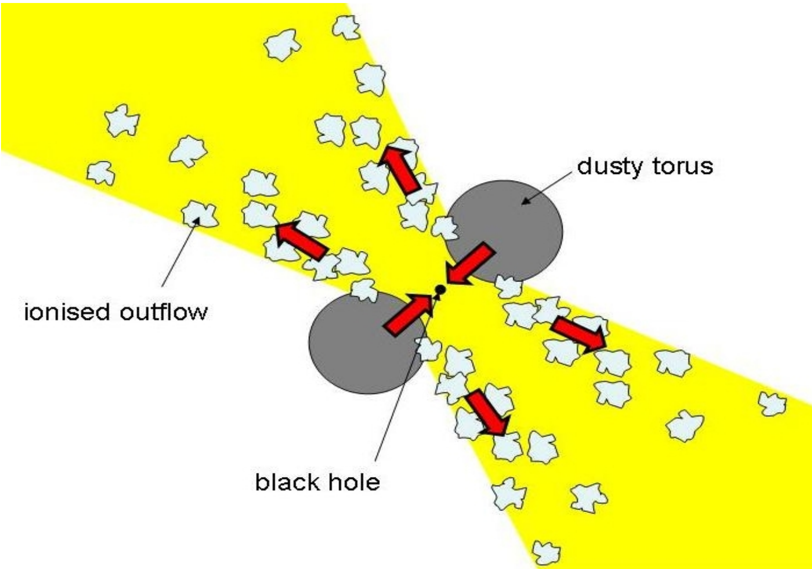

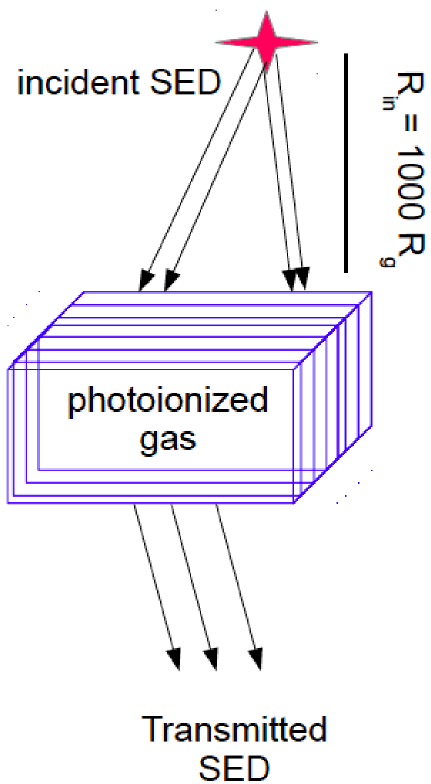

- Parameters: A_i – Solar :), R, n_0, N_{tot}, L_{ion}, *SED*, $C_f = 1$
- 1D non-LTE radiative transfer with ionization and thermal eq.: CLOUDY, XSTAR, TITAN, PHASE, PION, SPEX, XABS, SLAB
- Ionization parameter

$$\xi_0 = \frac{L_{ion}}{n_0 R^2}$$

- X-ray atomic data !!!

Photoionization calculations

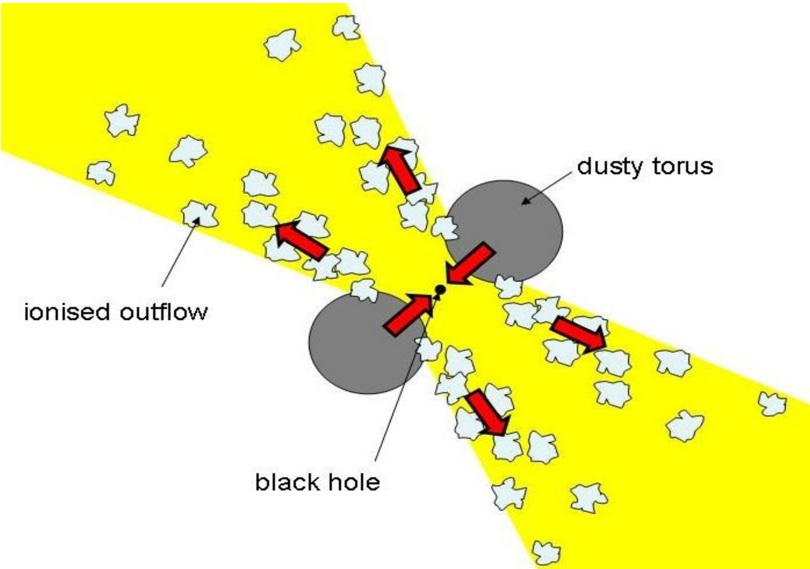

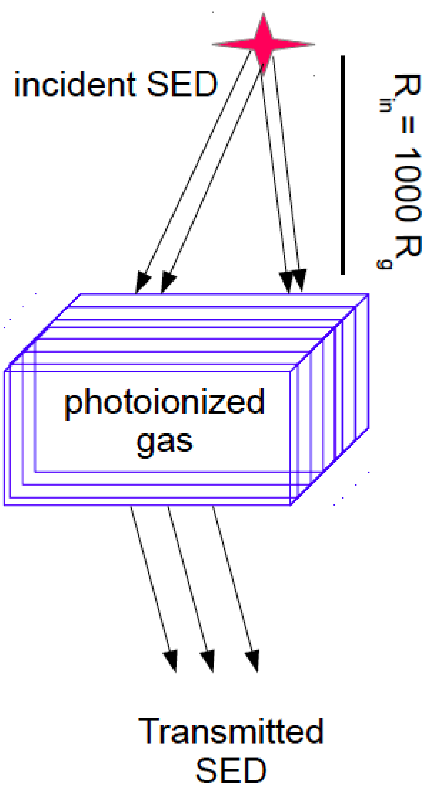

- Parameters: A_i – Solar :), $R, n_0, N_{tot}, L_{ion}, SED, C_f=1$
- 1D non-LTE radiative transfer with ionization and thermal eq.: CLOUDY, XSTAR, TITAN, PHASE, PION, SPEX, XABS, SLAB
- Ionization parameter

$$\xi_0 = \frac{L_{ion}}{n_0 R^2}$$

- X-ray atomic data !!!
- Energy balance:

$$\Gamma_{bb} + \Gamma_{bf} + \Gamma_{ff} = \Lambda_{bb} + \Lambda_{bf} + \Lambda_{ff}$$

One photoionization component

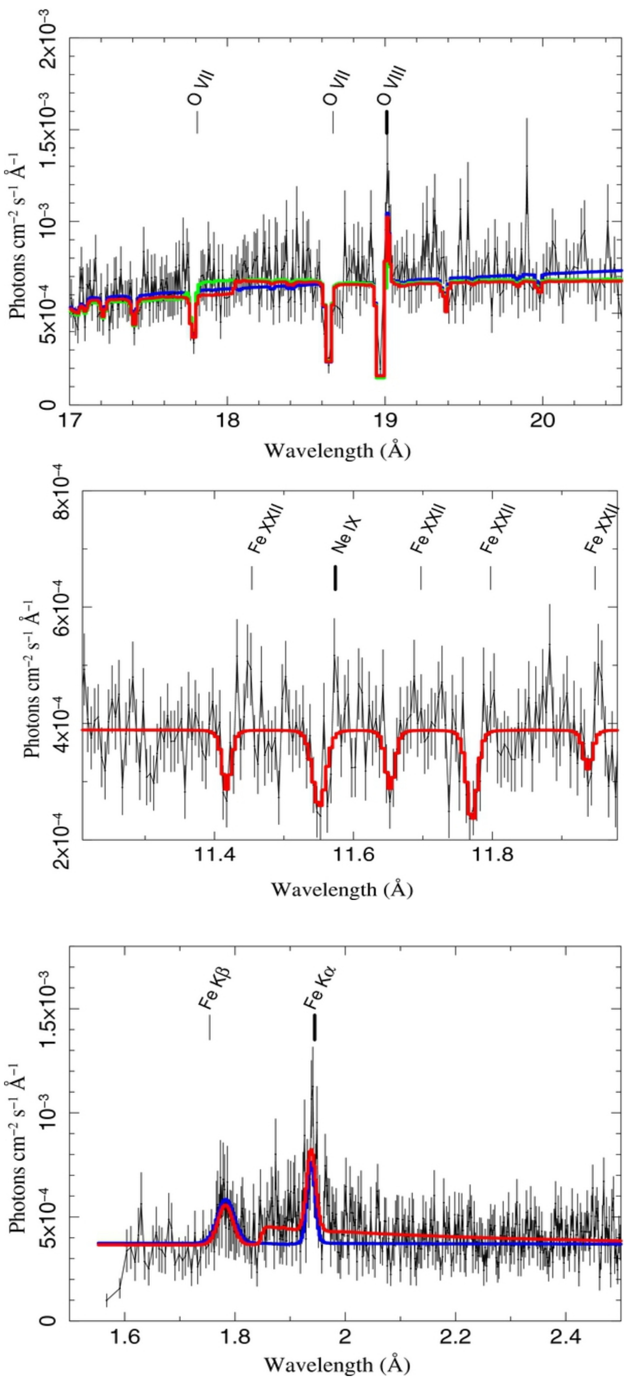

- Continuity equation:
  n=const, ξ = const, v=0

One photoionization component

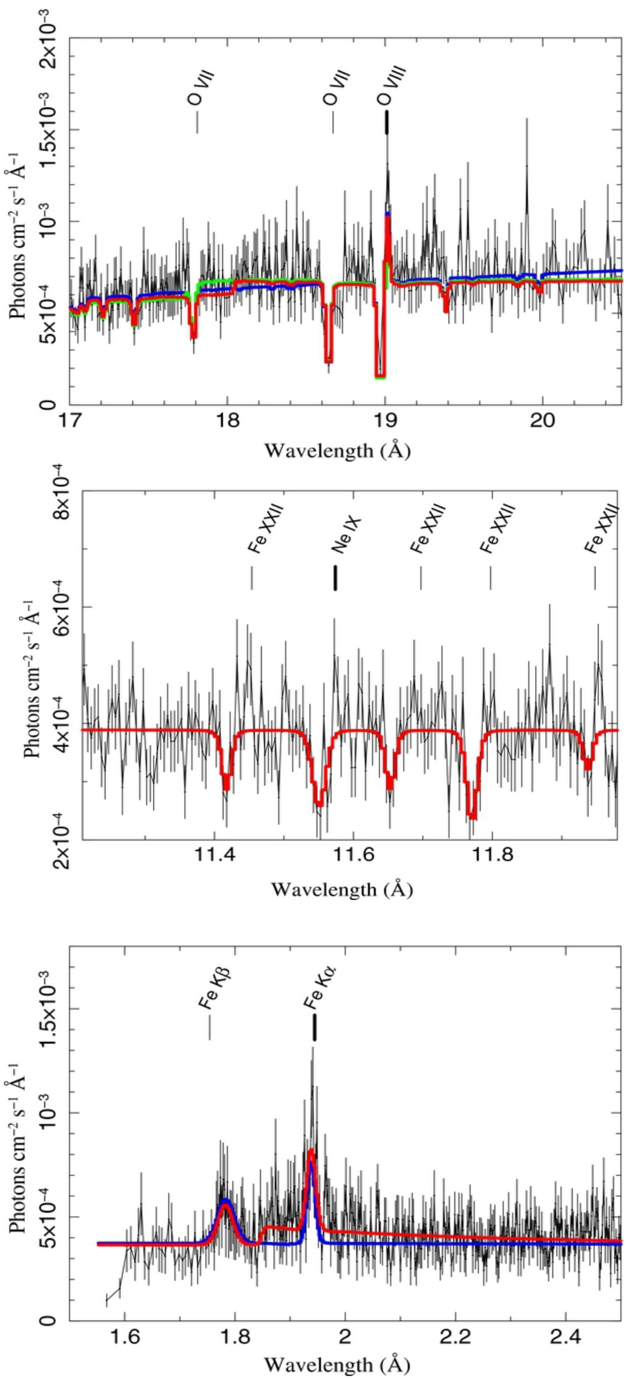

- Continuity equation: *$n=const$, $\xi = const$, $v=0$*
- All codes – T, N_{tot}, ξ, *EWs*

One photoionization component

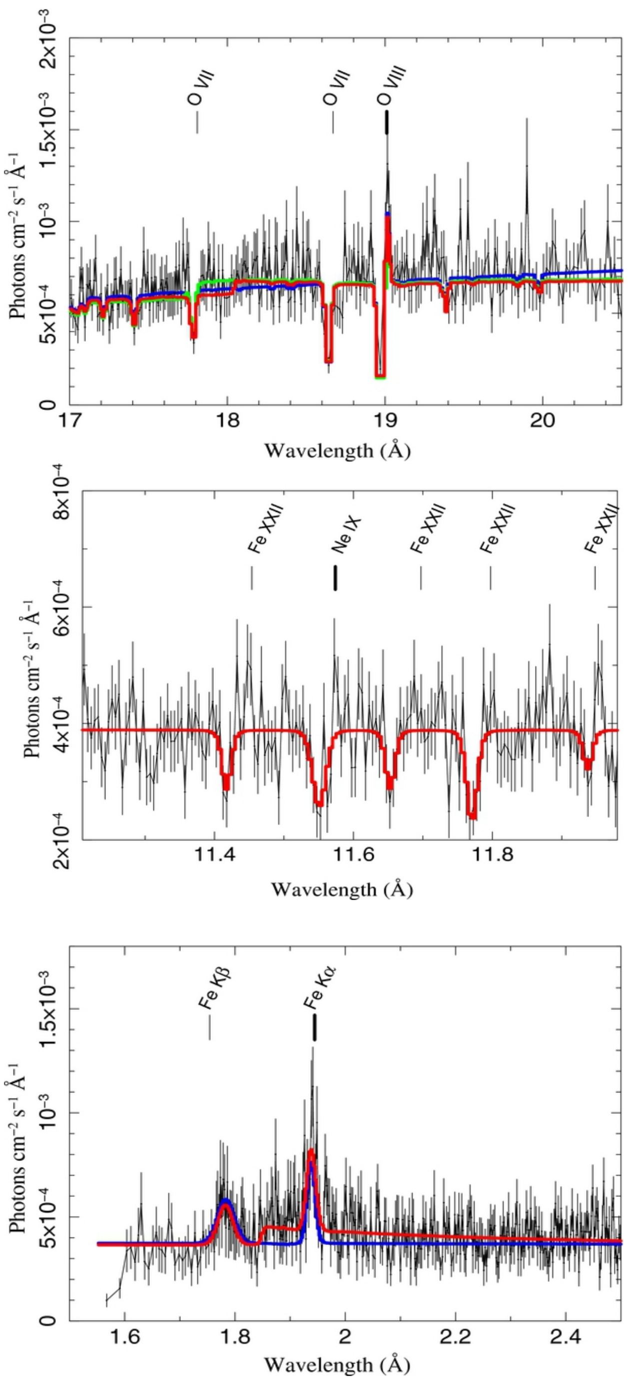

- Continuity equation:
  n=const, ξ = const, v=0

- All codes – T, N_{tot}, ξ, *EWs*

- Location does not depend on gravity of the central BH

One photoionization component

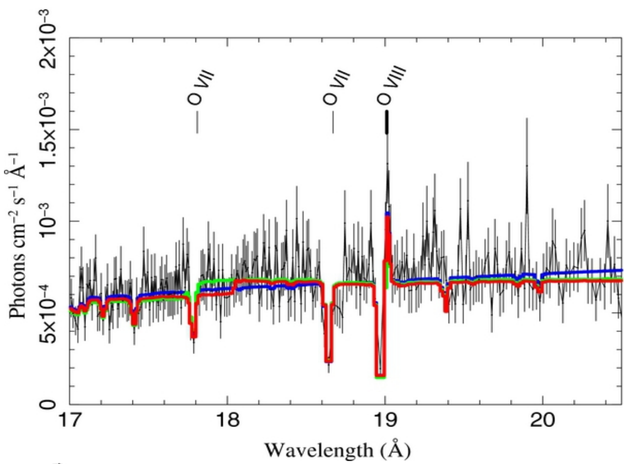

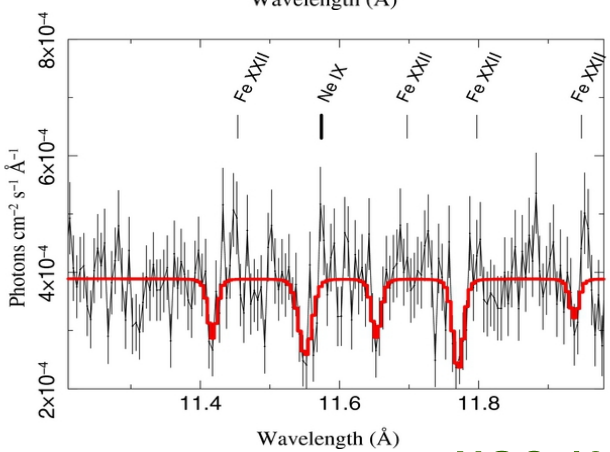

- Continuity equation:
  n=const, ξ = const, v=0
- All codes – *T*, N_{tot}, *ξ, EWs*
- Location does not depend on gravity of the central BH
- Three components:
  log(ξ)=4.5, 3.5, 1
  v = -580, -450, -310 km/s

NGC 4051, King +10

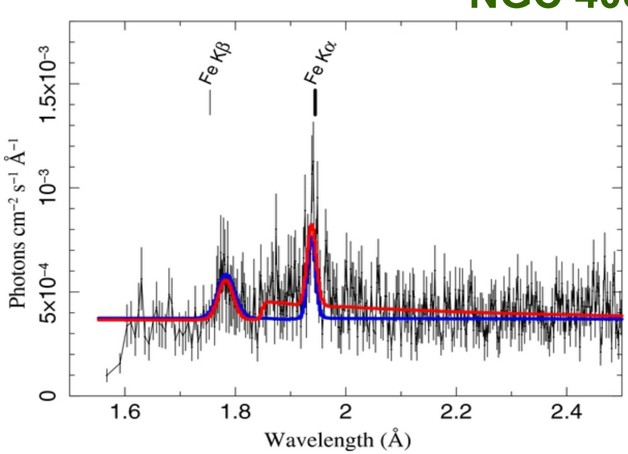

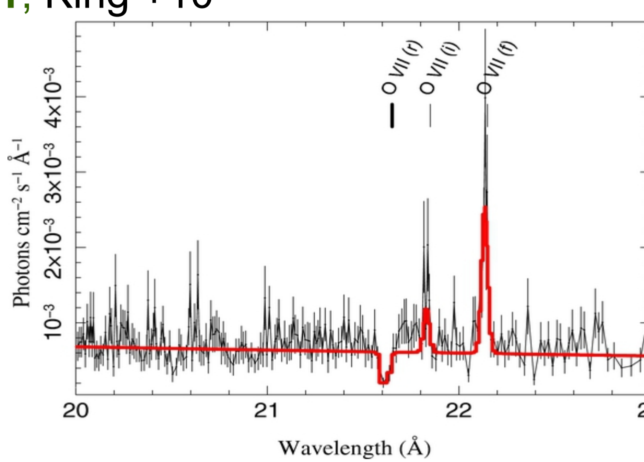

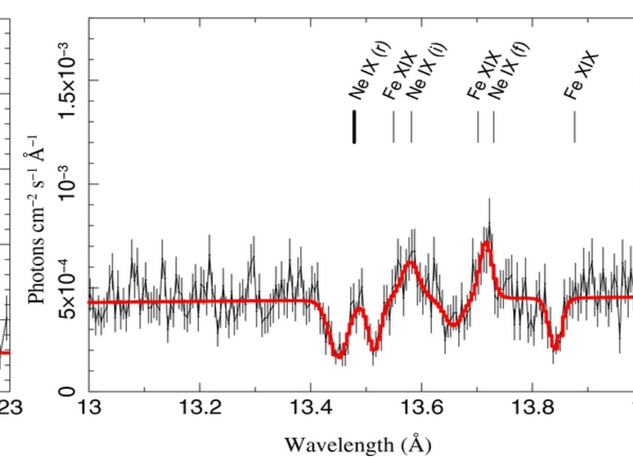

Continuous photoionization component, Różańska +06

NGC 3783, Goncalves +06

ξ = 2500, N_{tot} = 4×10^{22} cm^{-2}, v= 800 km/s

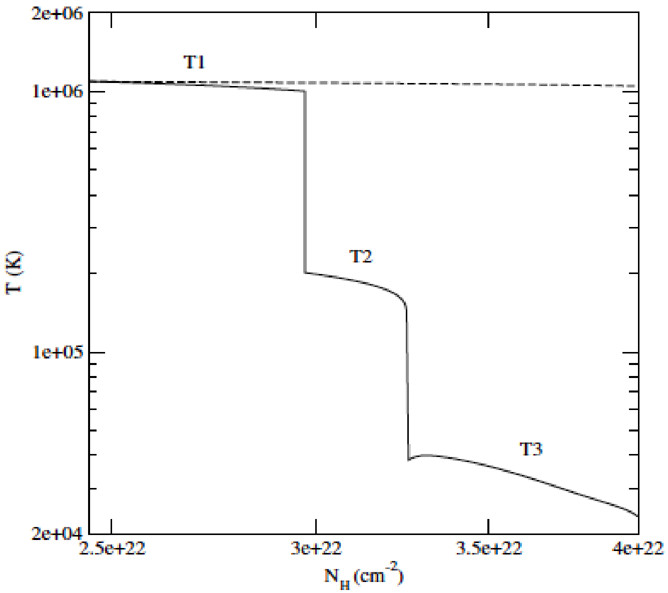

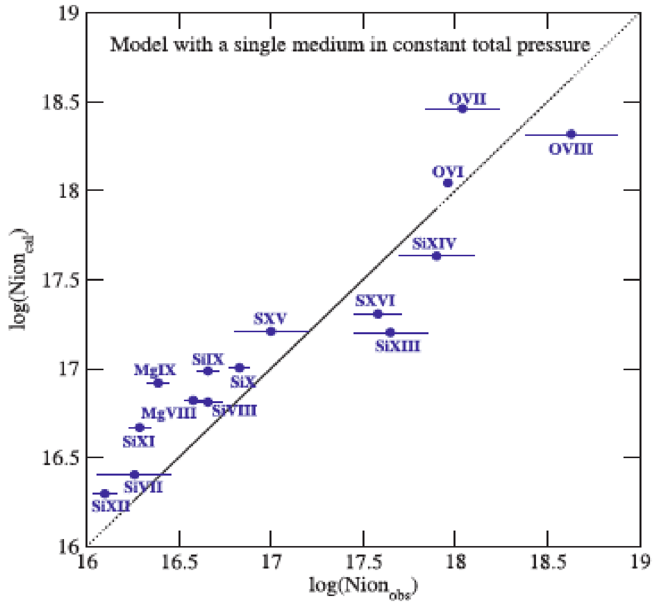

- Momentum equation: P_{tot}=const, v=0
- TITAN does this including calculations of $P_{rad}(\tau)$

Continuous photoionization component, Różańska +06

NGC 3783, Goncalves +06

ξ = 2500, N_{tot}= 4 x 10^{22} cm^{-2}, v= 800 km/s

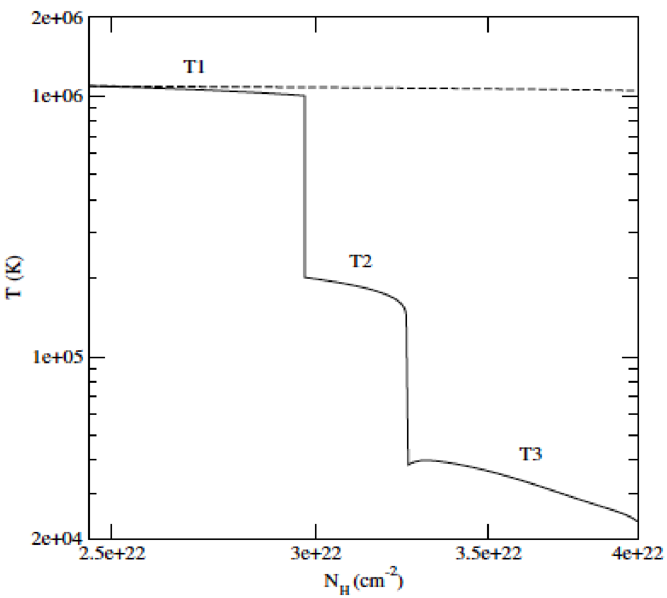

- Momentum equation: P_{tot}=const, v=0
- TITAN does this including calculations of $P_{rad}(\tau)$
- $T(\tau)$, $n(\tau)$, $\xi(\tau)$, N_{tot} , EWs
- Stability curve: T vs. Ξ

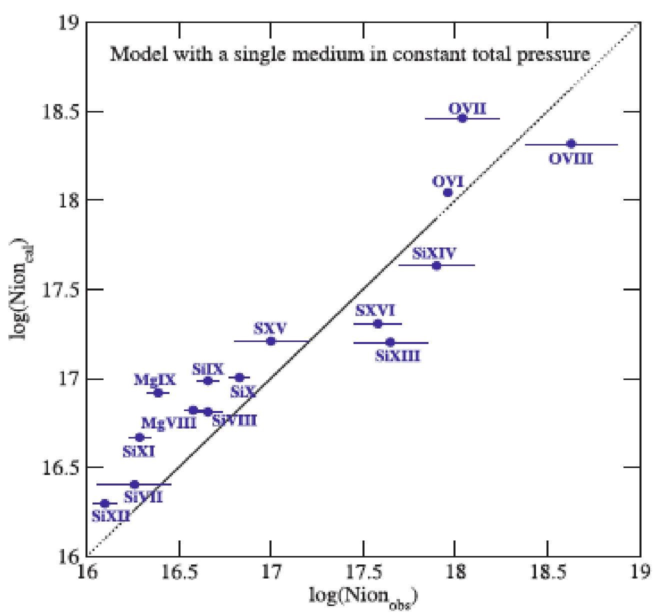

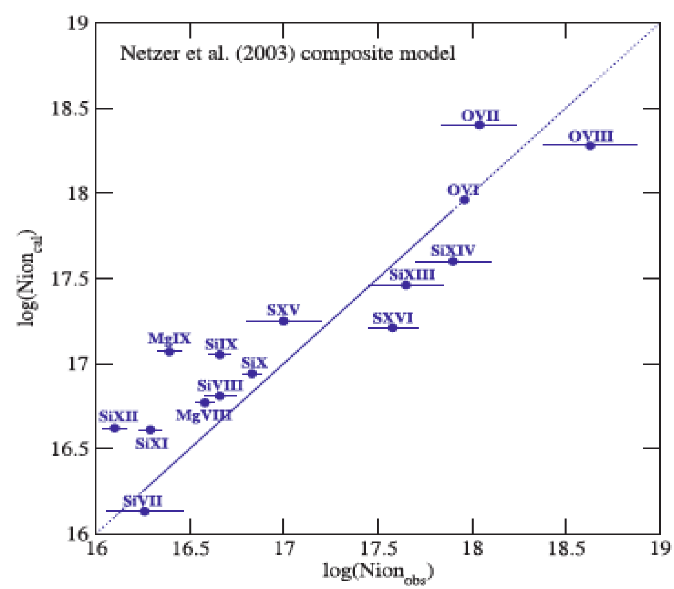

NGC 3783
Netzer +03

Questions to the audience

- Do we observe saturated lines in X-ray domain?
- Do we derive AMD for UV absorbers?
- Are we able to distinguish between ***const. P*** and ***const. n*** models from observations?

Dynamical ionization parameter

$$\Xi = \frac{\xi}{4\pi ckT} = \frac{L_{ion}}{4\pi cR^2}\frac{1}{nkT} = \frac{P_{rad}}{P_{gas}} = \frac{P_{rad}}{2.3\,P_{gas,H}},$$

Krolik +1981

Hess +1997, Stability curve

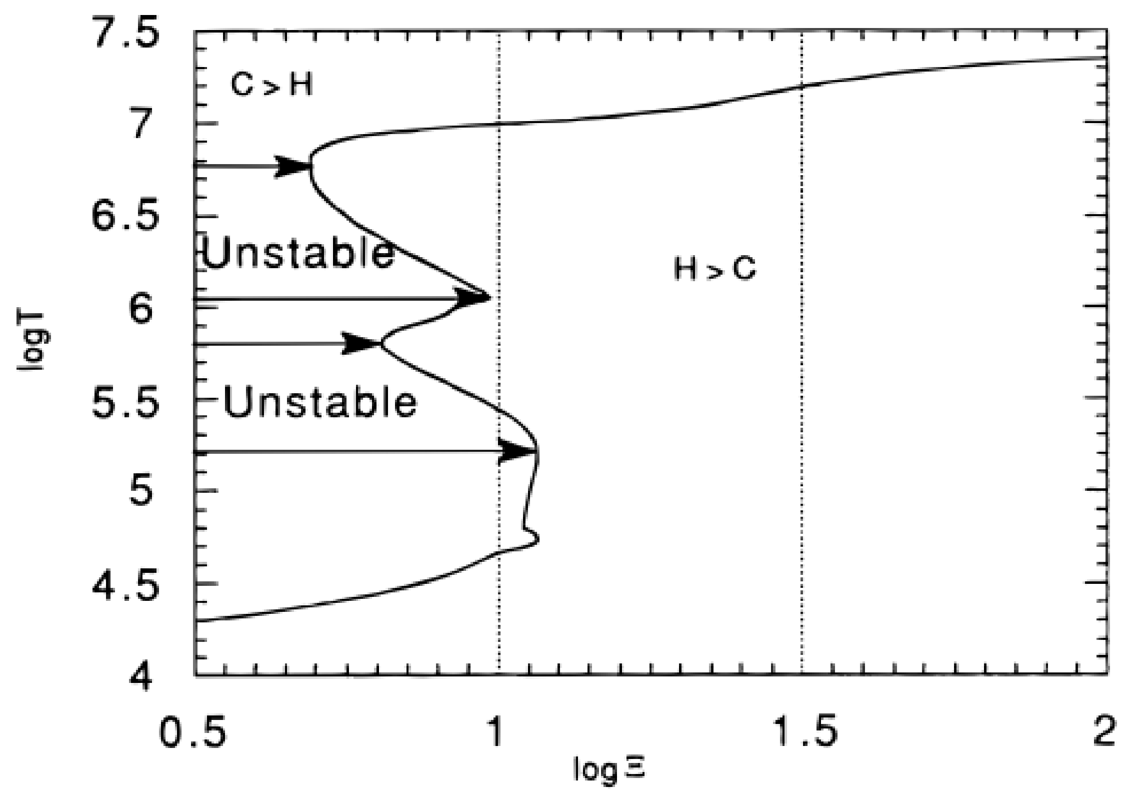

Dynamical ionization parameter

$$\Xi = \frac{\xi}{4\pi ckT} = \frac{L_{ion}}{4\pi cR^2}\frac{1}{nkT} = \frac{P_{rad}}{P_{gas}} = \frac{P_{rad}}{2.3\,P_{gas,H}},$$

Krolik +1981

Hess +1997, **Stability curve**, Influence of abundances

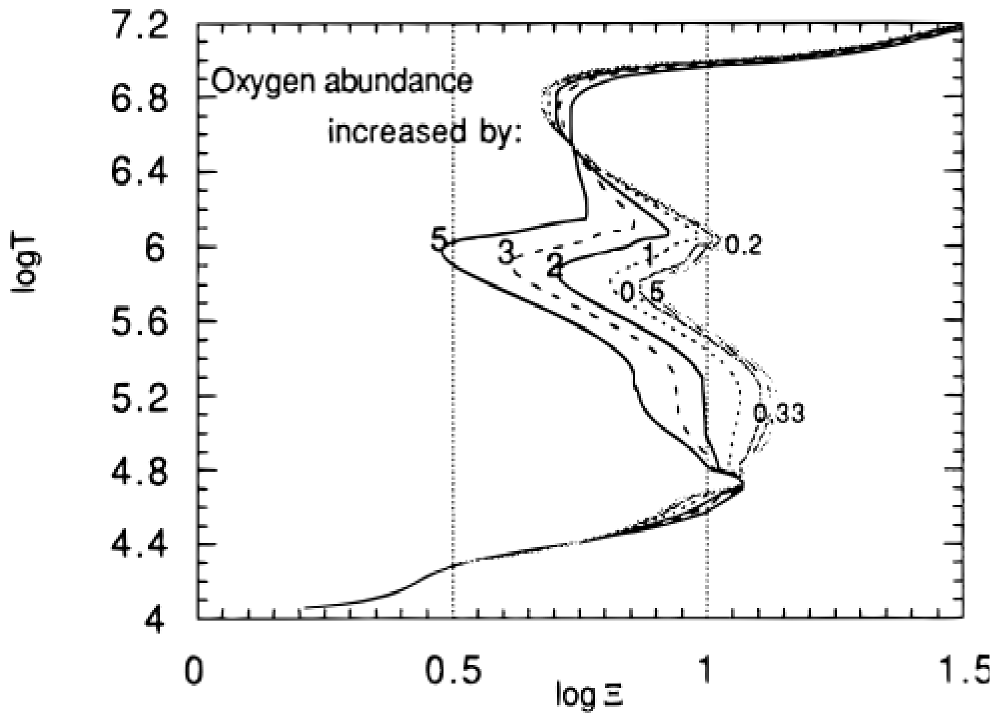

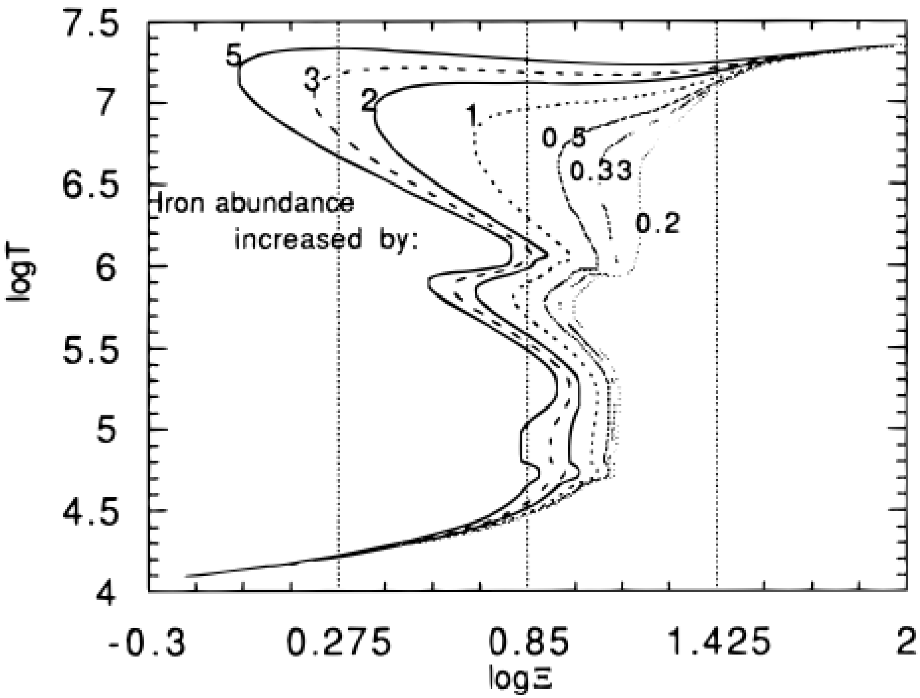

Stability curve

Chakravorty +12, **Different SEDs**

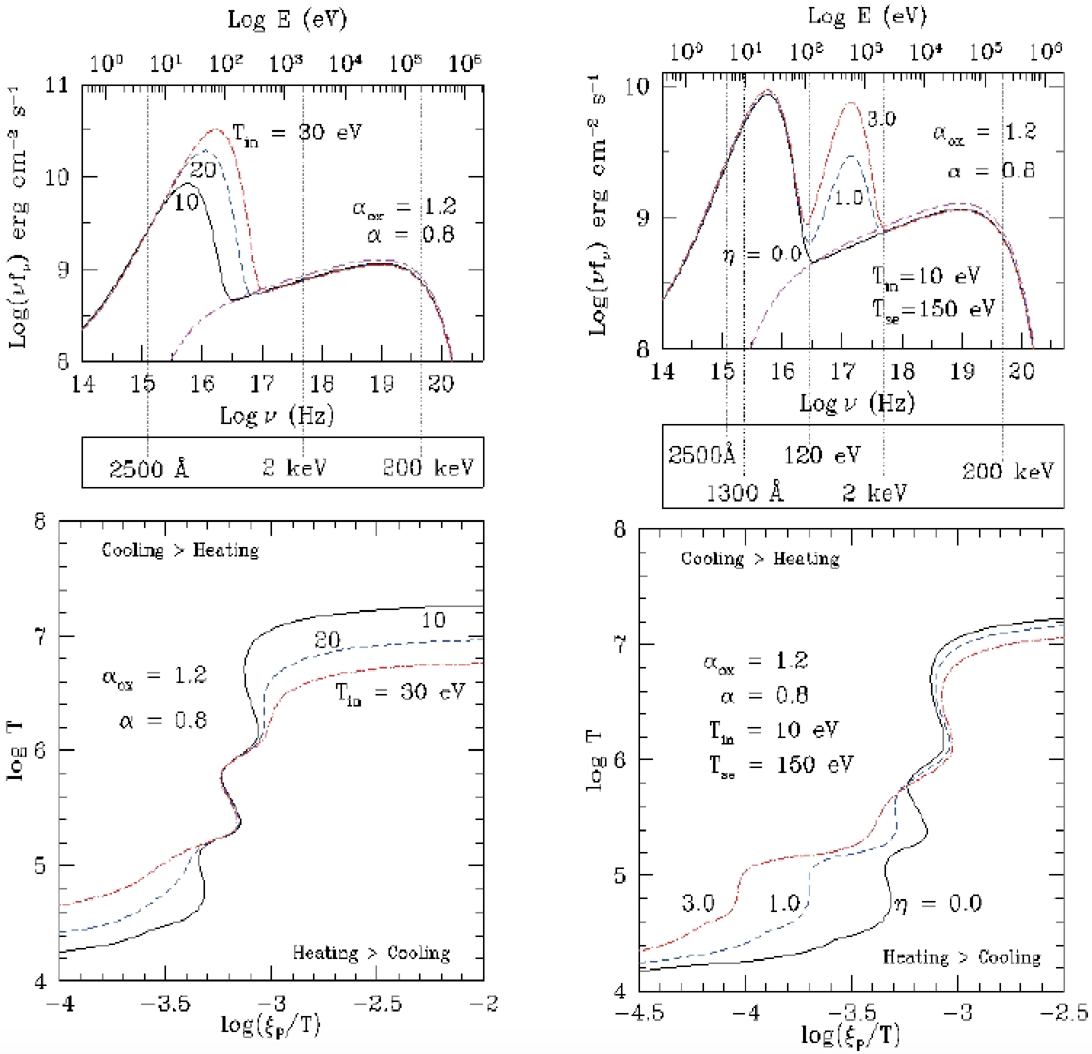

Stability curve

Chakravorty +12, **Different SEDs**

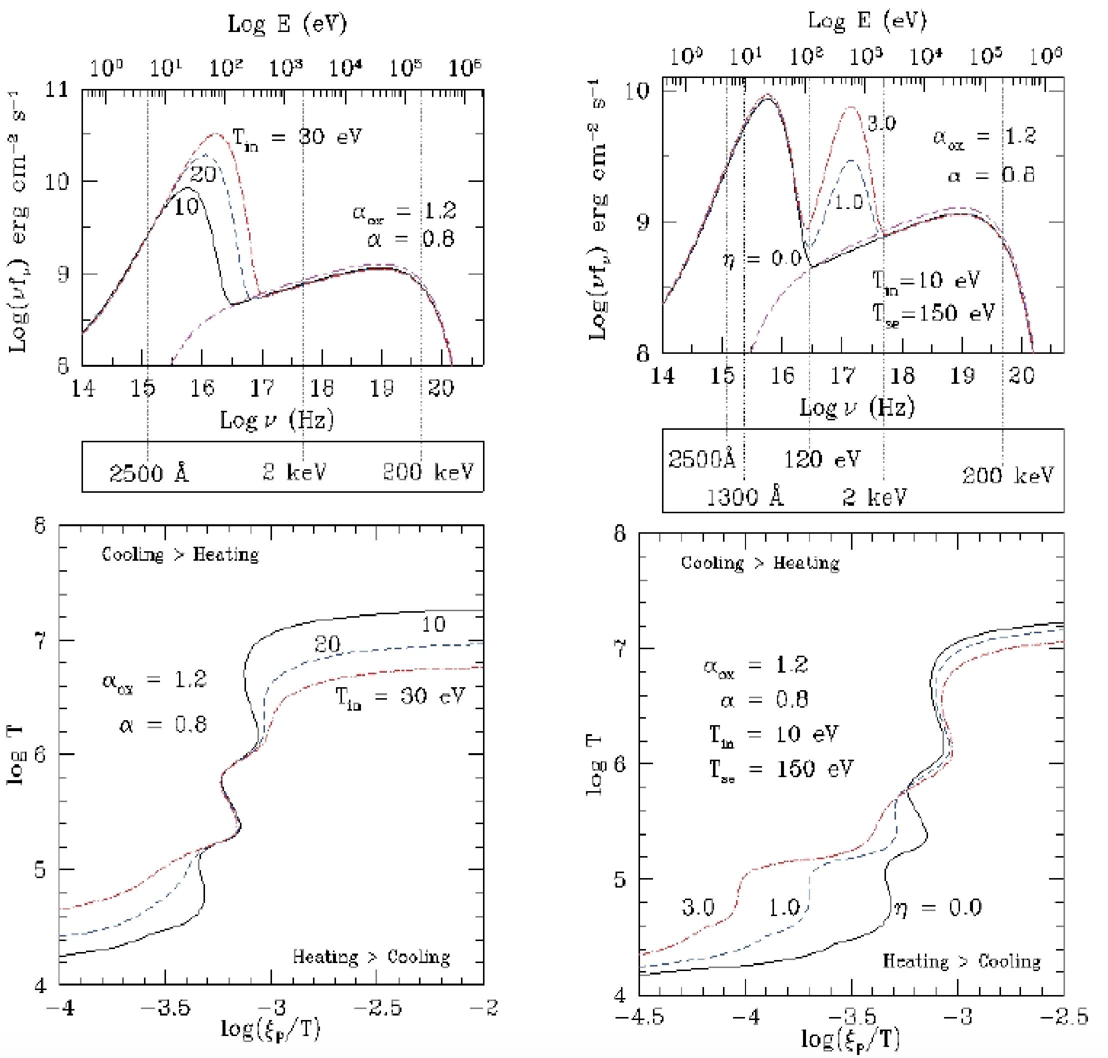

Różańska +08, **Processes**

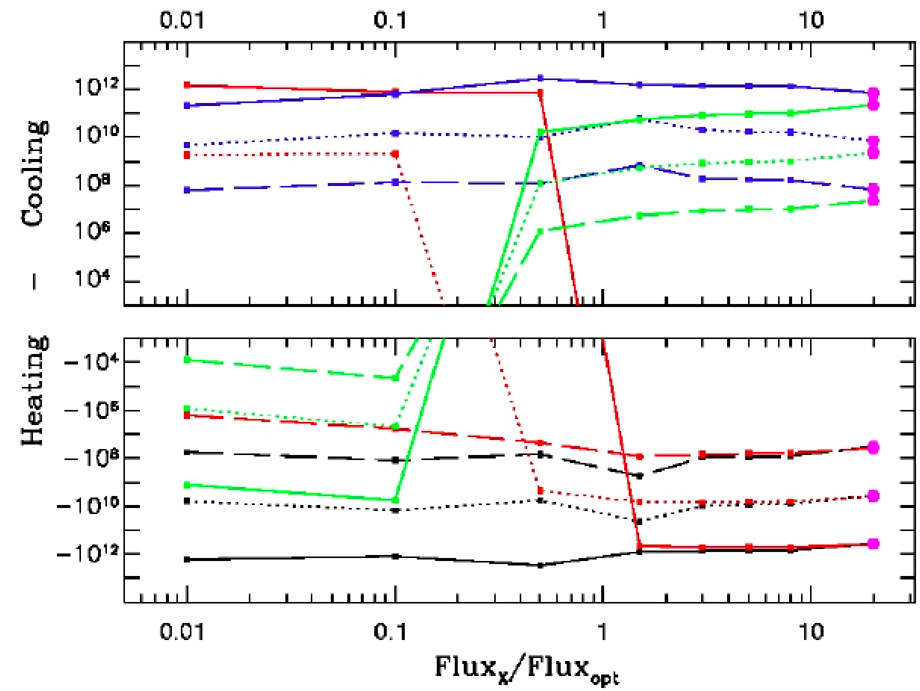

Net bound−free (Ion. − Rec.)

Net free−free (H − C)

Net Compton (H − C)

Net bound−bound (H − C) LINES

Solid line – n = 10^{10} cm^{-3}

Dotted line – n = 10^{8} cm^{-3}

Dashed line – n = 10^{6} cm^{-3}

Questions to the audience

- Do we observe saturated lines in X-ray domain?
- Do we derive AMD for UV absorbers?
- Are we able to distinguish between ***const. P*** and ***const. n*** models from observations?
- Are f-f winds more important than Compton winds?

Stability curve

One constant density component has constant ξ, and it occurs as the point on the stability curve:

NGC 3783, Krongold +03

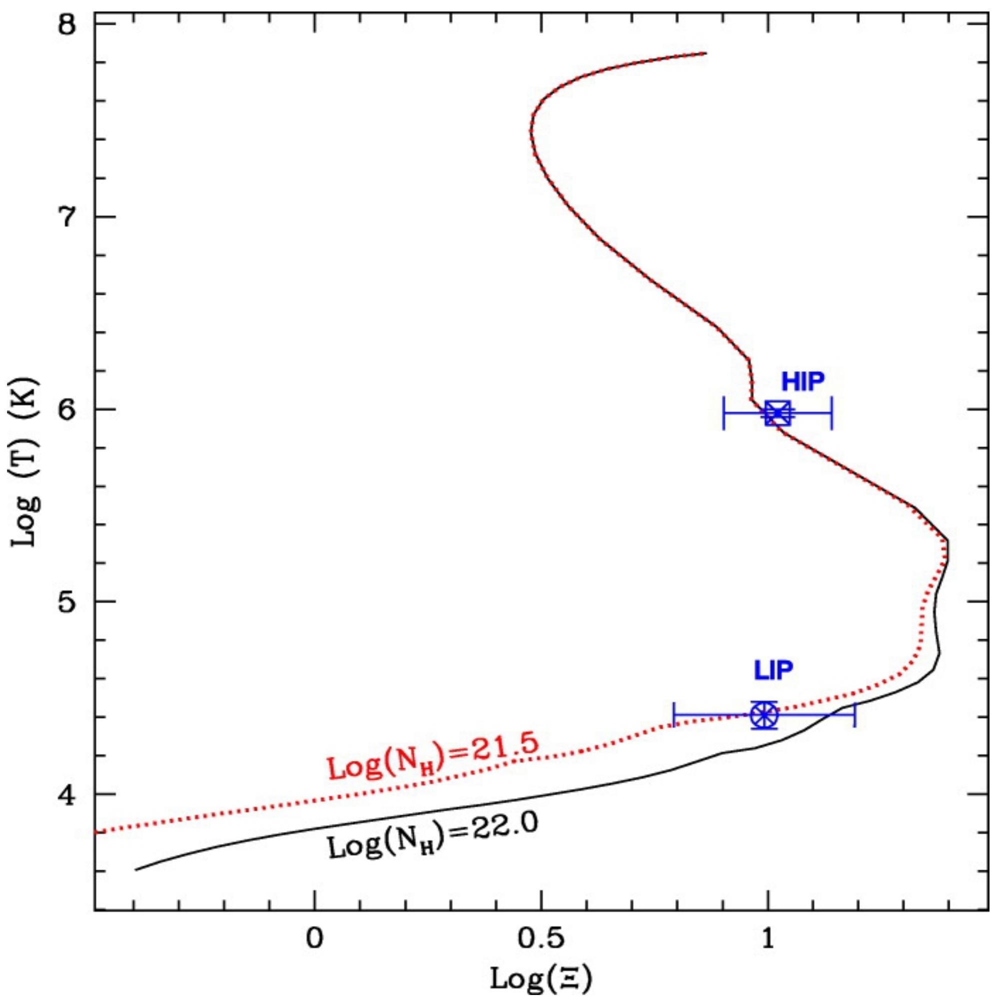

Stability curve

One constant density component has constant ξ, and it occurs as the point on the stability curve:

NGC 5548, Steenbrugge +05

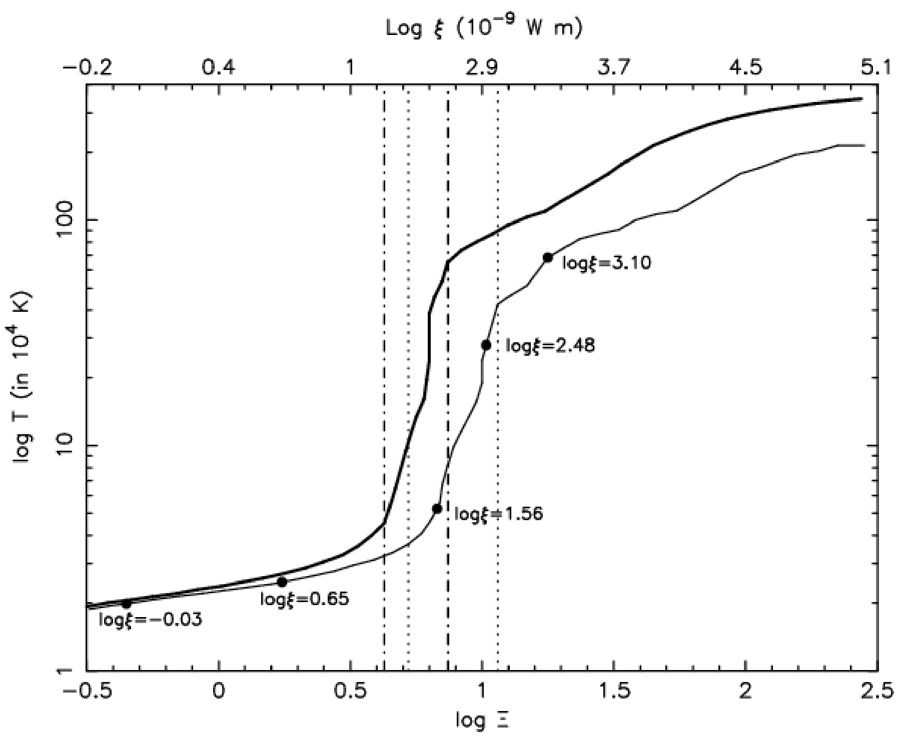

ESO 113-G010, Mehdipour +12

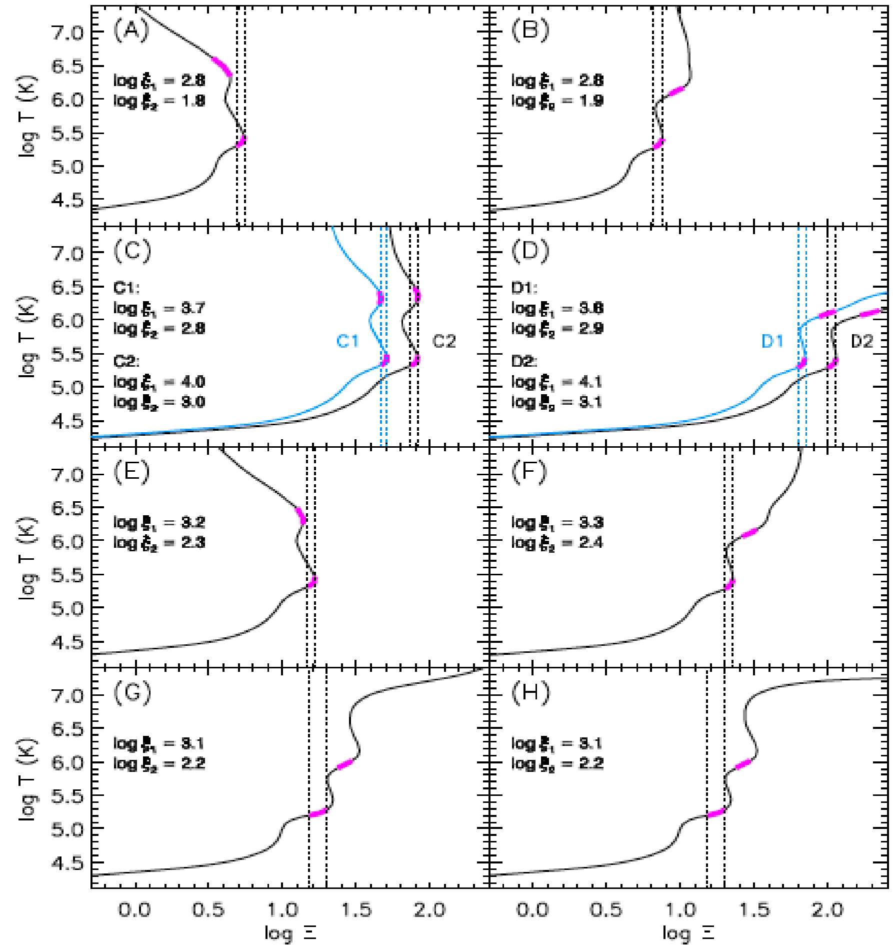

Stability curve

One constant density component has constant ξ, and it occurs as the point on the stability curve:

$$\Xi = \frac{L_{ion}}{4\pi c R^2}\frac{1}{nkT} = \frac{P_{rad}}{P_{gas}}$$

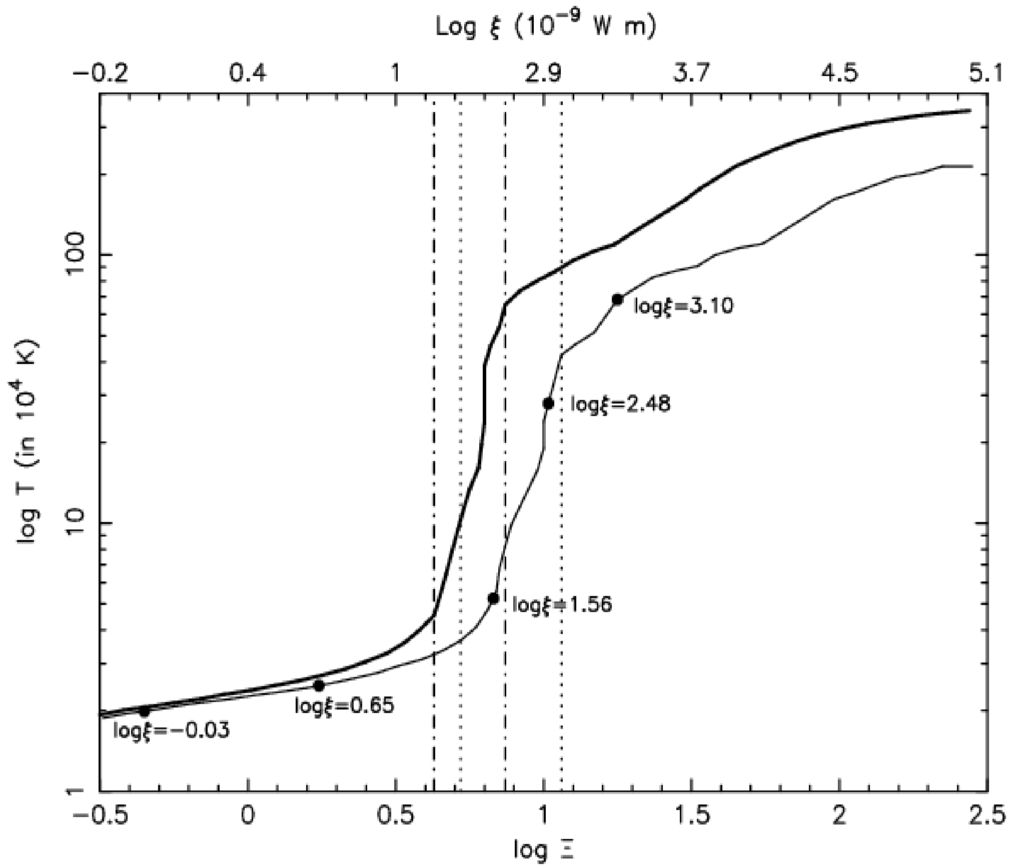

Stability curve

An absorber under constant total pressure, $P_{tot} = P_{rad} + P_{gas}$, solves the pressure structure: $P_{rad}(\tau)$ and $P_{gas}(\tau)$, and the whole stability curve is computed:

$$\Xi = \frac{P_{rad}(\tau)}{P_{gas}(\tau)}$$

SED dominated
by soft component

HS 1603+3820, Różańska +12

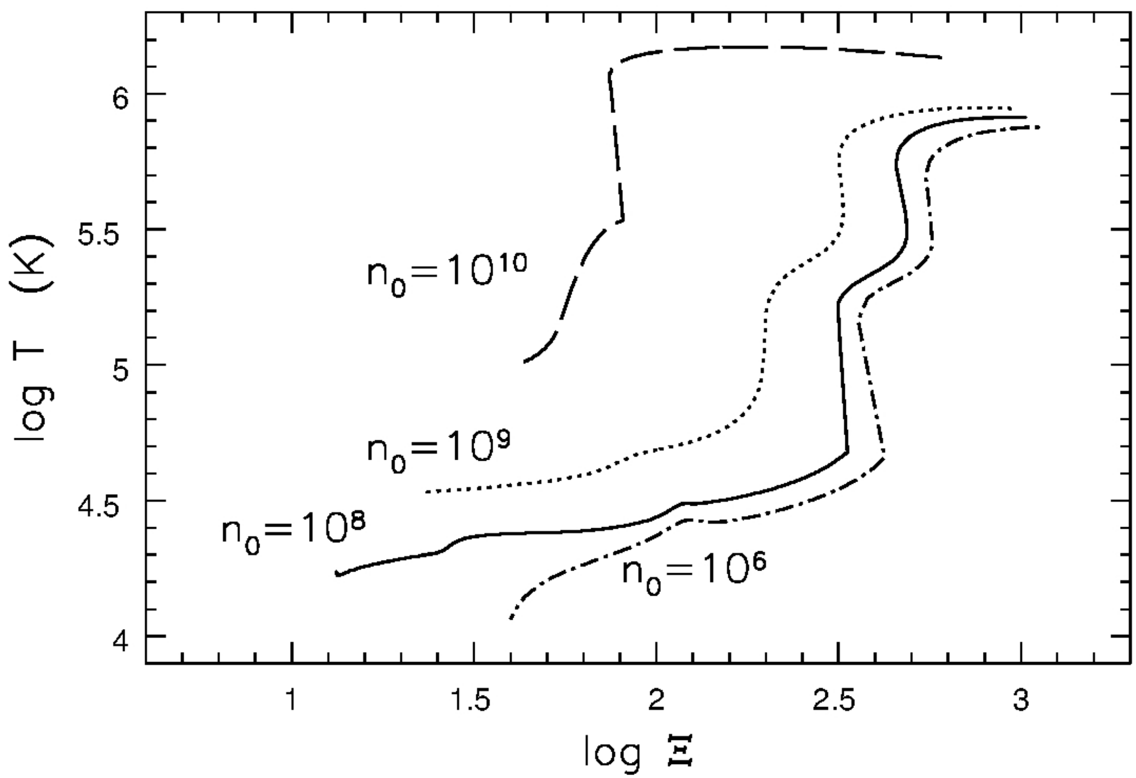

Conclusions:

- The fact that the photoionization models give the same results for broad range of densities is only valid for strong X-ray illumination, and weak optical/UV SED component.

High luminosity quasar, M_{BH}=5.26 x 10^9 M_{Sun}

HS 1603+3820, Różańska +12

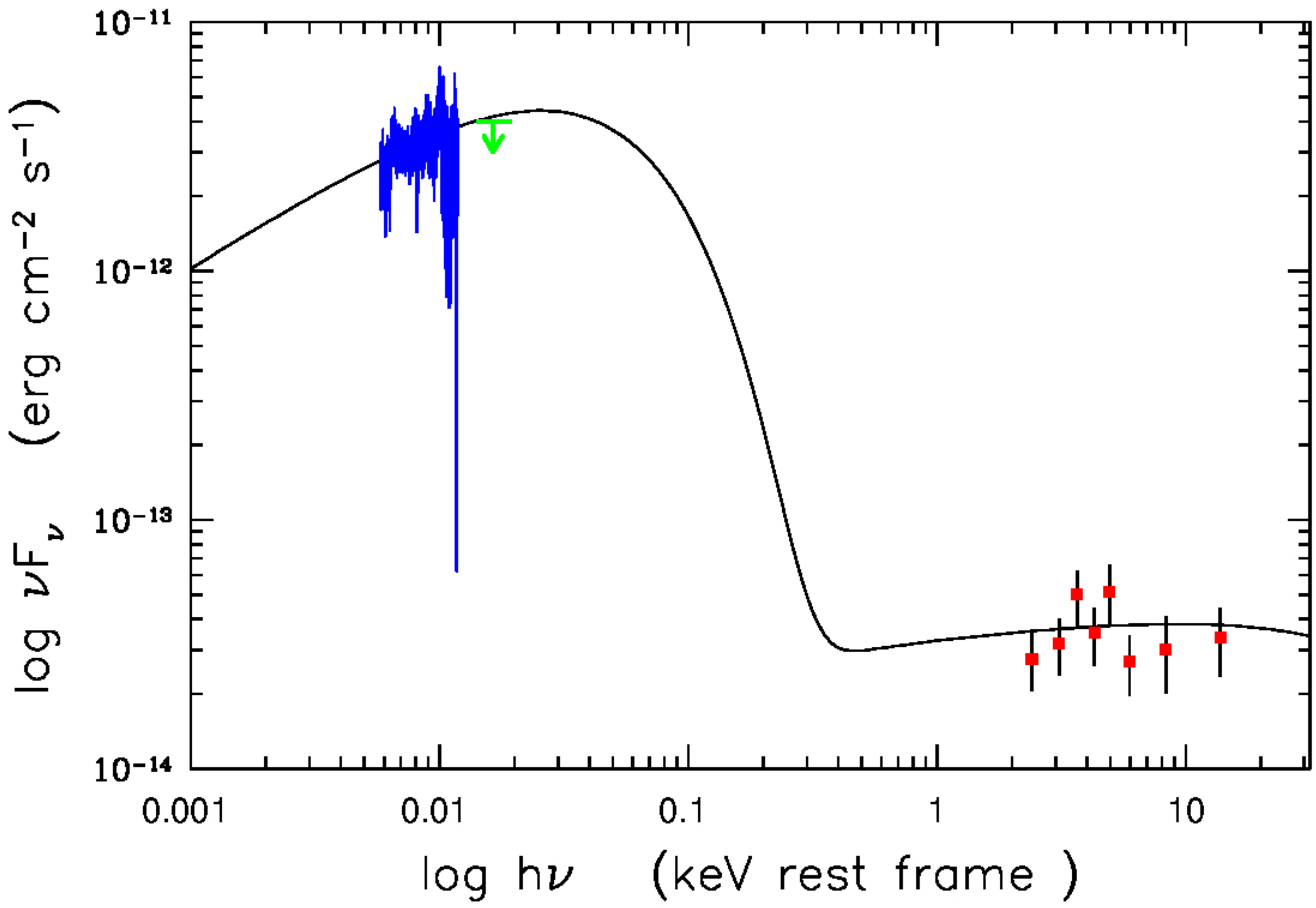

High luminosity quasar, M_{BH}=5.26 x 10^9 M_{Sun}

HS 1603+3820, Różańska +12

Par.	Unit	CLOUDY	TITAN
ξ	[erg s^{-1} cm^{-1}]	7	10^4
n_0	[cm^{-3}]	10^{12}	10^{10}
E^{UV}_{max}	[eV]	10	40
$\log(N_{CIV})$	[cm^{-2}]	14.97	14.71
N_{CIV}/N_{HI}		20.37	19.70
$L_{bol} = 7.7$	$\times 10^{47}$ [erg s^{-1}]	This paper	
log (R)	[cm]	17.52	16.94
R	[pc]	0.106	0.028

NLS1, Leighly +04

Radiation pressure

All clouds computed by TITAN code for ionized absorber are dominated by radiation pressure. Agrees with Stern +16

Różańska +08, **Double power-law SED with exp. cut-off**

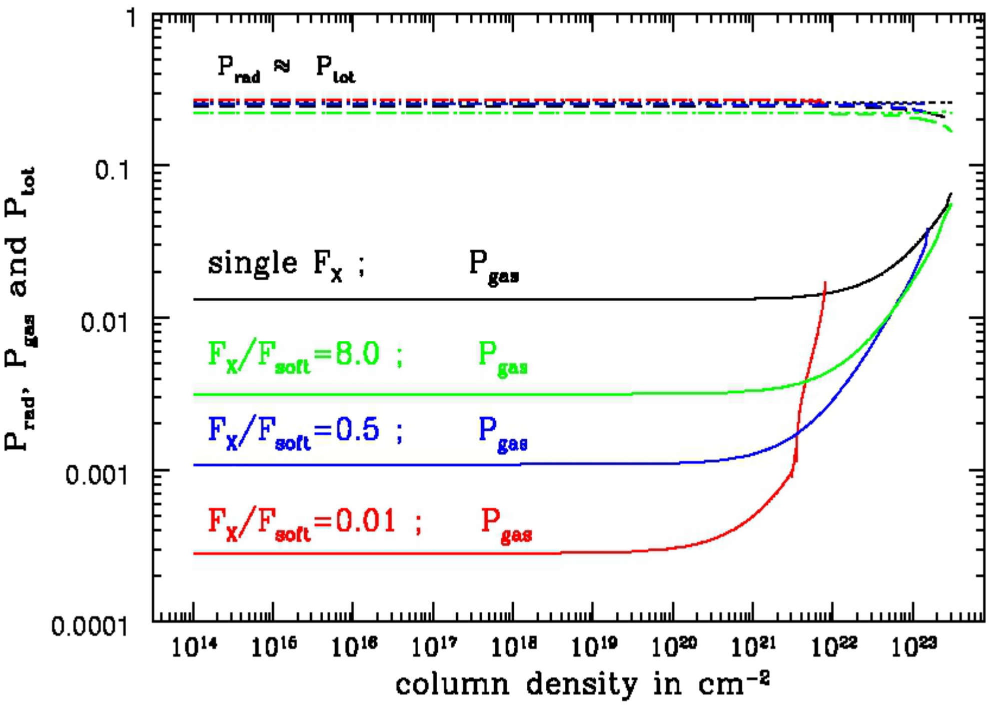

$n_0 = 10^6$ cm^{-3}, $\xi = 10^5$

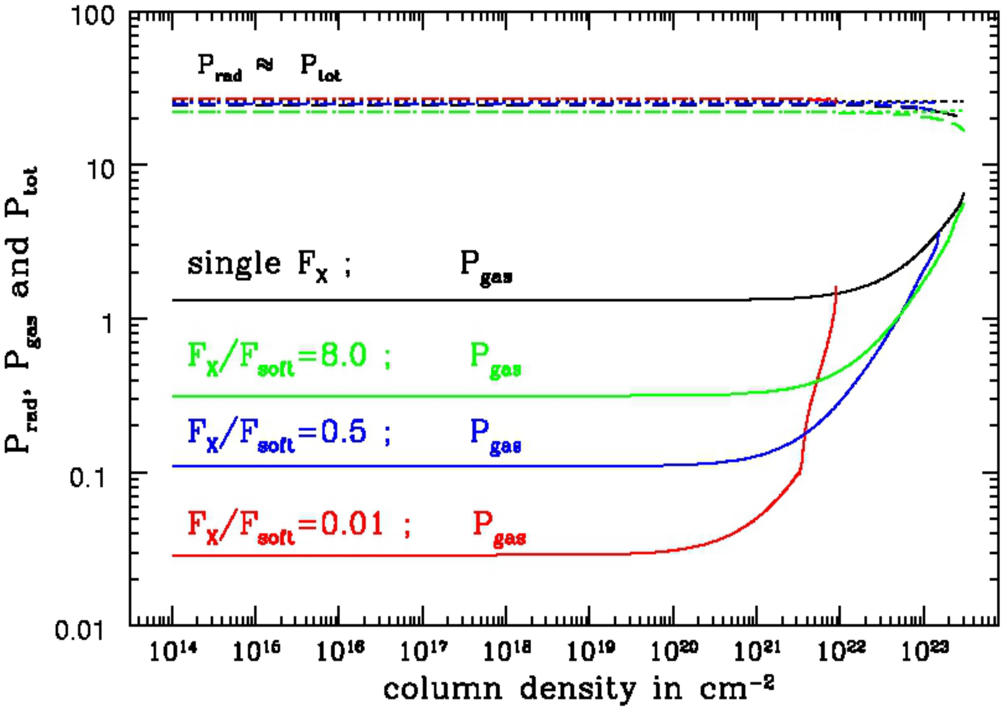

$n_0 = 10^8$ cm^{-3}, $\xi = 10^5$

Conclusions:

- The fact that the photoionization models give the same results for broad range of densities is only valid for strong X-ray illumination, and weak optical/UV SED component.

- The radiation pressure is dominant in the vicinity of BH.

Equivalenth Hydrogen column densities, ion by ion

NGC 5548, Steenbrugge +05

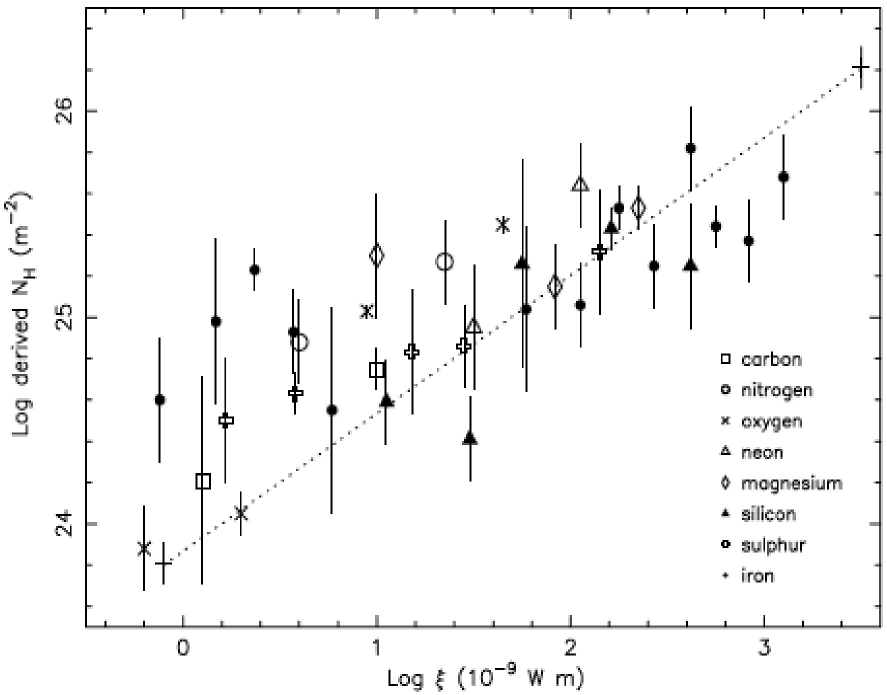

Fig. 11. The total hydrogen column density N_H, assuming solar abun dances (Anders & Grevesse 1989) derived using Eq. (3), plotted ver sus ionization parameter. The ionic column densities were taken fron Tables 4 and A.1 assuming a velocity broadening of 140 km s^{-1}. Fo clarity, no upper limits have been plotted. The best fit results fo model D are plotted as the two crosses connected by a dotted line.

Mrk 273, Costantini +07

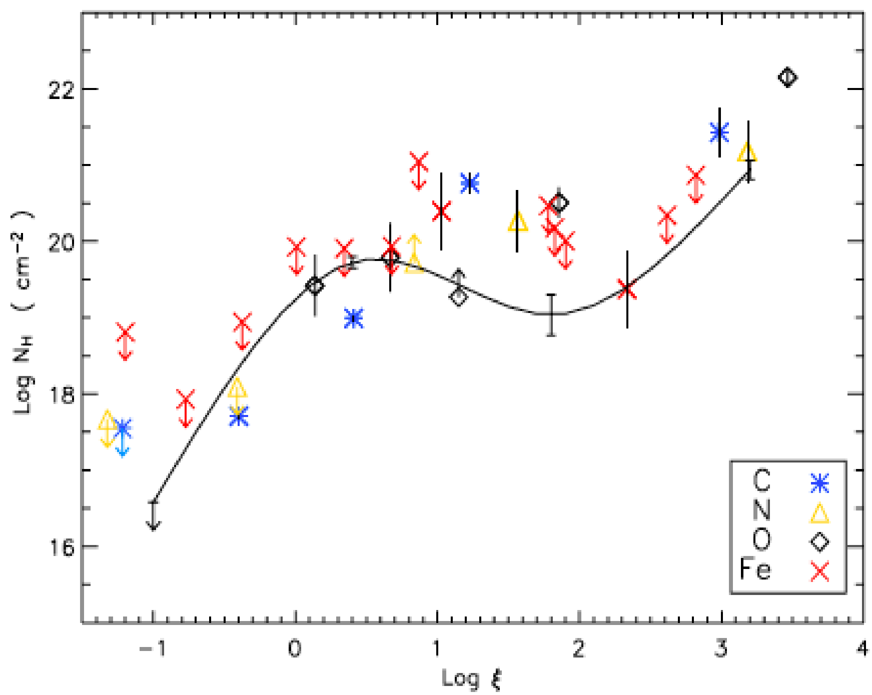

Fig. 10. The hydrogen column density as a function of the ionization parameter determined for: single ions (individual points) and an N_H continuous distribution model (solid line). See Sect. 2.4.2 for a full description.

Equivalenth Hydrogen column densities, ion by ion

Holczer +07

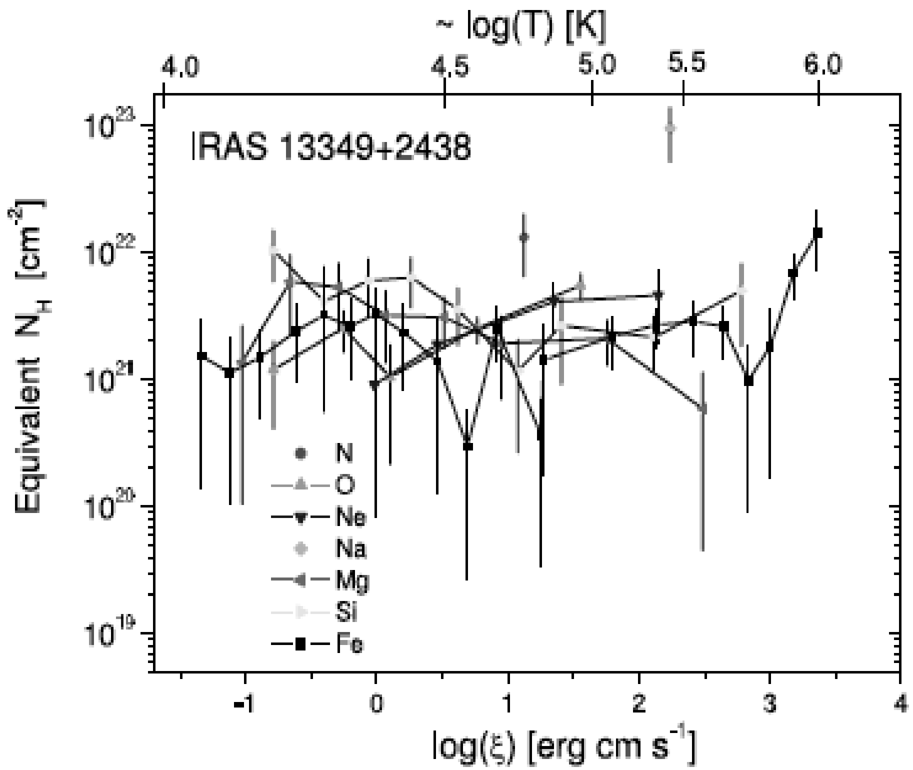

FIG. 4.—Equivalent N_H distribution (eq. [8]) obtained for the IRAS 13349+2438 outflow, assuming that ions form at ξ_{max} and assuming solar abundances (Asplund et al. 2005). Lines are drawn between data points to guide the eye. Vertical offsets between elements indicate deviations from solar abundances. The corresponding temperature scale obtained from the XSTAR computation is shown at the top of the figure. [*See the electronic edition of the Journal for a color version of this figure.*]

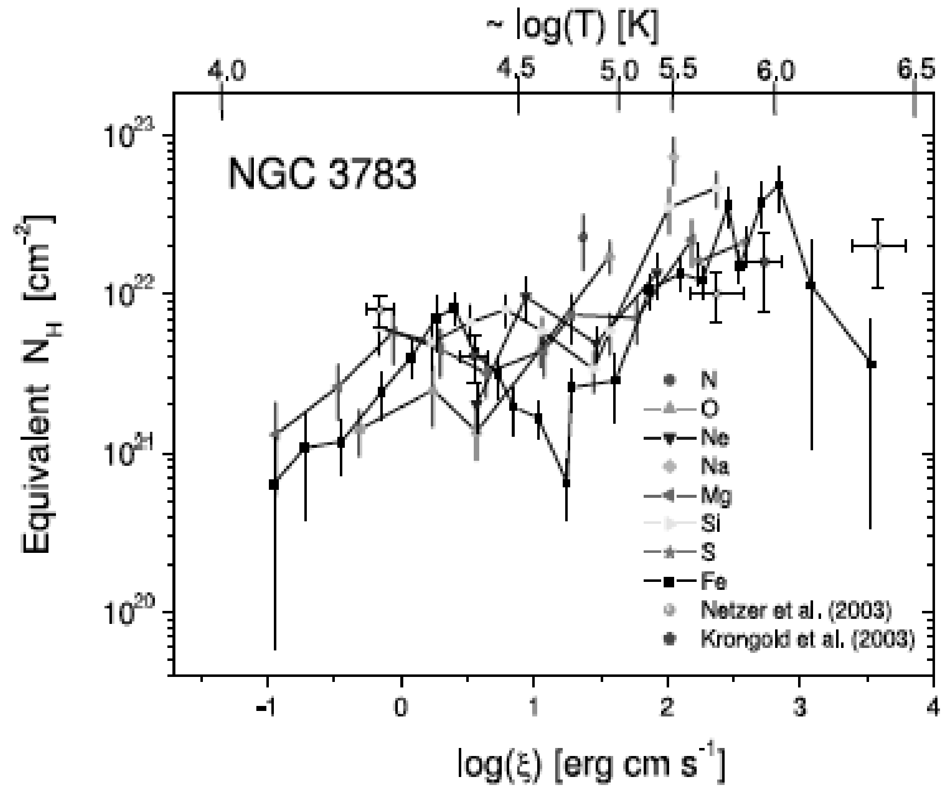

FIG. 6.—Equivalent N_H distribution (eq. [8]) obtained for the NGC 3783 outflow, assuming that ions form at ξ_{max} and assuming solar abundances (Asplund et al. 2005). Lines are drawn between data points to guide the eye. Vertical offsets between elements indicate deviations from solar abundances. The corresponding temperature scale obtained from the XSTAR computation is shown at the top of the figure. The Netzer et al. (2003) three-component model results and the Krongold et al. (2003) two-component model results are plotted for comparison. [*See the electronic edition of the Journal for a color version of this figure.*]

Absorption measure distribution

Holczer +07, **constant density slabs**

AMD is: $\xi \frac{dN_H}{d\xi}$ vs. $\log(\xi)$

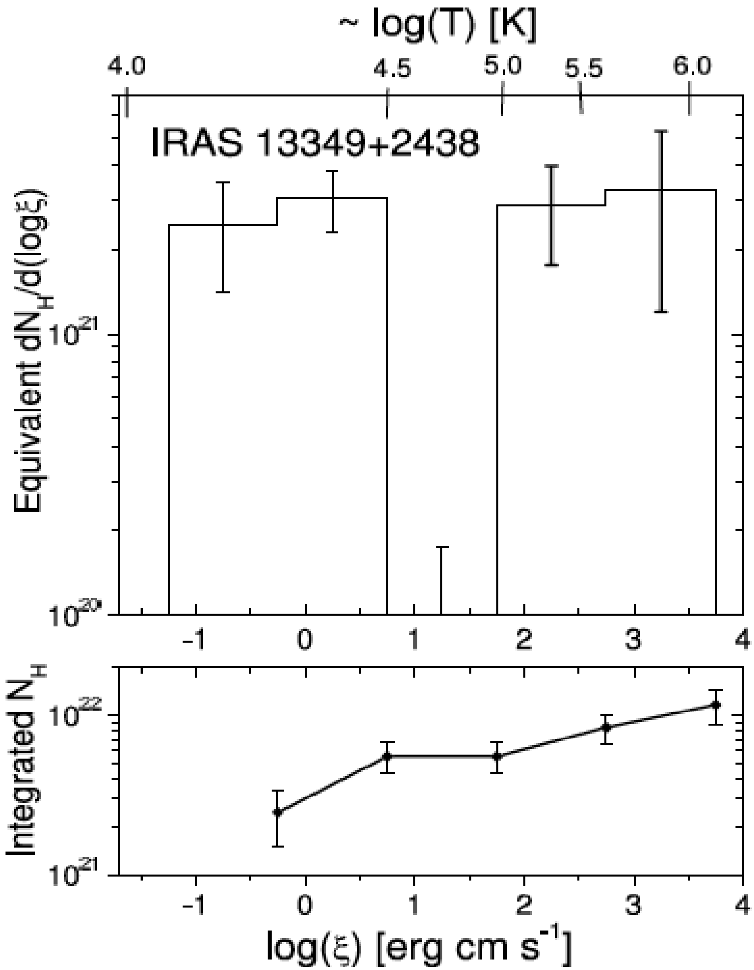

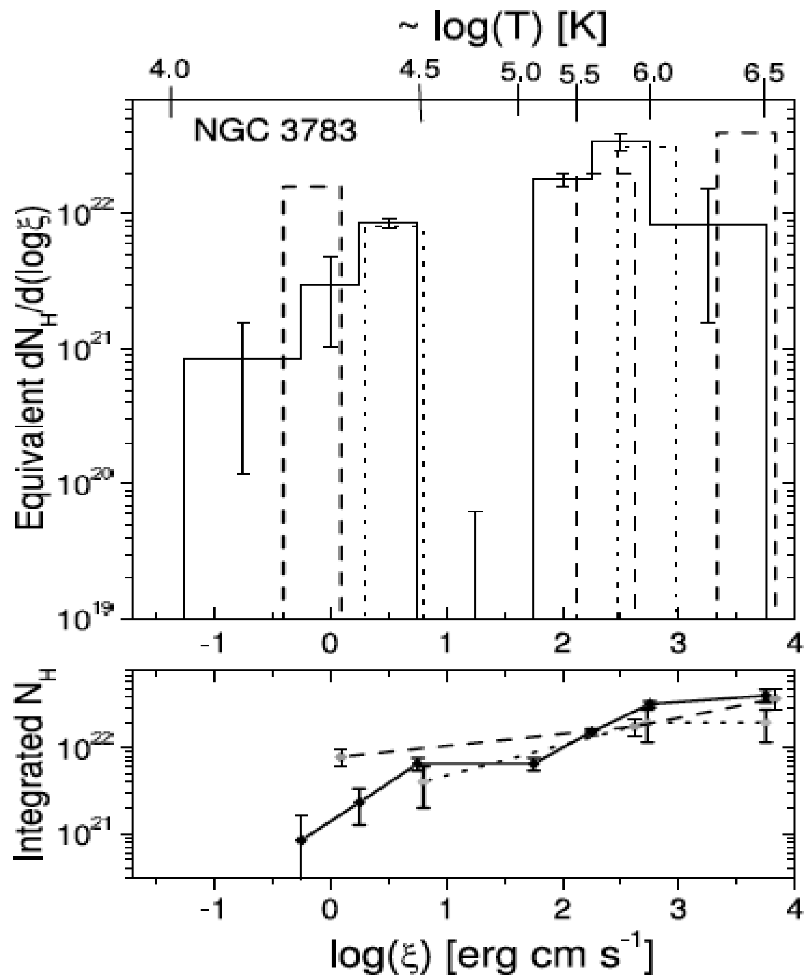

Observed AMD

Stern +14

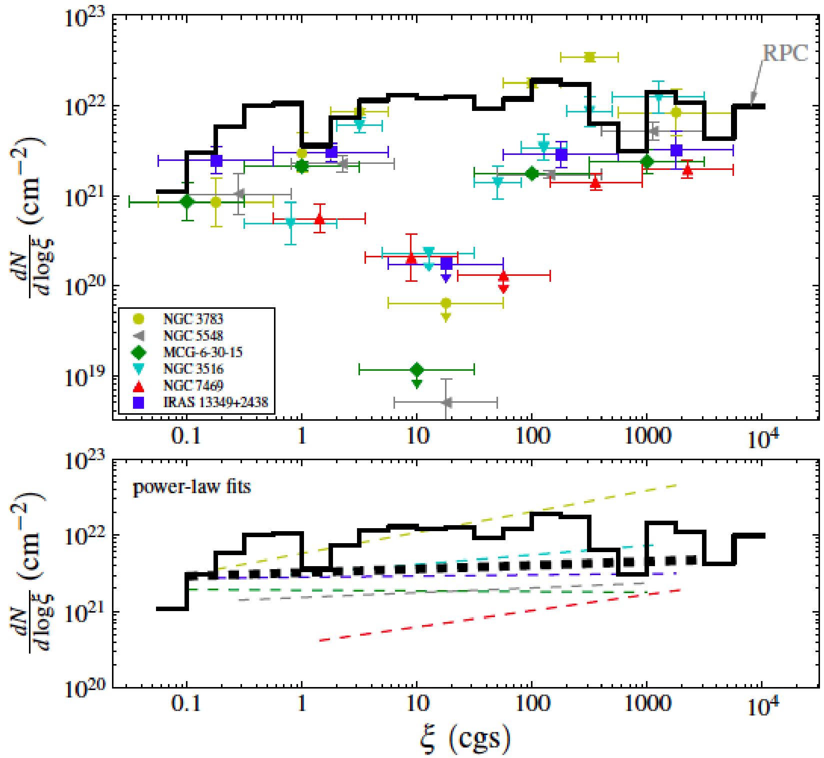

Behar +09

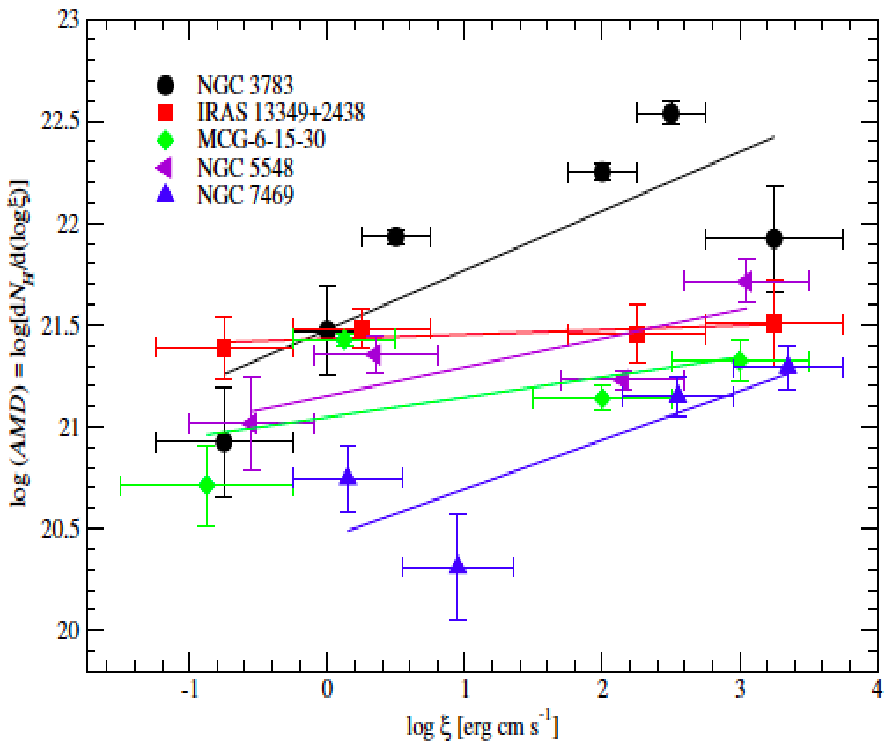

Observed AMD modelled by CLOUDY

Stern +14, **constant pressure slabs**

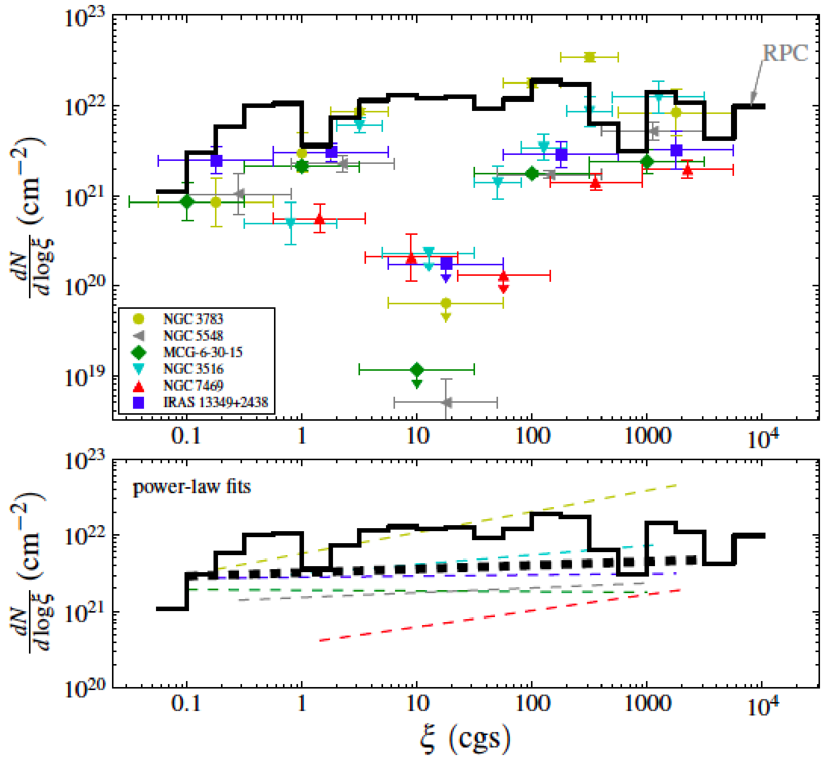

- Radiation Pressure Confinement

$$dP_{gas}(\tau) = P_{rad}\, e^{-\tau}\, d\tau$$

Observed AMD modelled by CLOUDY

Stern +14, **constant pressure slabs**

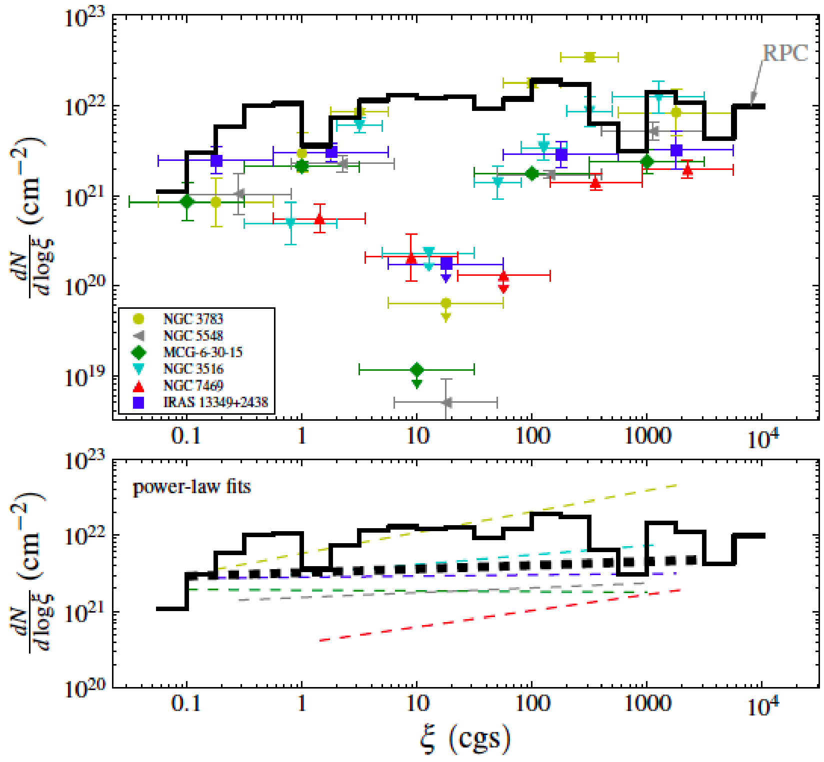

- Radiation Pressure Confinement

$$dP_{gas}(\tau) = P_{rad}\, e^{-\tau}\, d\tau$$

- CLOUDY computations under constant pressure

$$P_{gas}(\tau = 0) = const$$

Observed AMD modelled by CLOUDY

Stern +14, **constant pressure slabs**

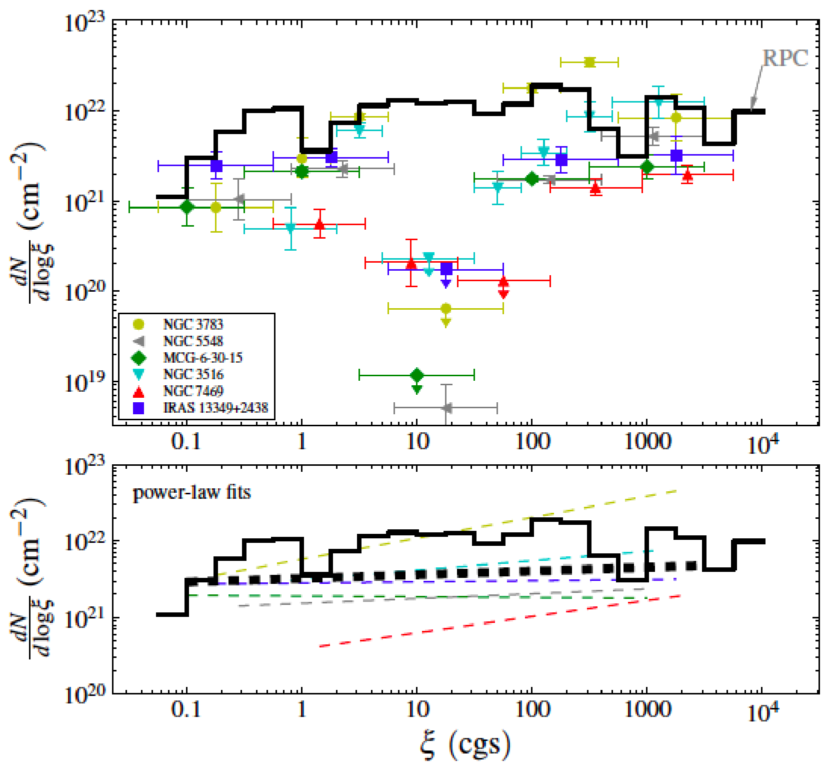

- Radiation Pressure Confinement

$$dP_{gas}(\tau) = P_{rad} e^{-\tau} d\tau$$

- CLOUDY computations under constant pressure

$$P_{gas}(\tau = 0) = const$$

- AMD deep structure is not reconstructed by the model

Radiation pressure in TITAN

$$\mu \frac{dI_\nu}{d\tau_\nu} = I_\nu - \frac{j_\nu}{\kappa_\nu + \sigma_\nu} = I_\nu - S_\nu$$

Emission coefficient j_ν is the sum of three terms, $j_\nu = j_\nu^{th} + j_\nu^{sc} + j_\nu^{fl}$.

Requires iteration with gas(X,Y,Z) structure due to equilibrium equations:

- Hydrostatic equil. => $\frac{dP}{dz}$
- Radiative equil. => $\frac{dT}{dz}$
- EoS - usually ideal gas

Radiation pressure in TITAN

$$\mu \frac{dI_\nu}{d\tau_\nu} = I_\nu - \frac{j_\nu}{\kappa_\nu + \sigma_\nu} = I_\nu - S_\nu$$

Emission coefficient j_ν is the sum of three terms, $j_\nu = j_\nu^{th} + j_\nu^{sc} + j_\nu^{fl}$.

Requires iteration with gas(X,Y,Z) structure due to equilibrium equations:

- Hydrostatic equil. => $\frac{dP}{dz}$
- Radiative equil. => $\frac{dT}{dz}$
- EoS - usually ideal gas

Radiation pressure is computed from the radiation field and goes into the gas structure directly.

Observed AMD modelled by TITAN

Adhikari +15, **constant pressure single model**

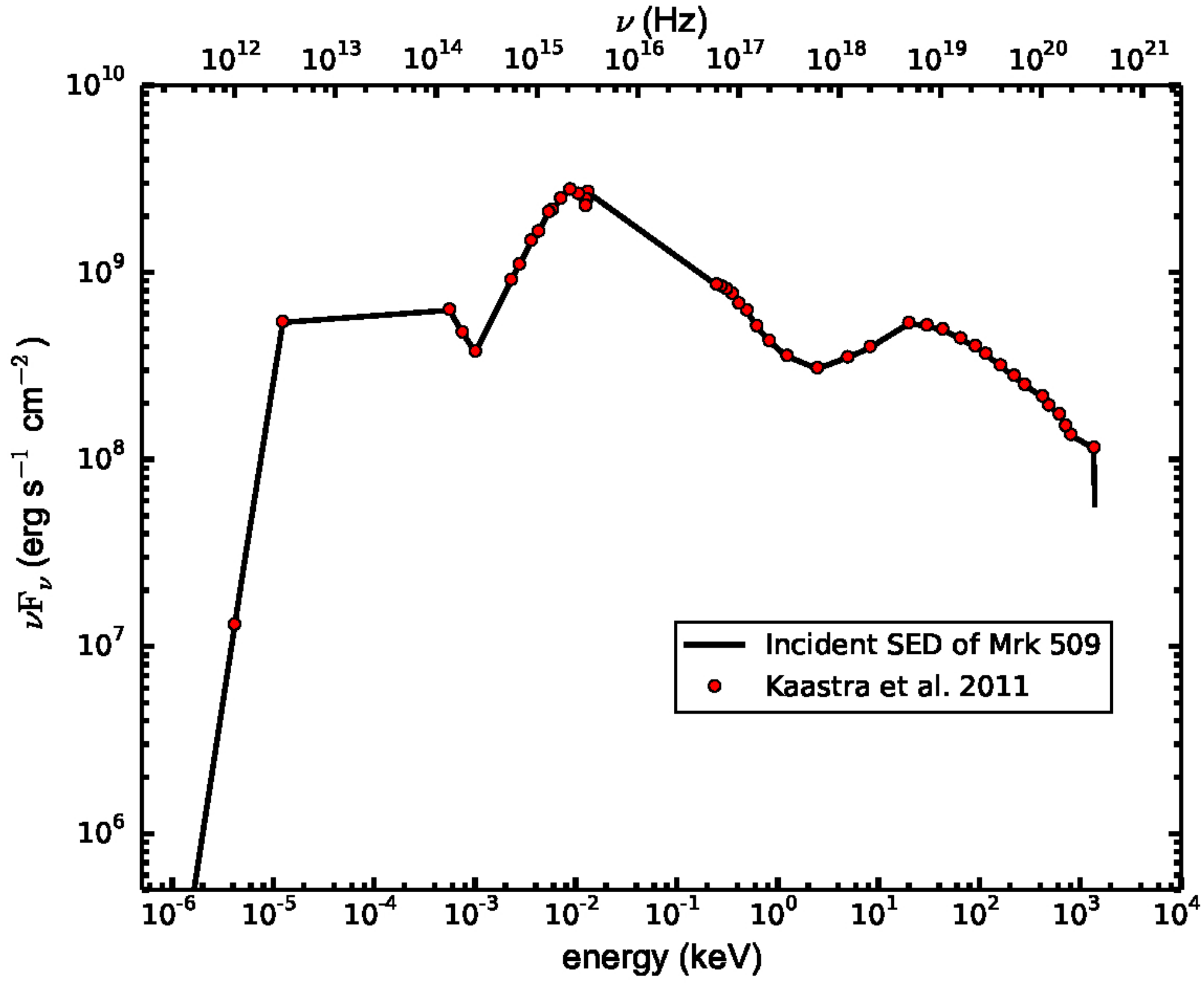

Observed AMD modelled by TITAN

Adhikari +15, **constant pressure single model**

const. n

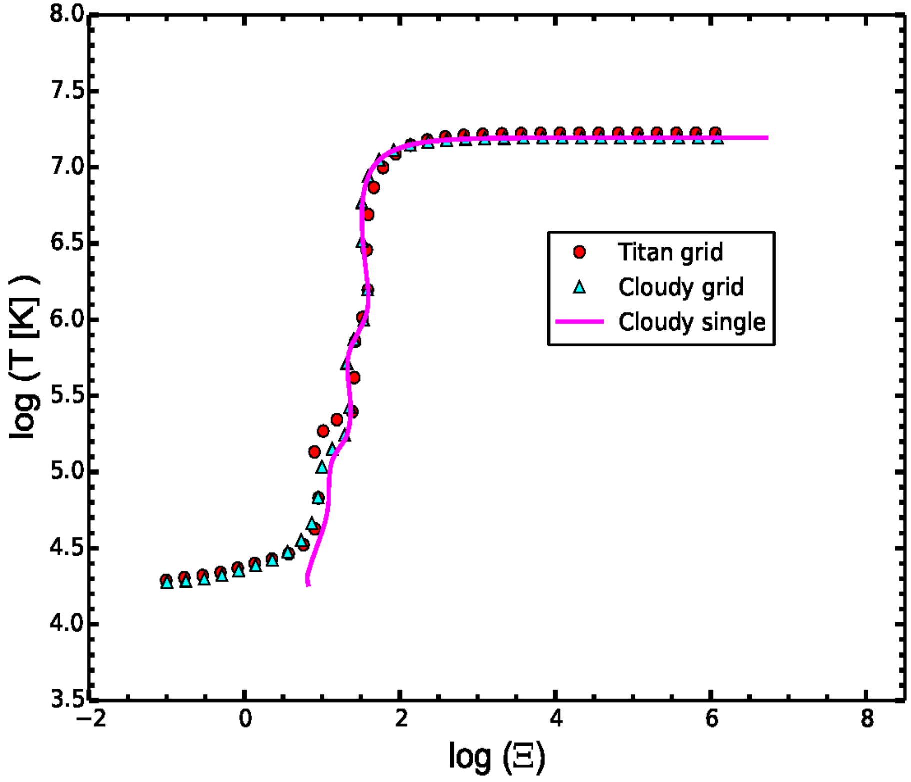

CLOUDY:

$$\Xi = \frac{L_{ion}}{4\pi c R^2} \frac{1}{nkT}$$

Observed AMD modelled by TITAN

Adhikari +15, **constant pressure single model**

const. n

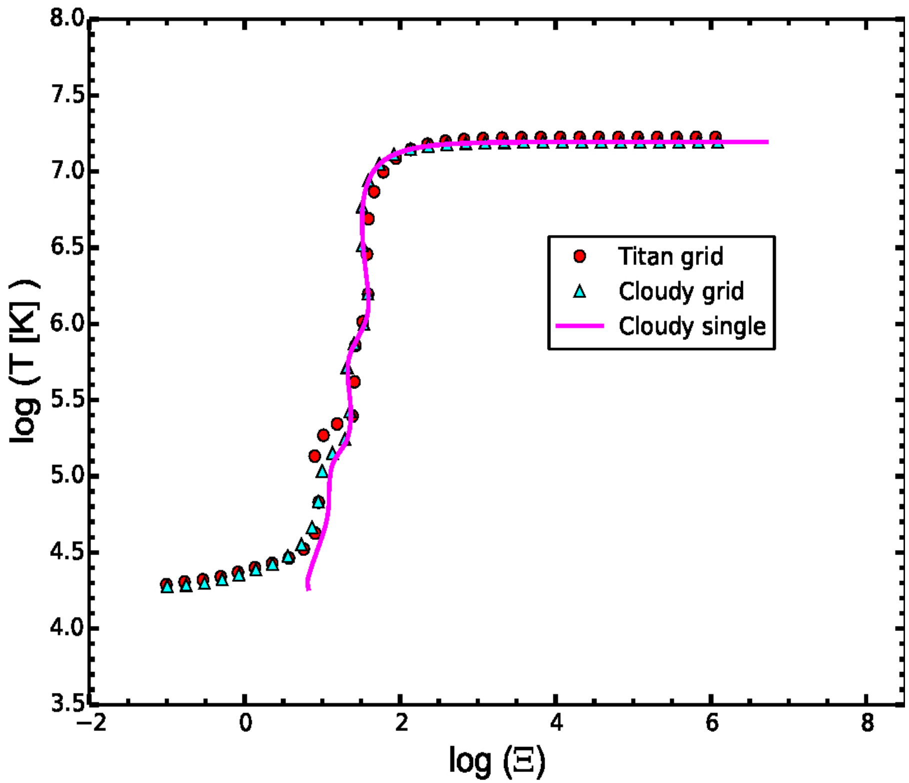

const. P

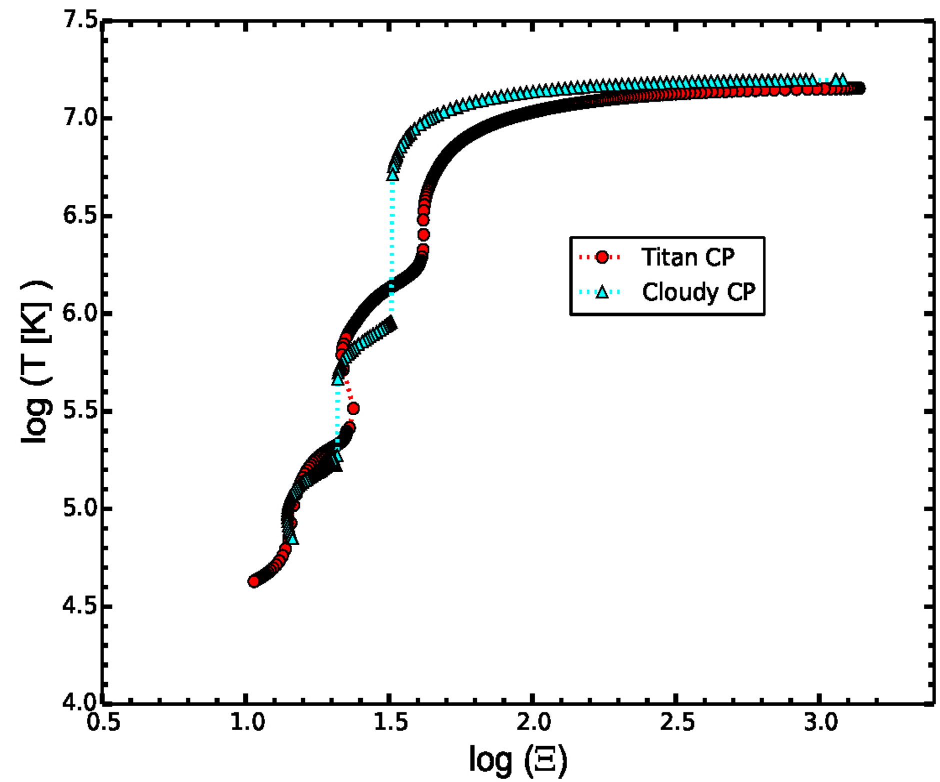

CLOUDY:

$$\Xi = \frac{L_{ion}}{4\pi c R^2} \frac{1}{nkT}$$

TITAN:

$$\Xi = \frac{P_{rad}(\tau)}{P_{gas}(\tau)}$$

Thermal instability in transition layer between disk and corona

Różańska +96, **CLOUDY cooling and heating**

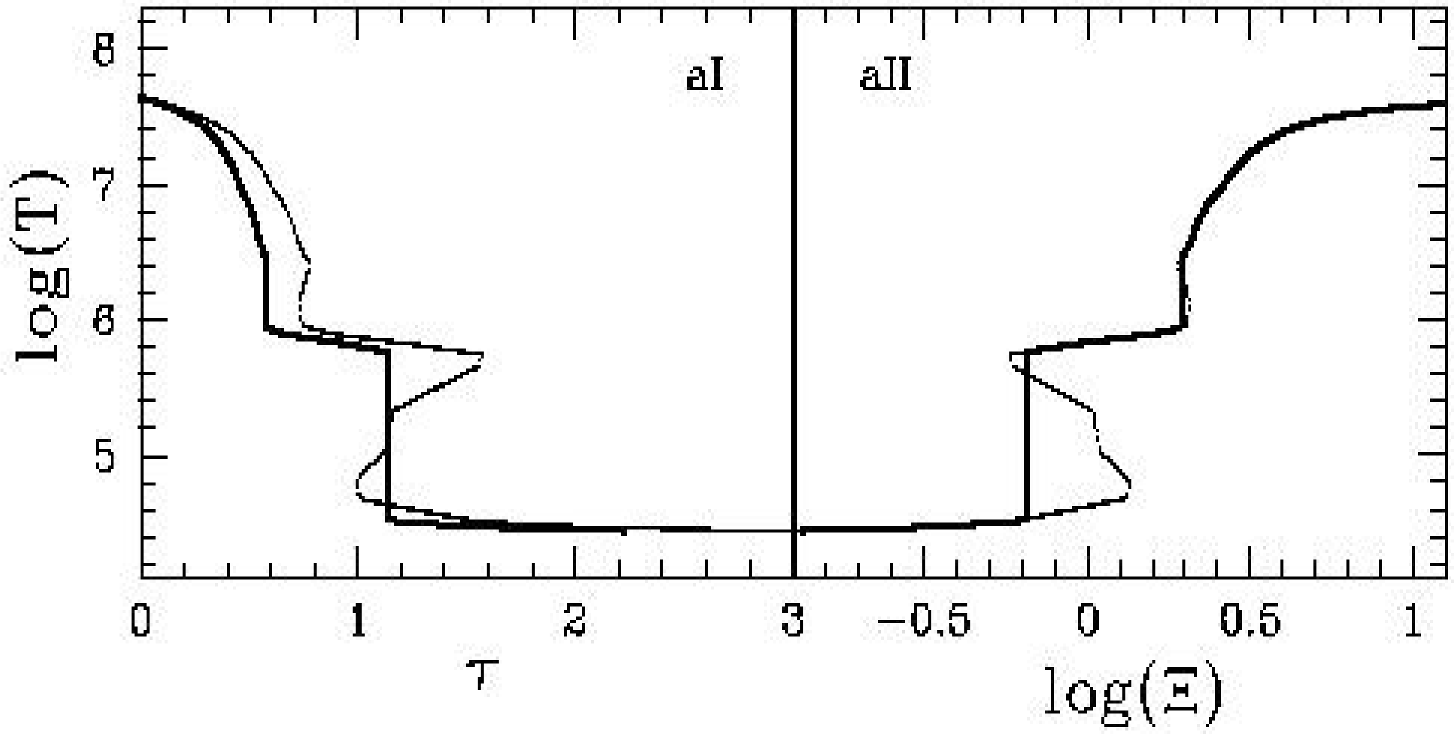

The disk in hydrostatic equillibrium

Conclusions:

- The fact that the photoionization models give the same results for broad range of densities is only valid for strong X-ray illumination, and weak optical/UV SED component.
- The radiation pressure is dominant in the vicinity of BH.
- Thermal Instability occurs only when hydrostatic equilibrium is solved.

Thermal instability in illuminated disk

The transition layer between an accretion disk and corona:

Nayakshin et al. 2000

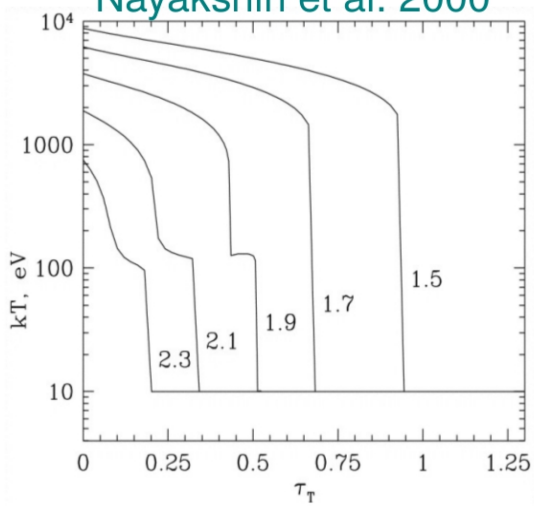

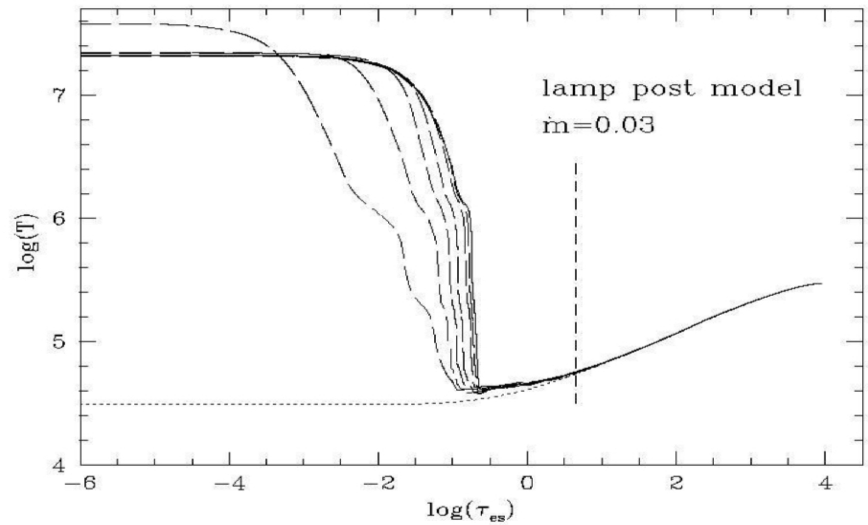

Ballantyne et al. 2001

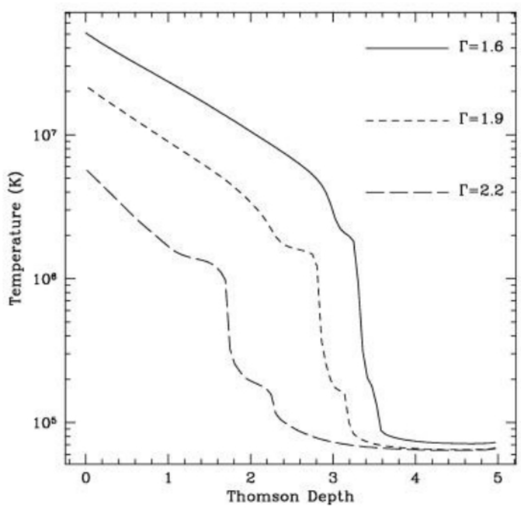

TITAN , Różańska et al 2002

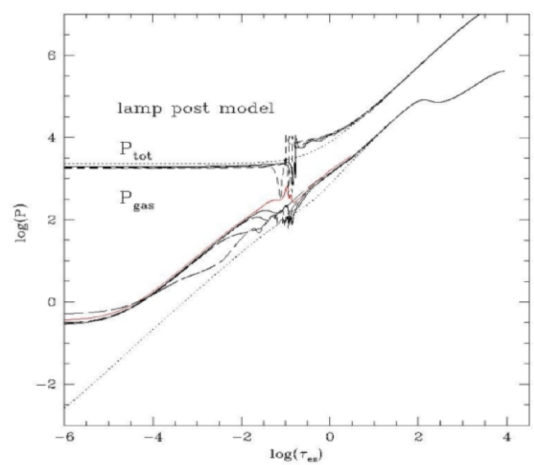

Thermal instability in illuminated disk

The transition layer between an accretion disk and corona:

Comparing of work by: Nayakshin, Ballantyne and **TITAN** :

non-LTE,
external illumination
900 atomic
bound-bound
transitions.

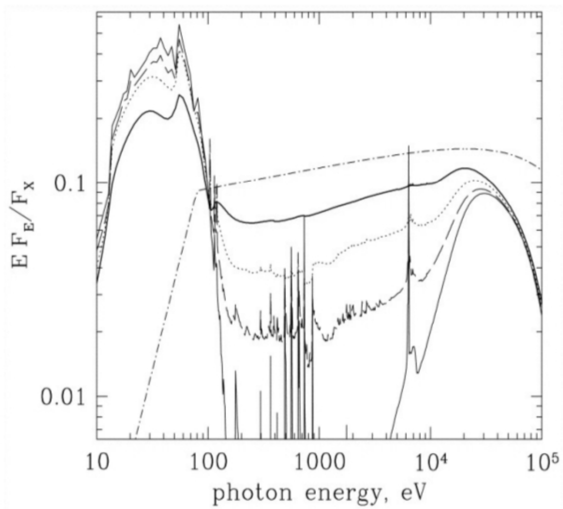

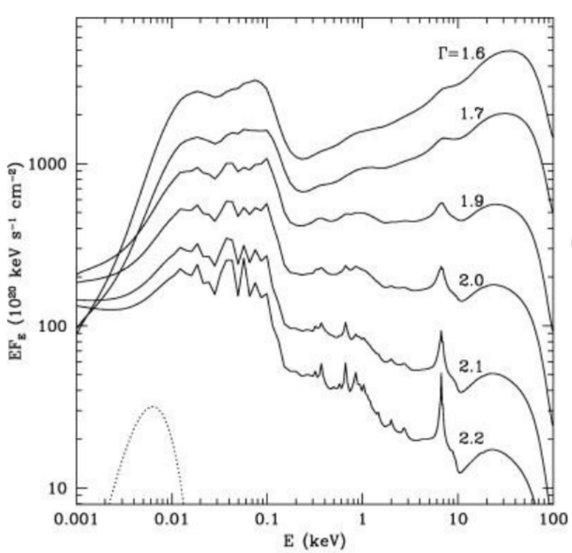

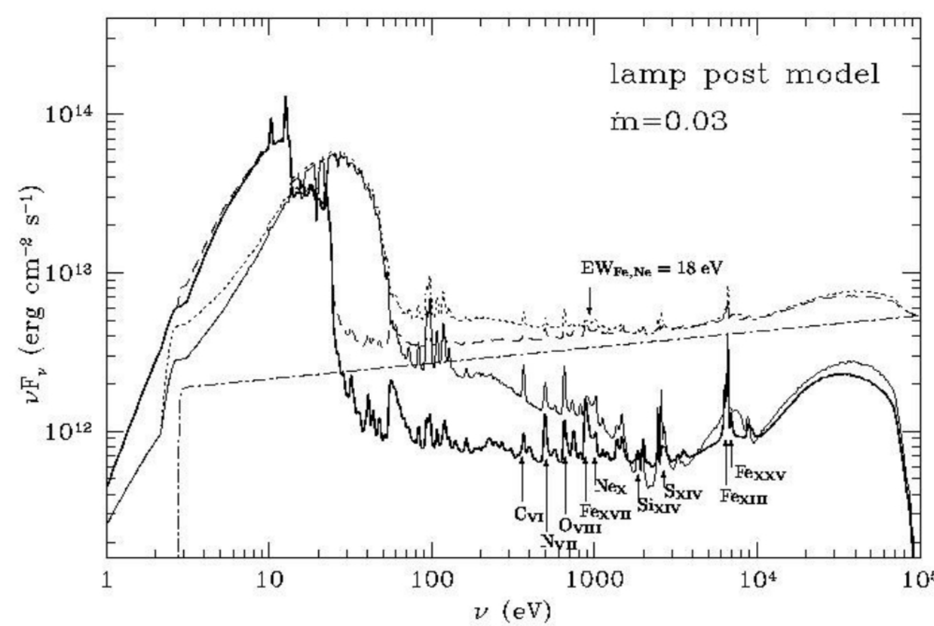

Observed AMD modelled by TITAN

Adhikari +15, **constant pressure single model**

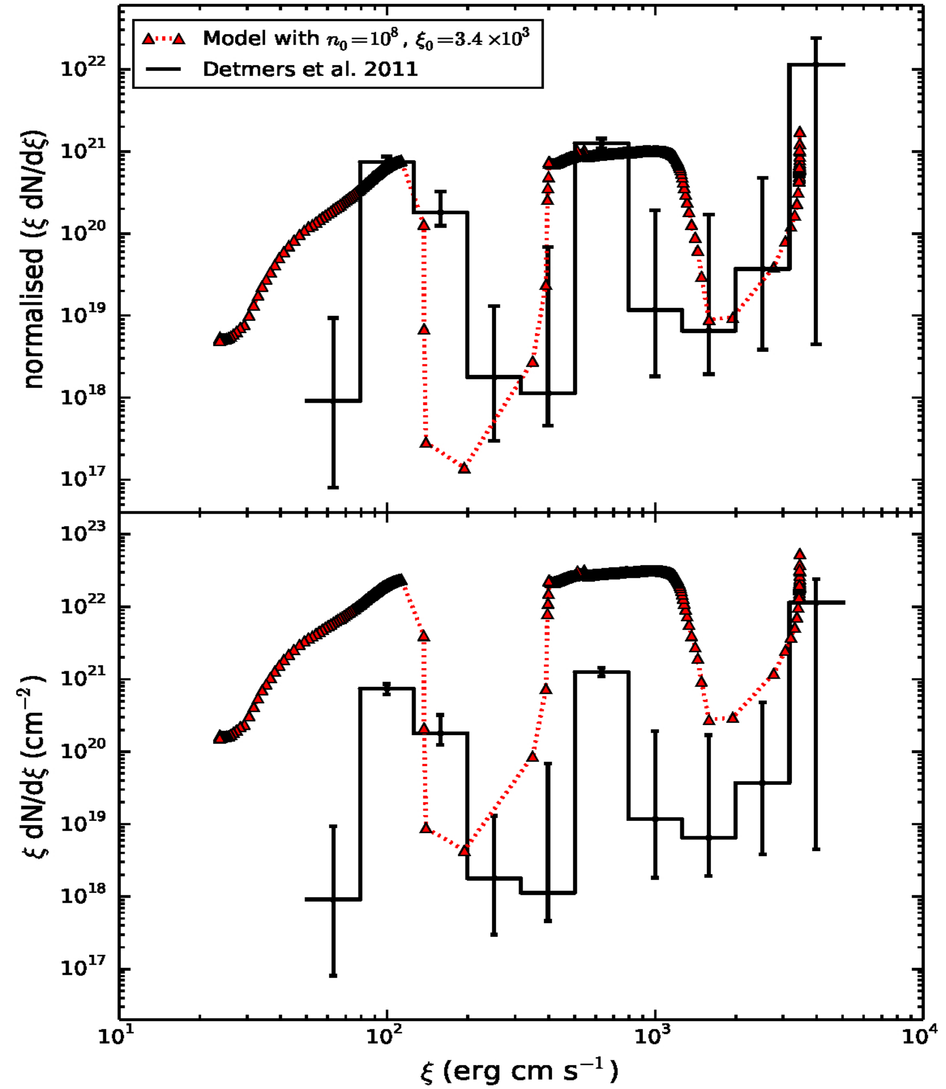

Observed AMD modelled by TITAN

Goosmann +16, **constant pressure model – two clouds, NGC 3783**

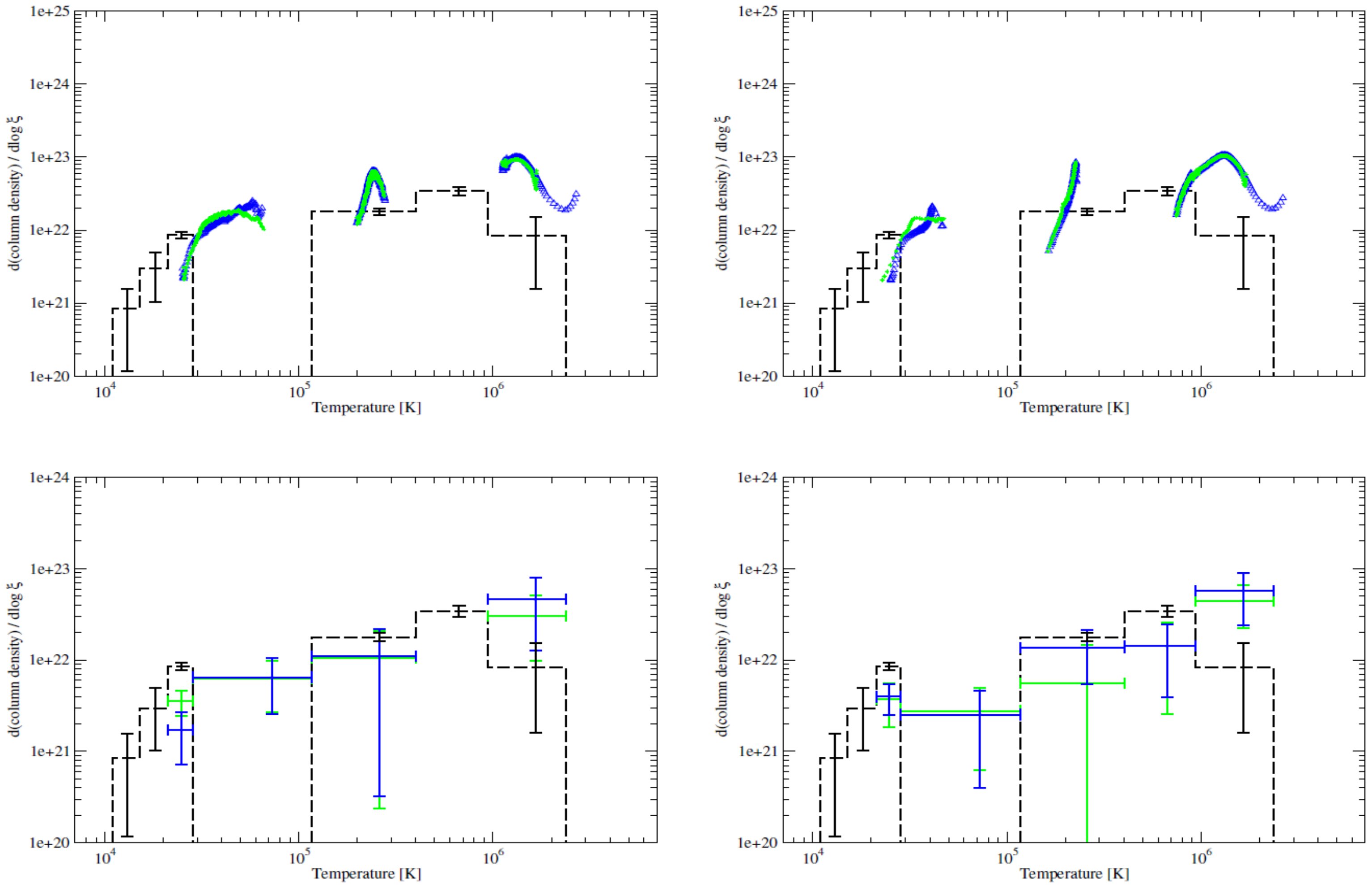

Fig. 7. Comparison between the observed and the modeled AMD as a function of temperature inside the medium (see Sect. 3). We construct theoretical AMD curves for the cold (*left*) and hot (*right*) solutions of the cases ξ_{tot} = 4000 (green) and ξ_{tot} = 8000 (blue). The observational AMD is denoted by the dashed line. The botom panels show the same theoretical AMDs as above but degraded to the resolution of the observed AMD and plotted on a larger vertical scale.

Modelled AMD structure

Stern +14, **constant pressure slabs**

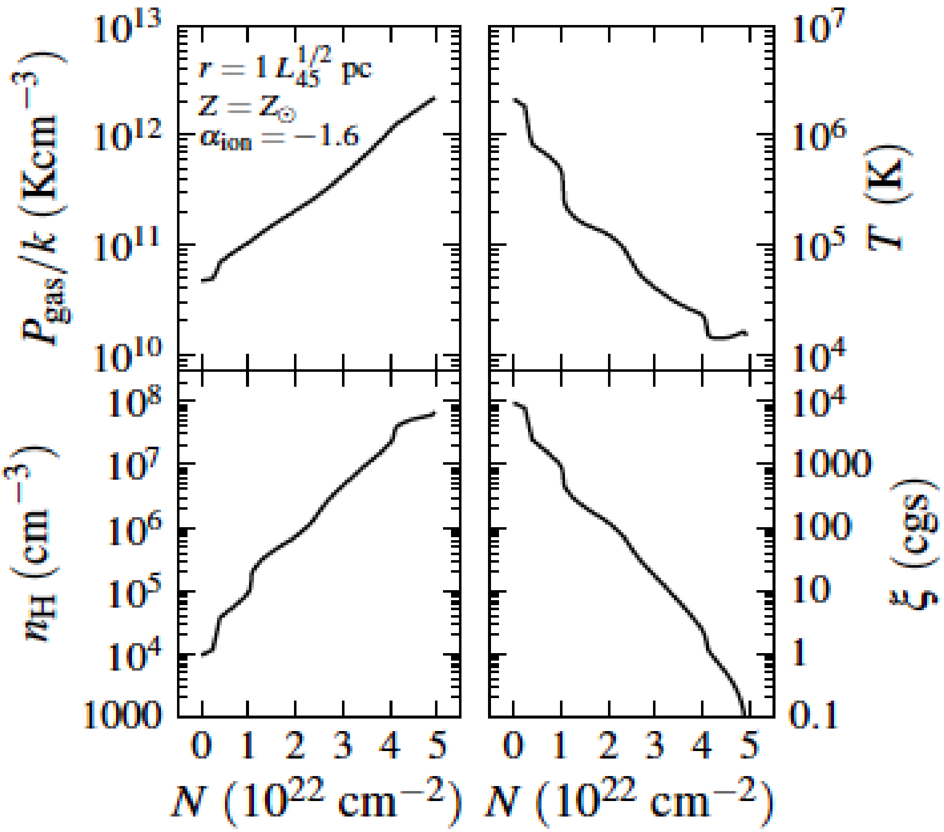

Adhikari +15, **constant pressure slab**

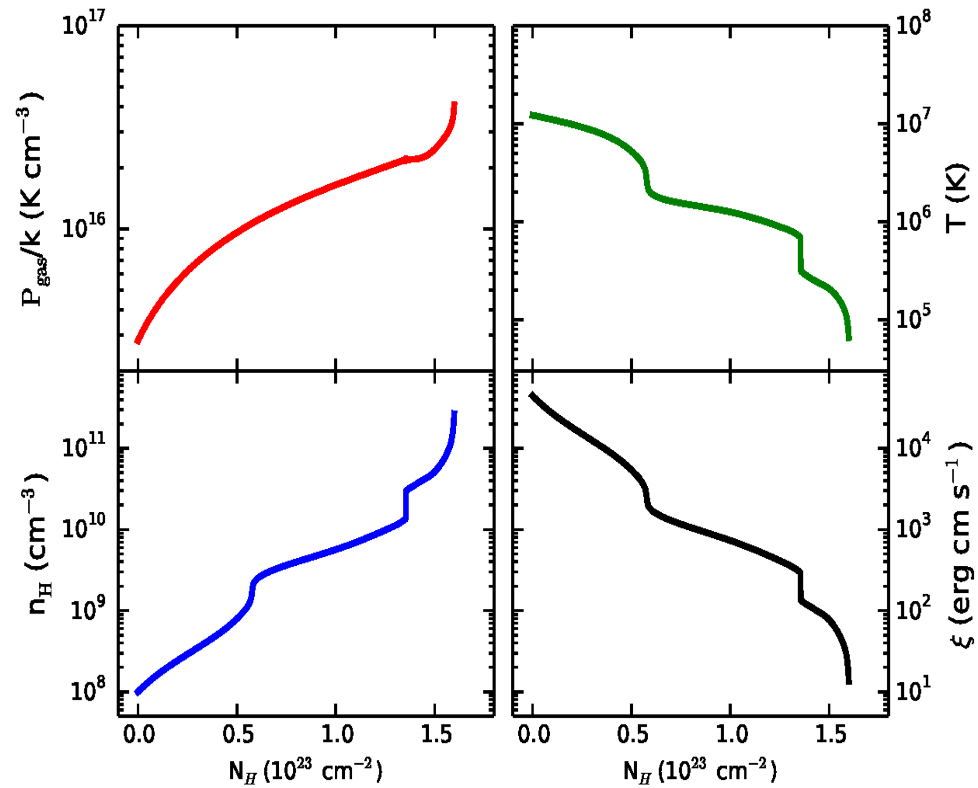

Modelled AMD structure

Stern +14, **constant pressure slabs**

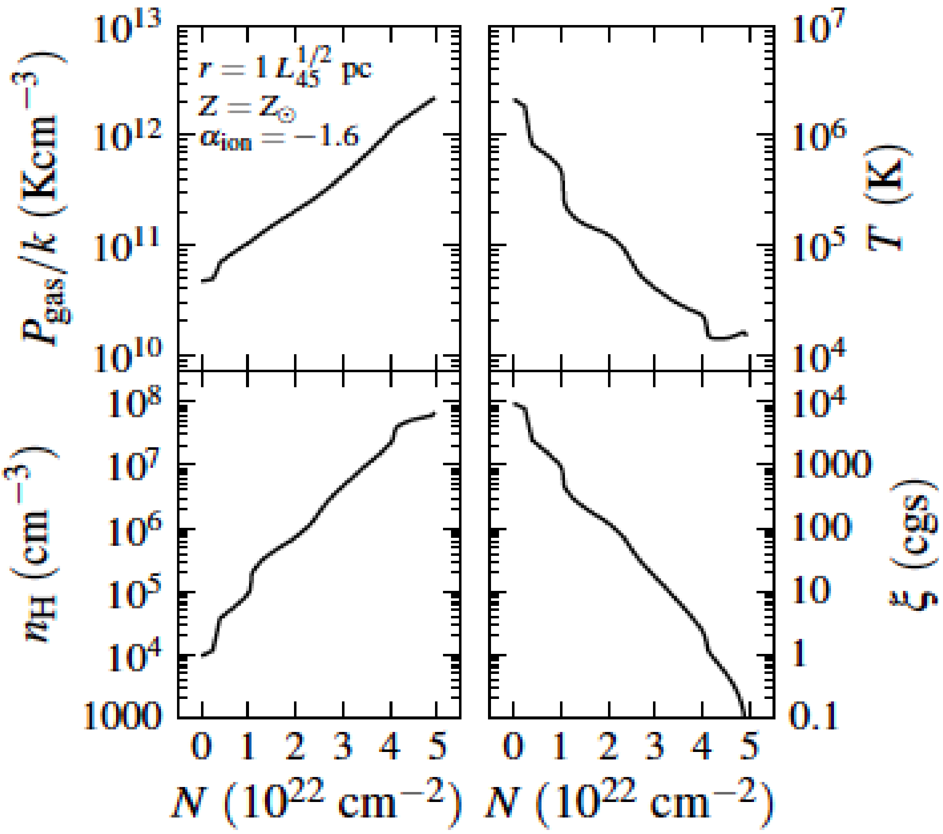

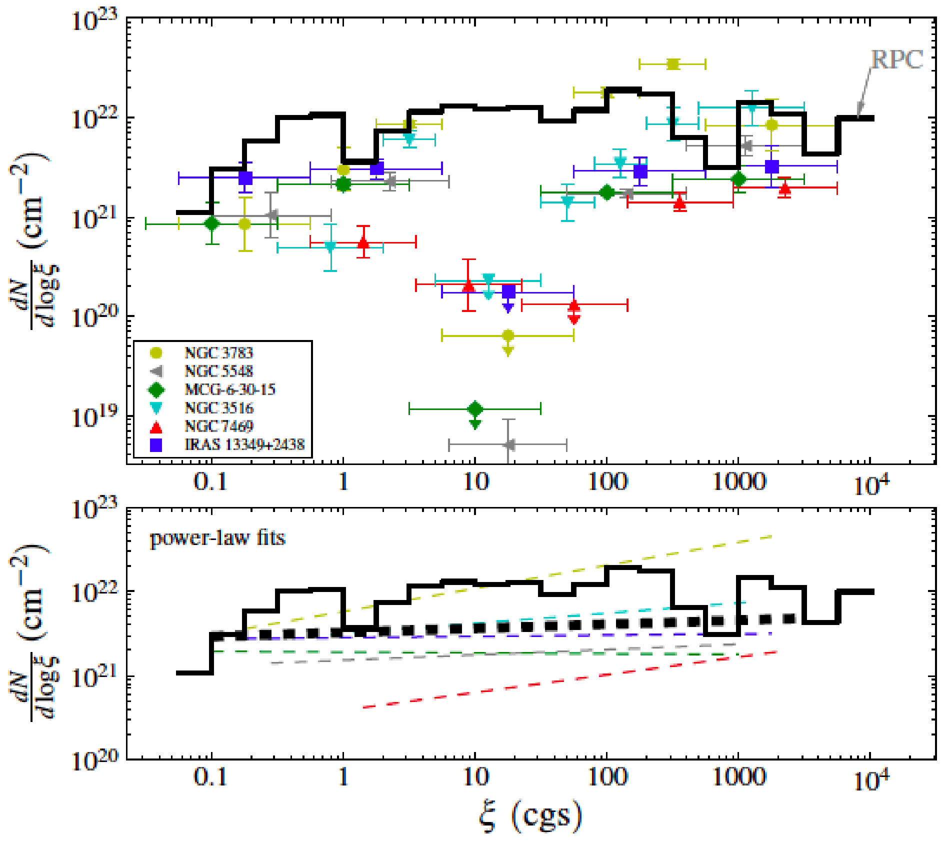

Modelled AMD structure

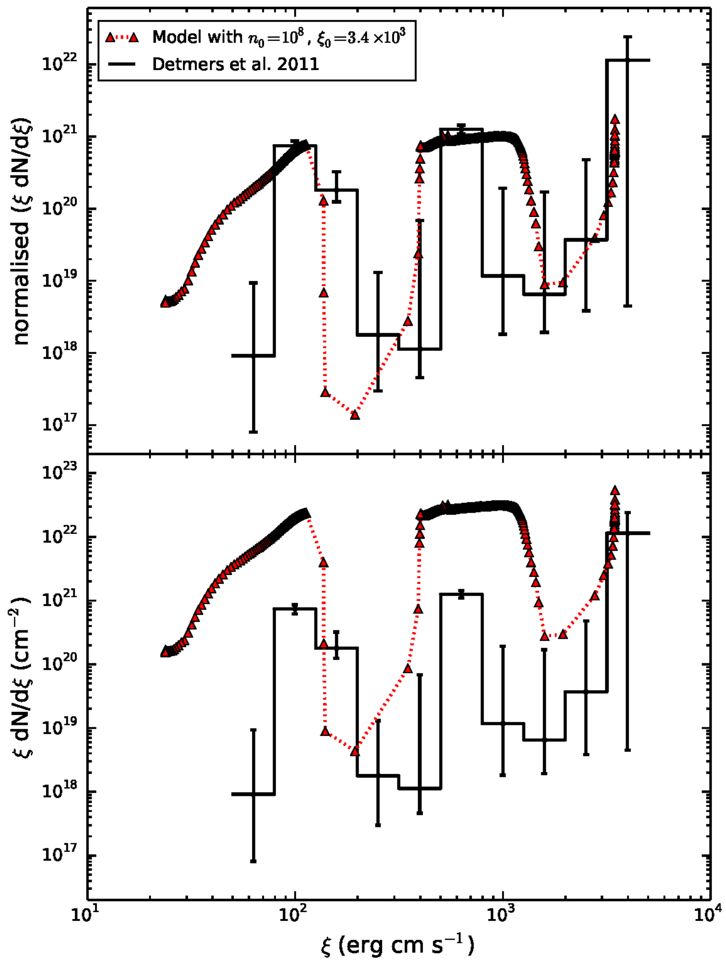

Adhikari +15, **constant pressure slab**

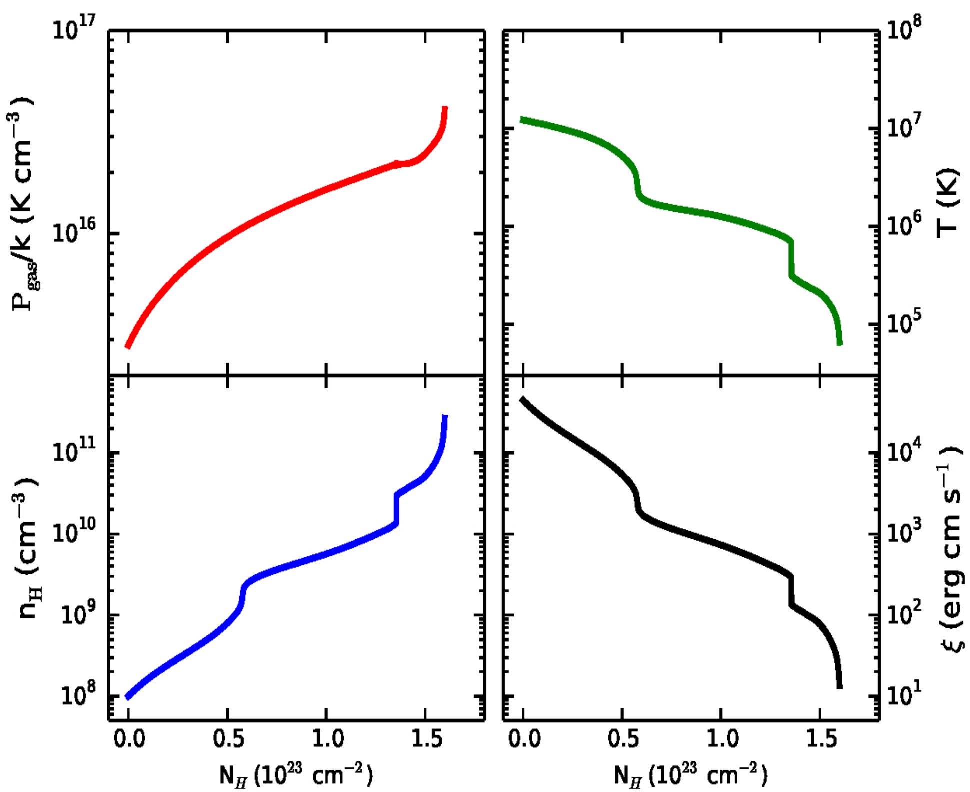

Modelled AMD structure

Adhikari +15, **constant pressure slab,** compared to Goosmann +16

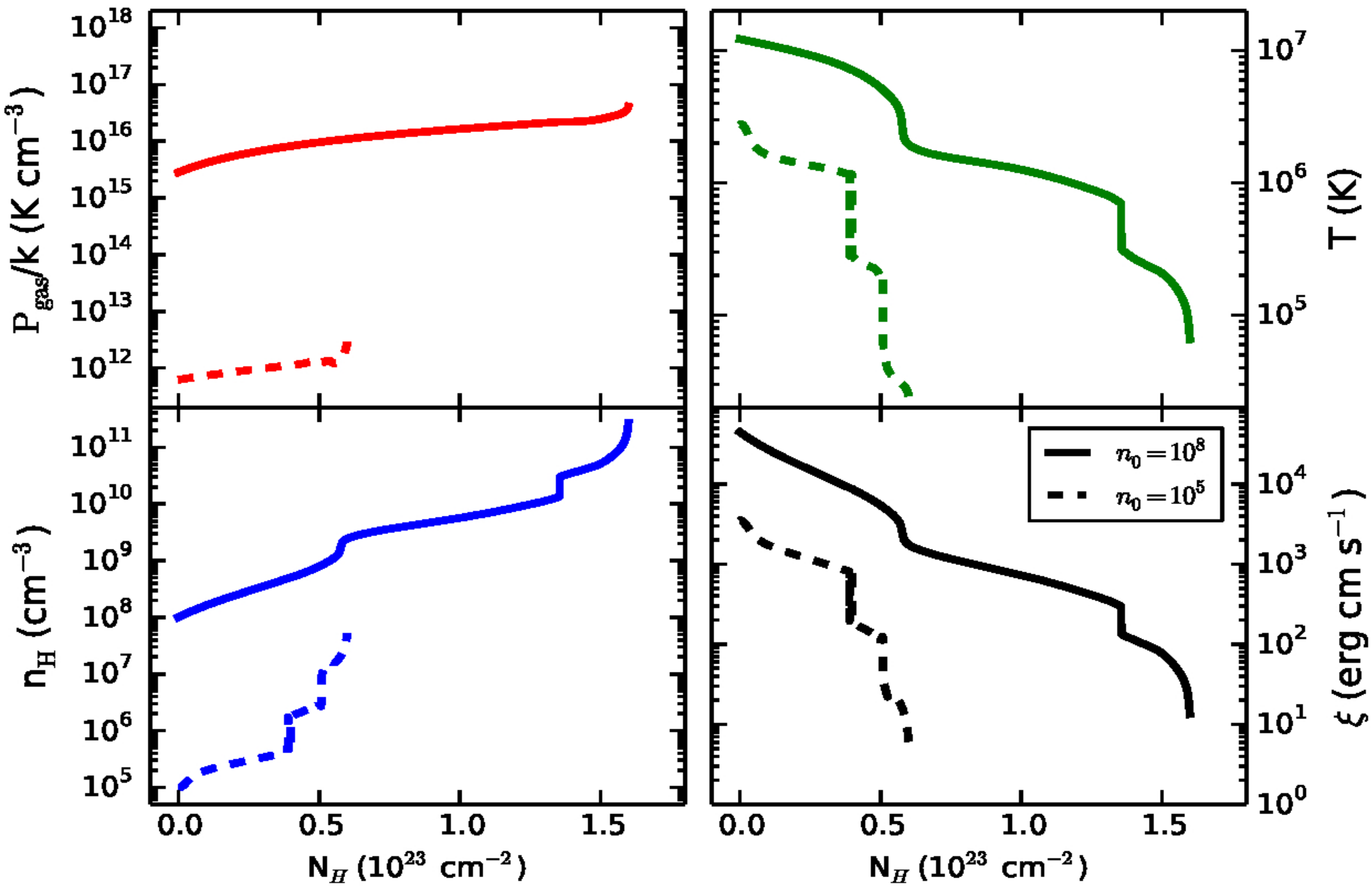

Questions to the audience

- Do we observe saturated lines in X-ray domain?
- Do we derive AMD for UV absorbers?
- Are we able to distinguish between ***const. P*** and ***const. n*** models from observations?
- Are f-f winds more important than Compton winds?
- Can we distinguish volume density of the absorber?

Systematic studies of AMD with TITAN

n=10^8 cm^{-3}, different SEDs, L_{tot} ~ 10^{45} erg/s

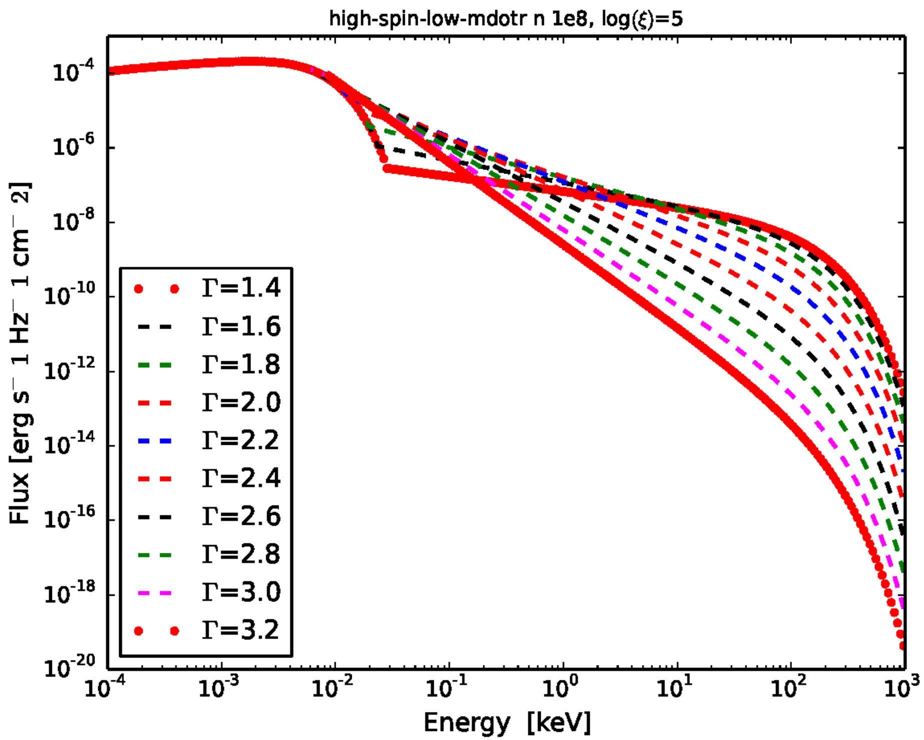

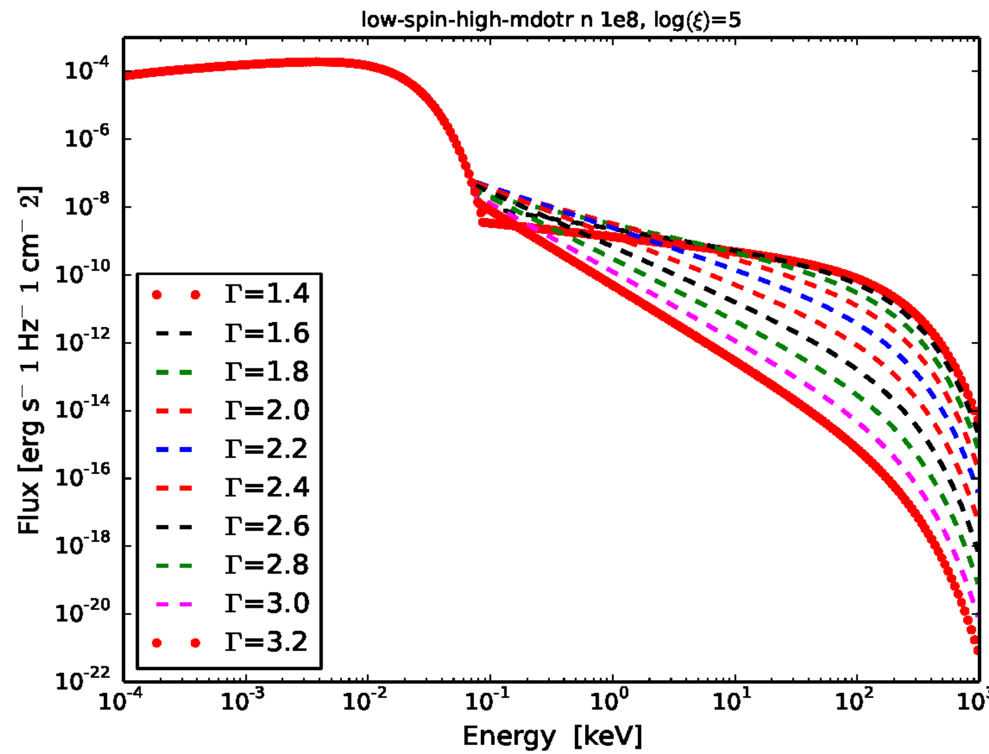

Systematic studies of AMD with TITAN

n=10^8 cm^{-3}, different SEDs, L_{tot} ~ 10^{45} erg/s

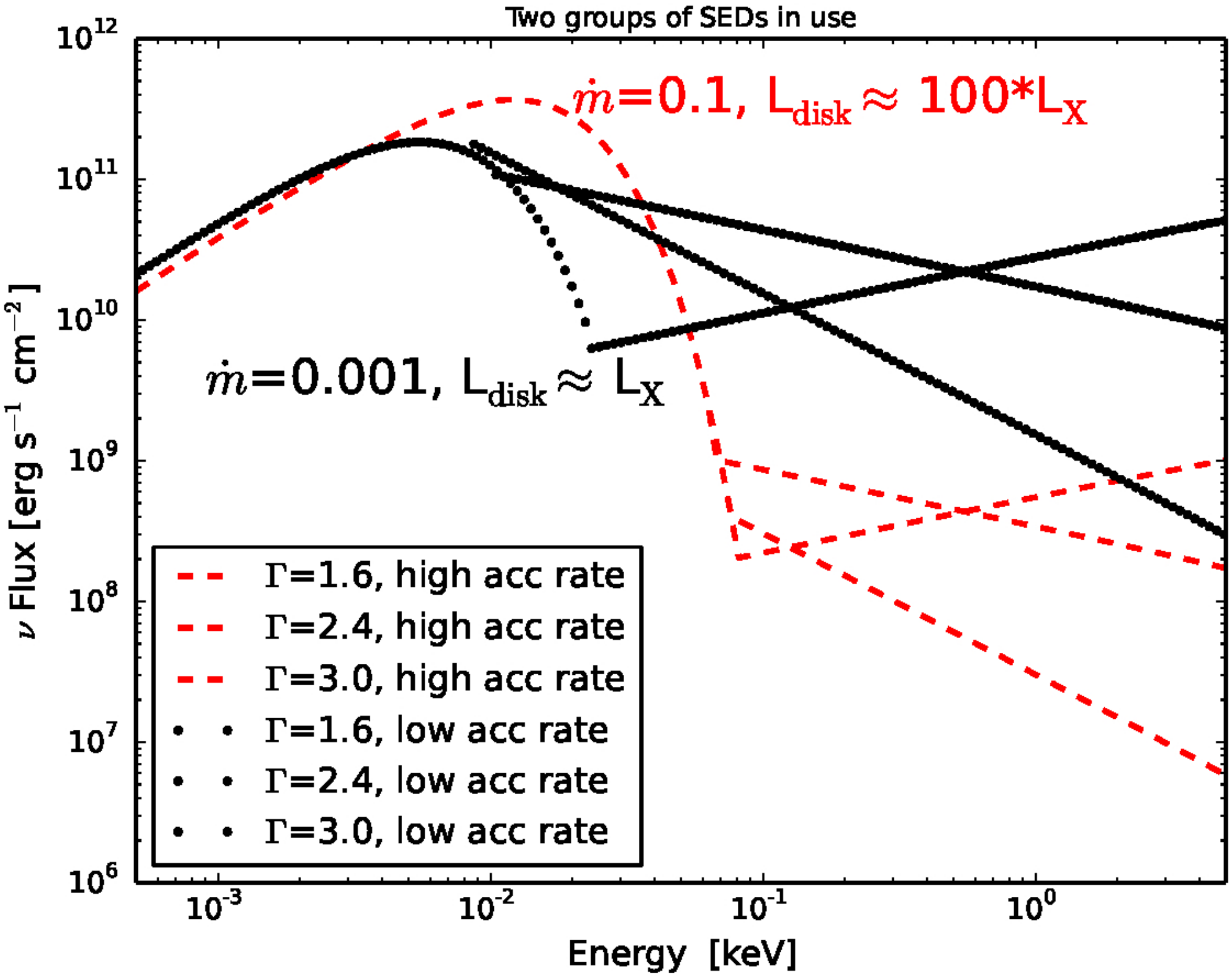

Systematic studies of AMD with TITAN

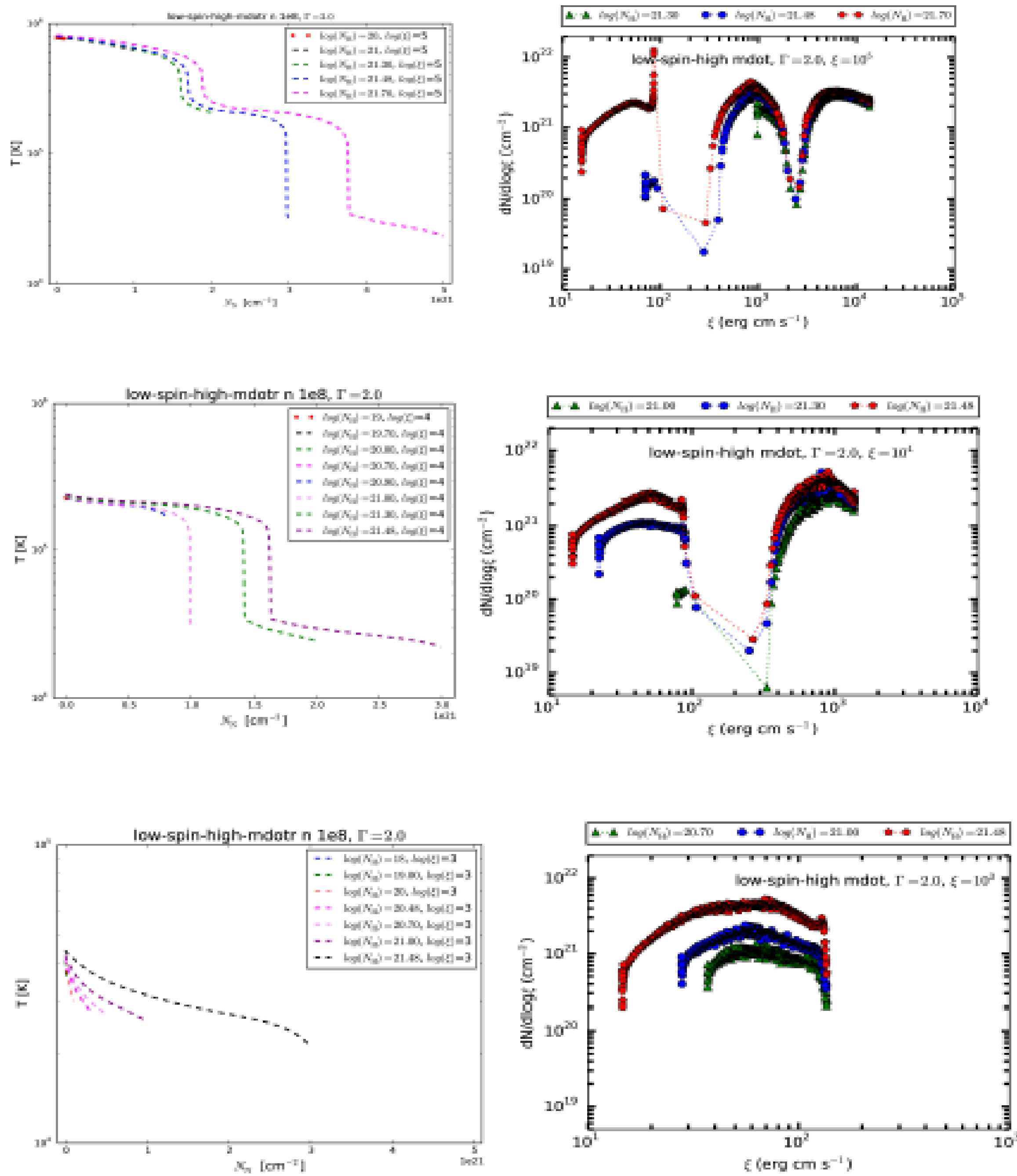

Normalization of AMD with TITAN

$N_{tot} \geq 10^{23}$ cm^{-2}

SED – **NO** soft X-ray bump

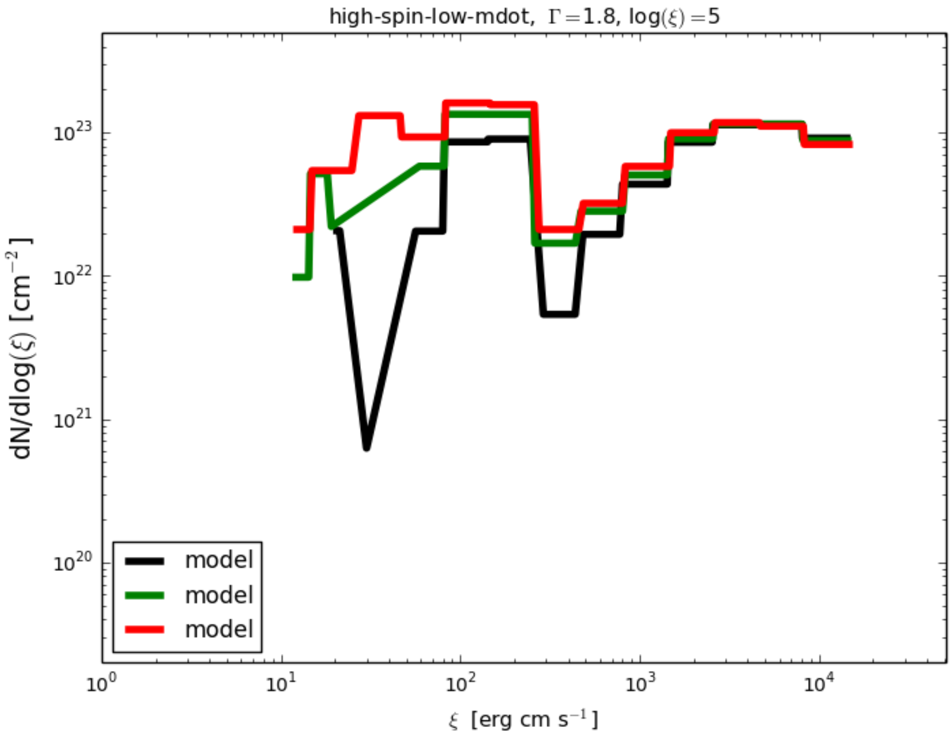

Normalization of AMD with TITAN

$N_{tot} \geq 10^{23}$ cm^{-2}

SED – **NO** soft X-ray bump

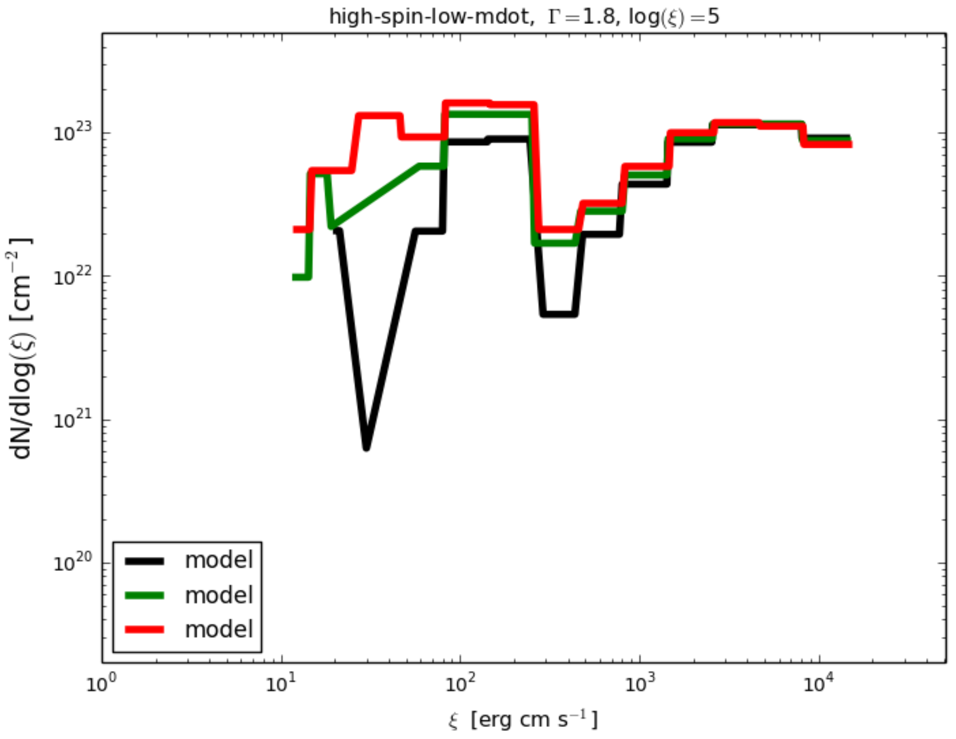

$N_{tot} \sim 10^{21-22}$ cm^{-2}

SED – soft X-ray bump

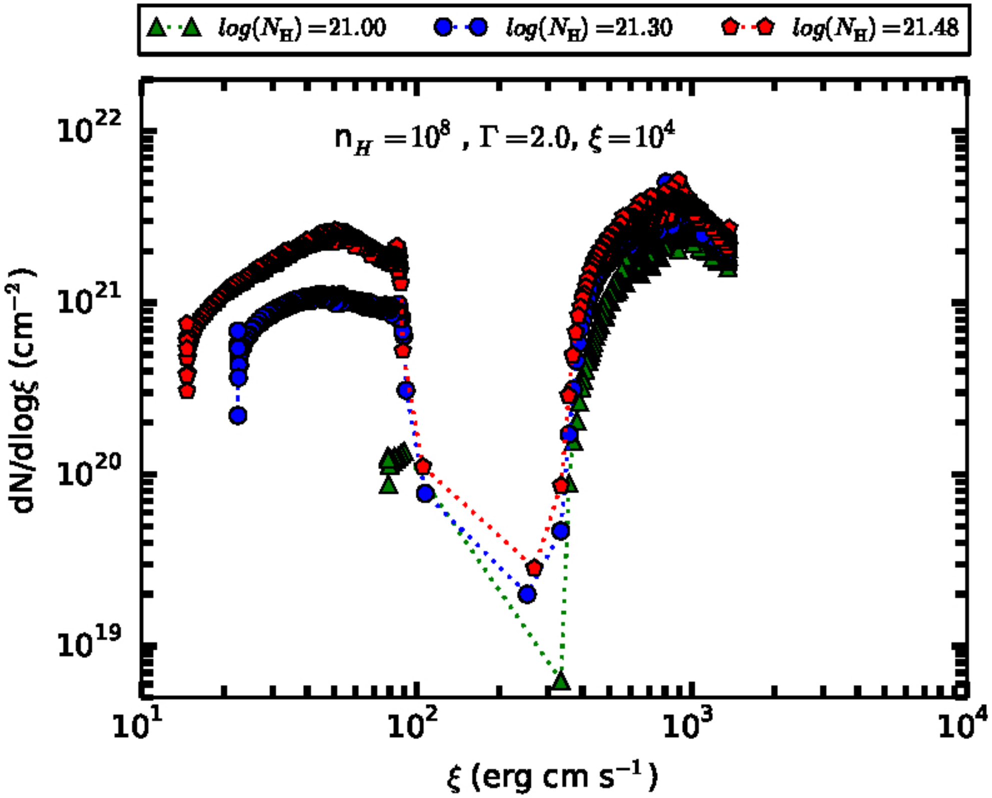

Conclusions:

- The fact that the photoionization models give the same results for broad range of densities is only valid for strong X-ray illumination, and weak optical/UV SED component.
- The radiation pressure is dominant in the vicinity of BH.
- Thermal Instability occurs only when hydrostatic equilibrium is solved.
- AMD normaliztion is higher for SED with strong X-ray component and weak optical UV component

Position of the drop of AMD with TITAN

$N_{tot} \sim 10^{21\text{-}22}$ cm^{-2} , SED – soft X-ray bump

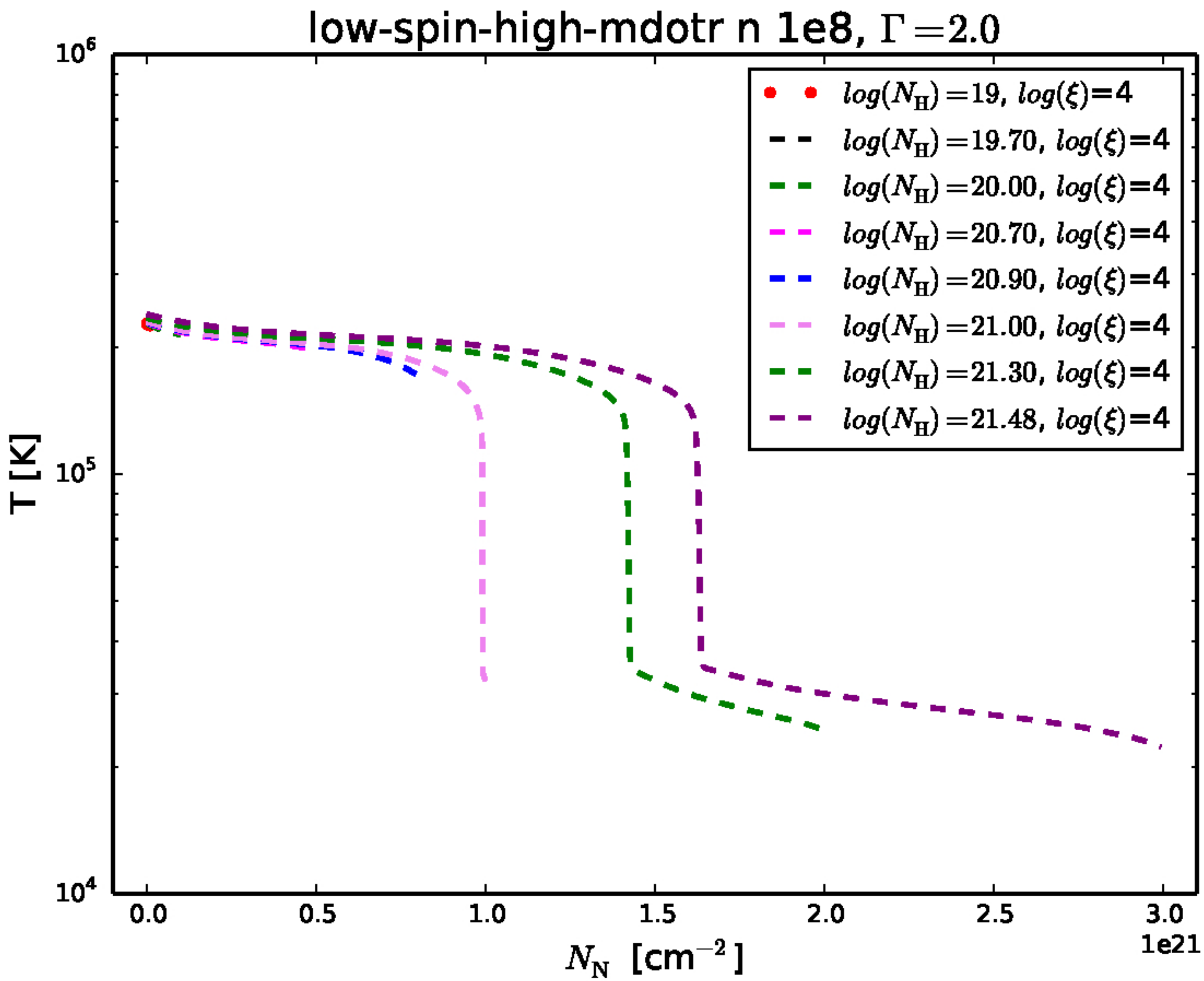

Position of the drop of AMD with TITAN

$N_{tot} \sim 10^{21\text{-}22}$ cm^{-2} , SED – soft X-ray bump

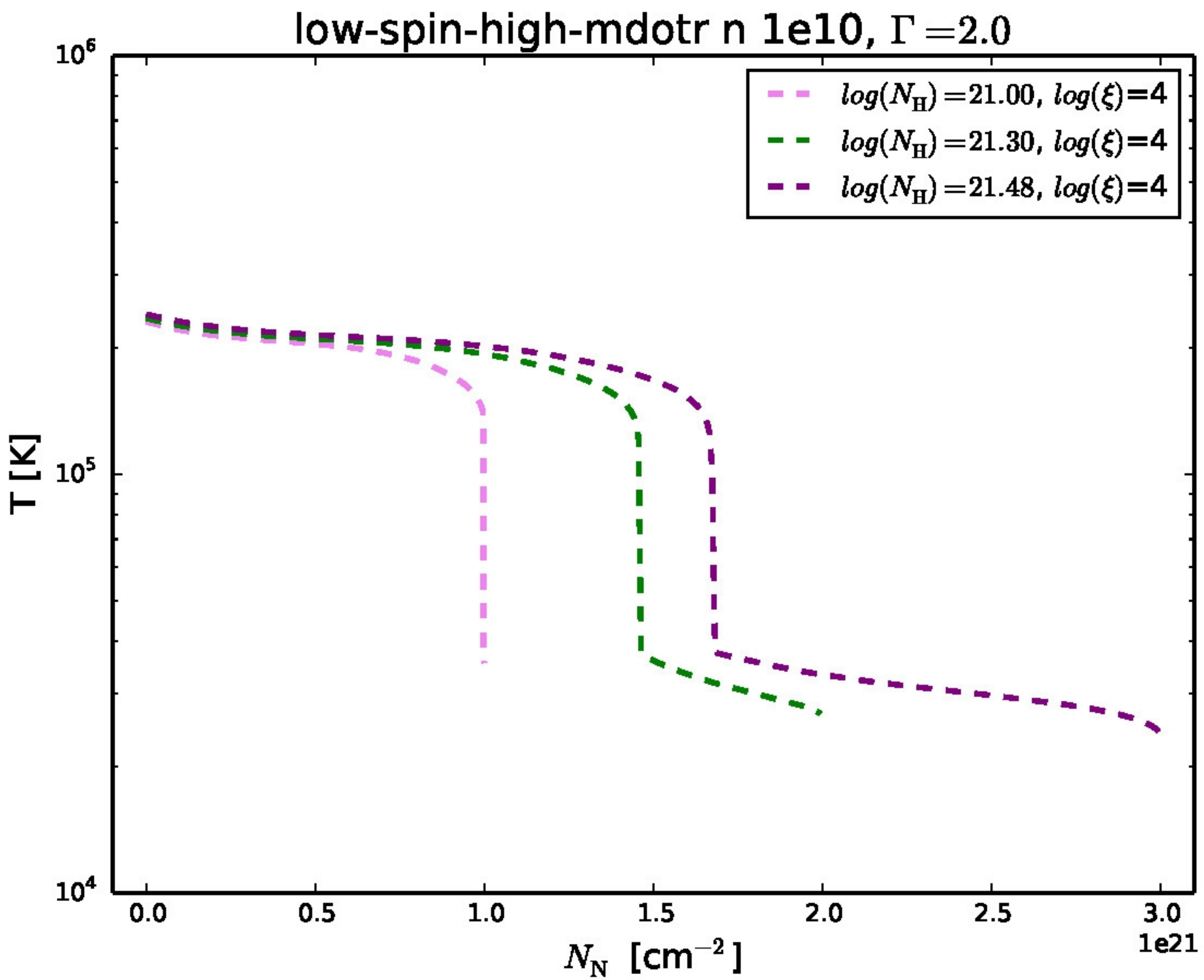

Position of the drop of AMD with TITAN

$N_{tot} \sim 10^{21\text{-}22}$ cm^{-2} , SED – soft X-ray bump

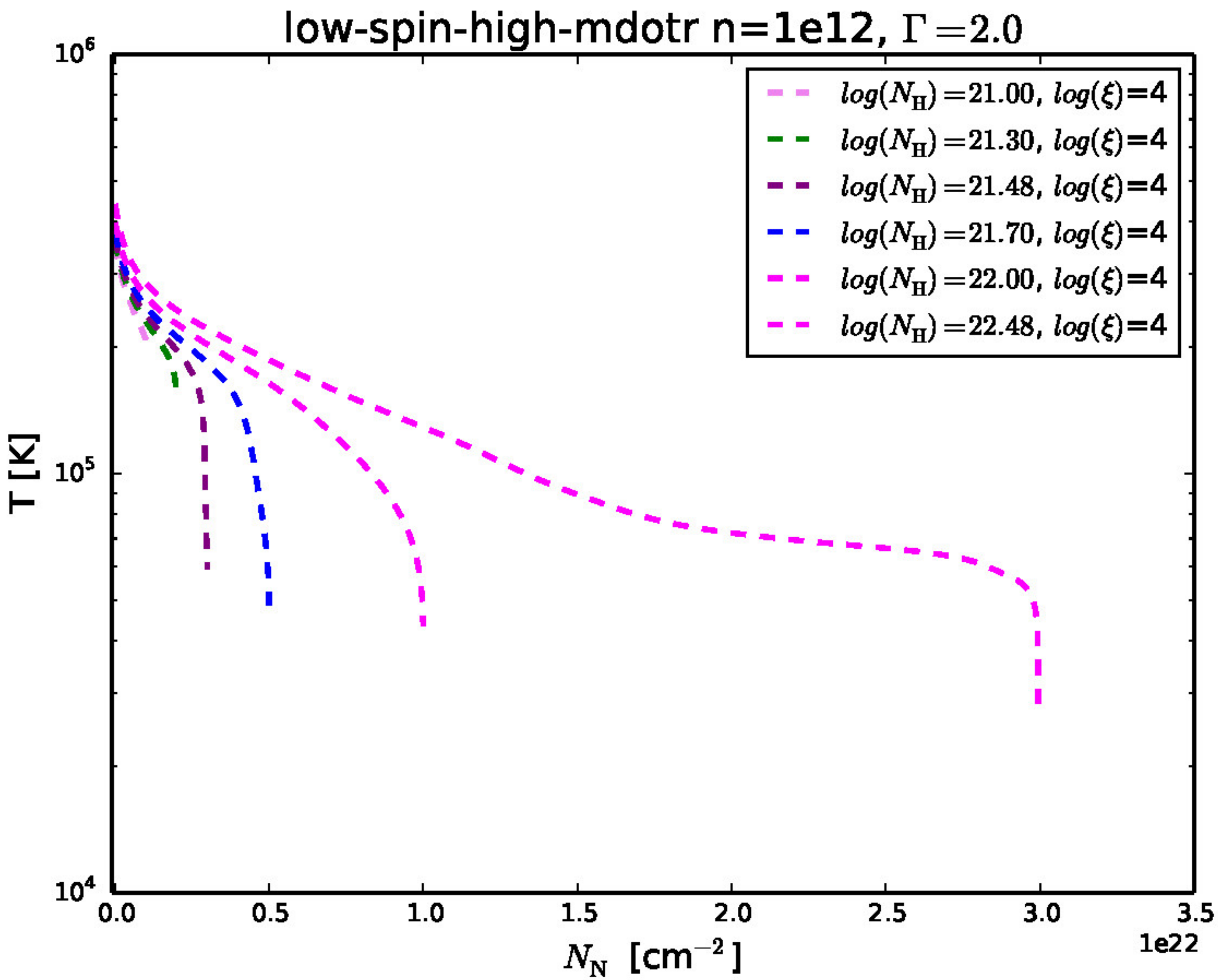

Conclusion first

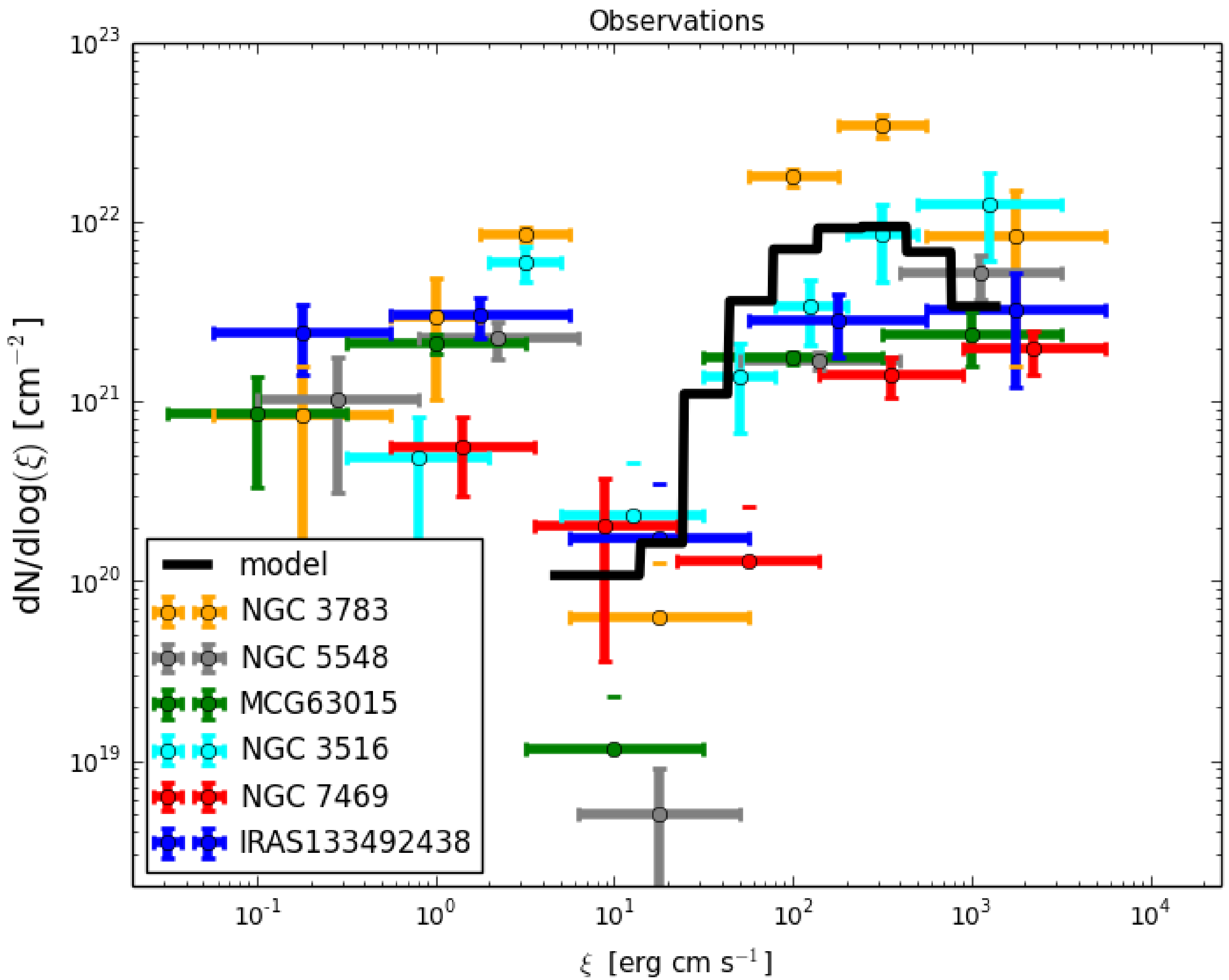

AMD data provided by Ehud Behar

Model computed with TITAN (Anne-Marie Dumont)

Conclusions:

- The fact that the photoionization models give the same results for broad range of densities is only valid for strong X-ray illumination, and weak optical/UV SED component.

- The radiation pressure is dominant in the vicinity of BH.

- Thermal Instability occurs only when hydrostatic equilibrium is solved.

- AMD normaliztion is higher for SED with strong X-ray component and weak optical UV component.

- For the given SED the position of the AMD drop position depends on the volume density.

Density matters

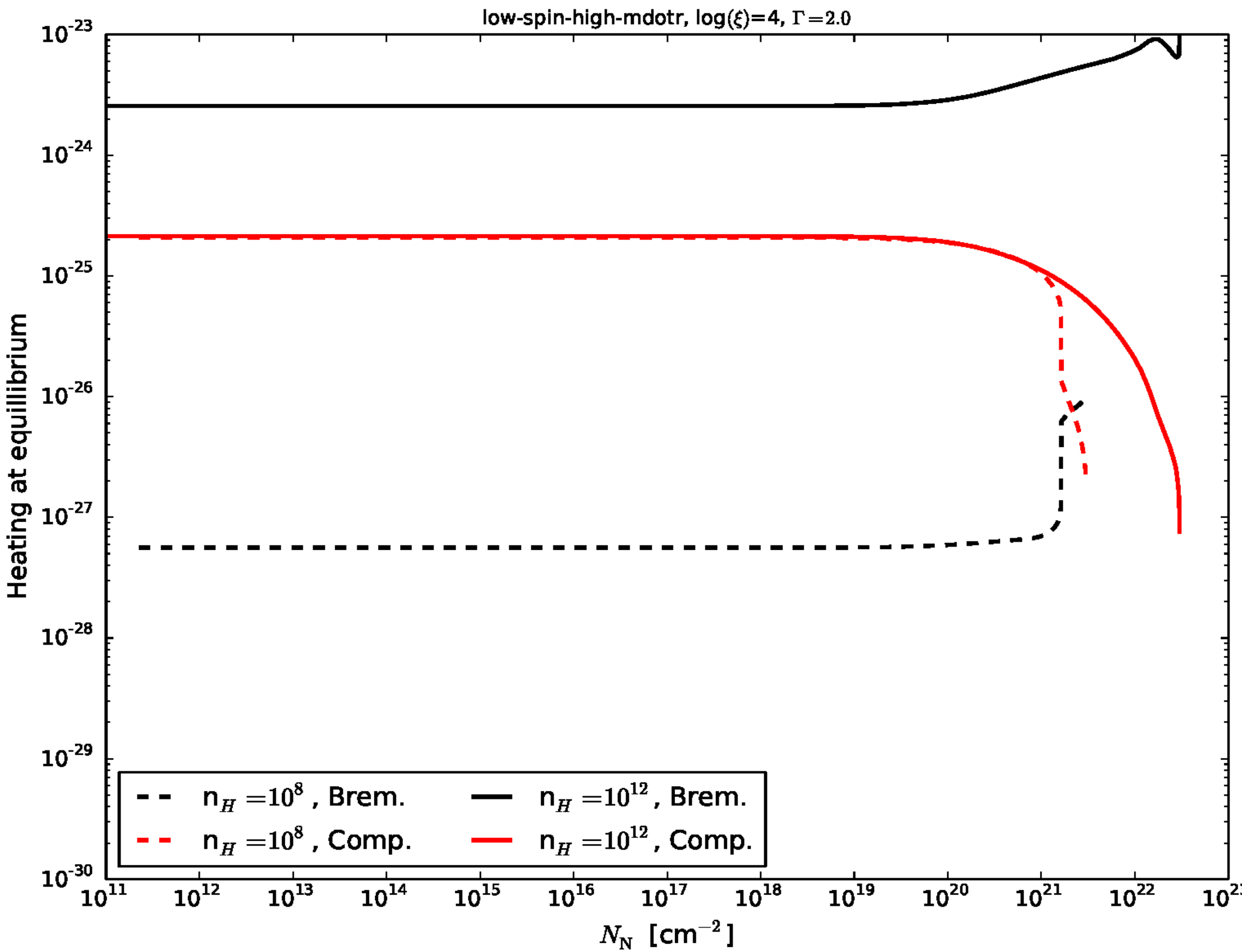

Density matters

Adhikari +15, **constant pressure slab**

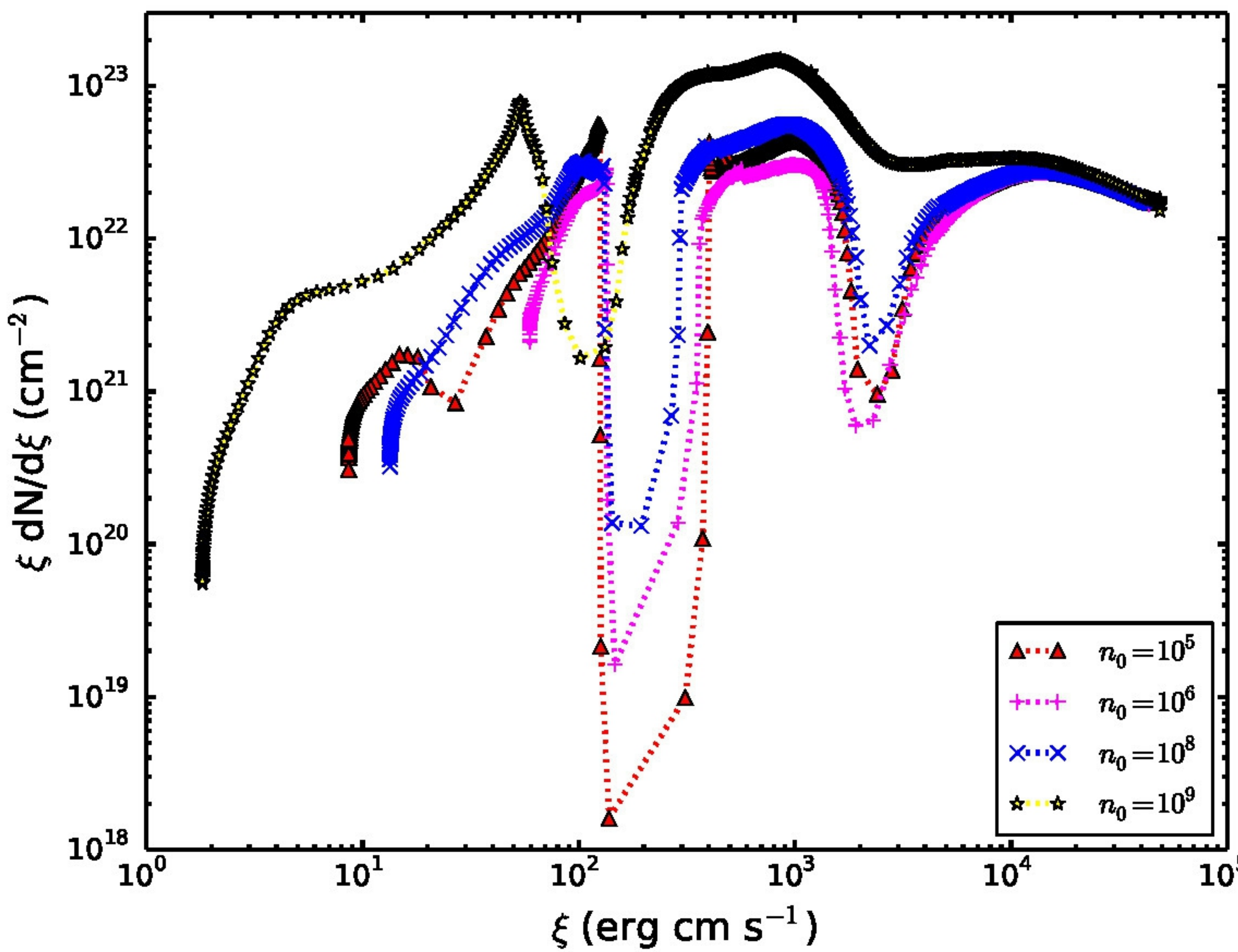

Density matters

Netzer & Laor 1993, **BLR** and **NLR**

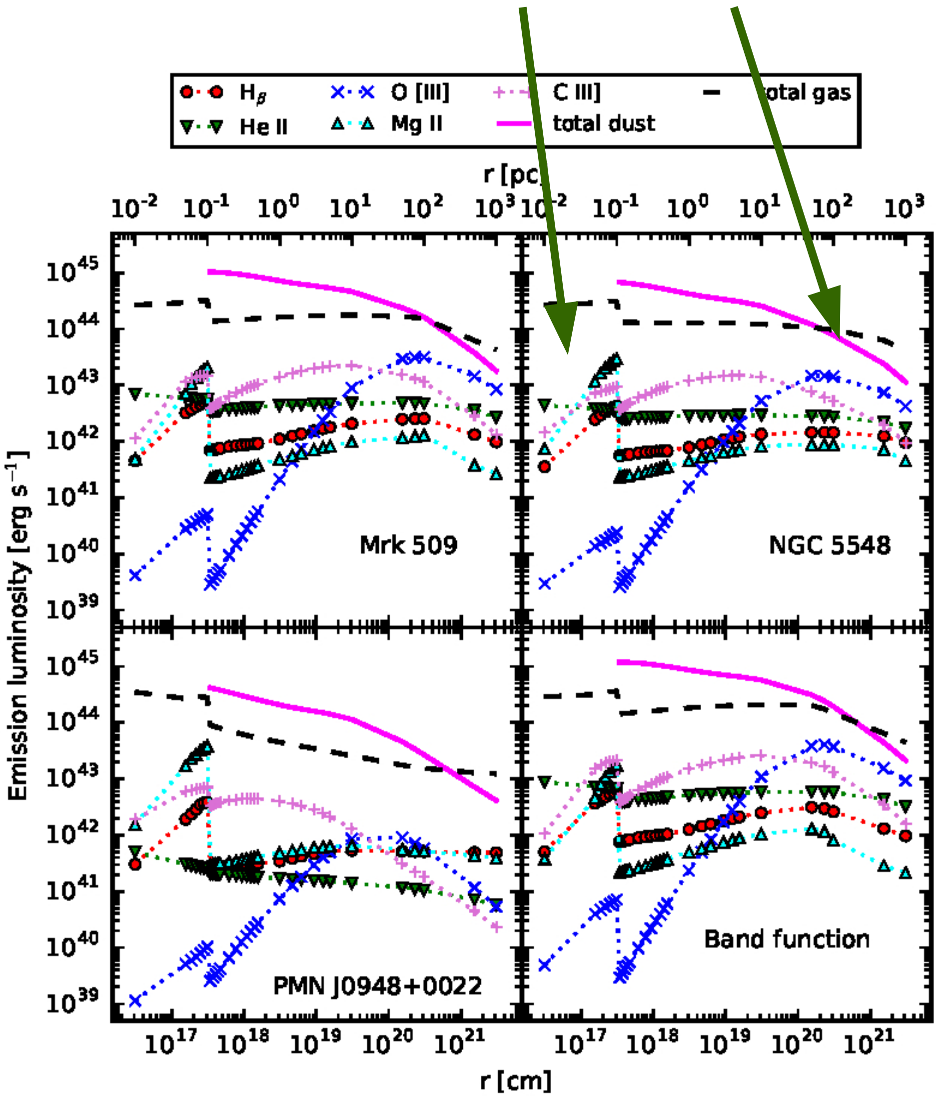

Density matters

Netzer & Laor 1993, **BLR** and **NLR**

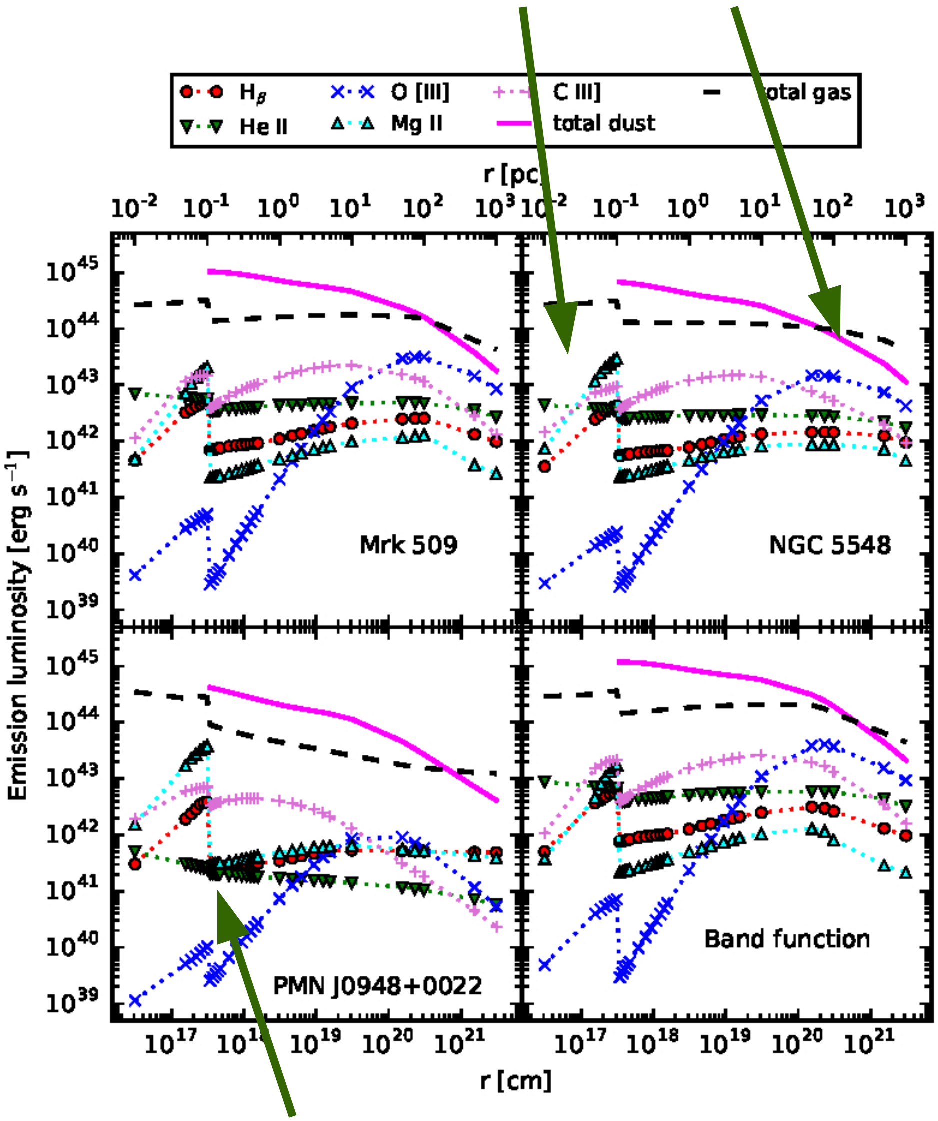

n (R_{sub}) = $10^{9.4}$ cm^{-3}

Density matters

Netzer & Laor 1993, **BLR** and **NLR**

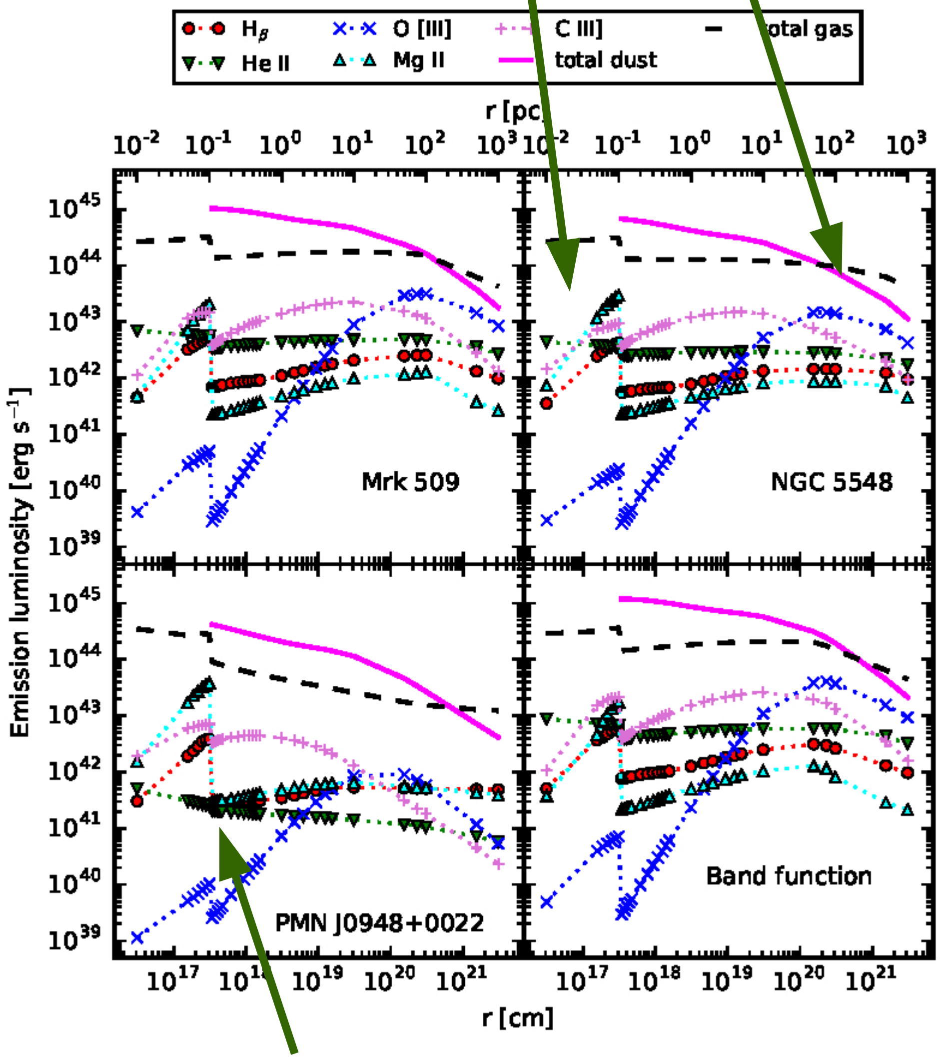

$n\ (R_{sub}) = 10^{9.4}\ cm^{-3}$

Adhikari +16, **const. n CLOUDY, ILR**

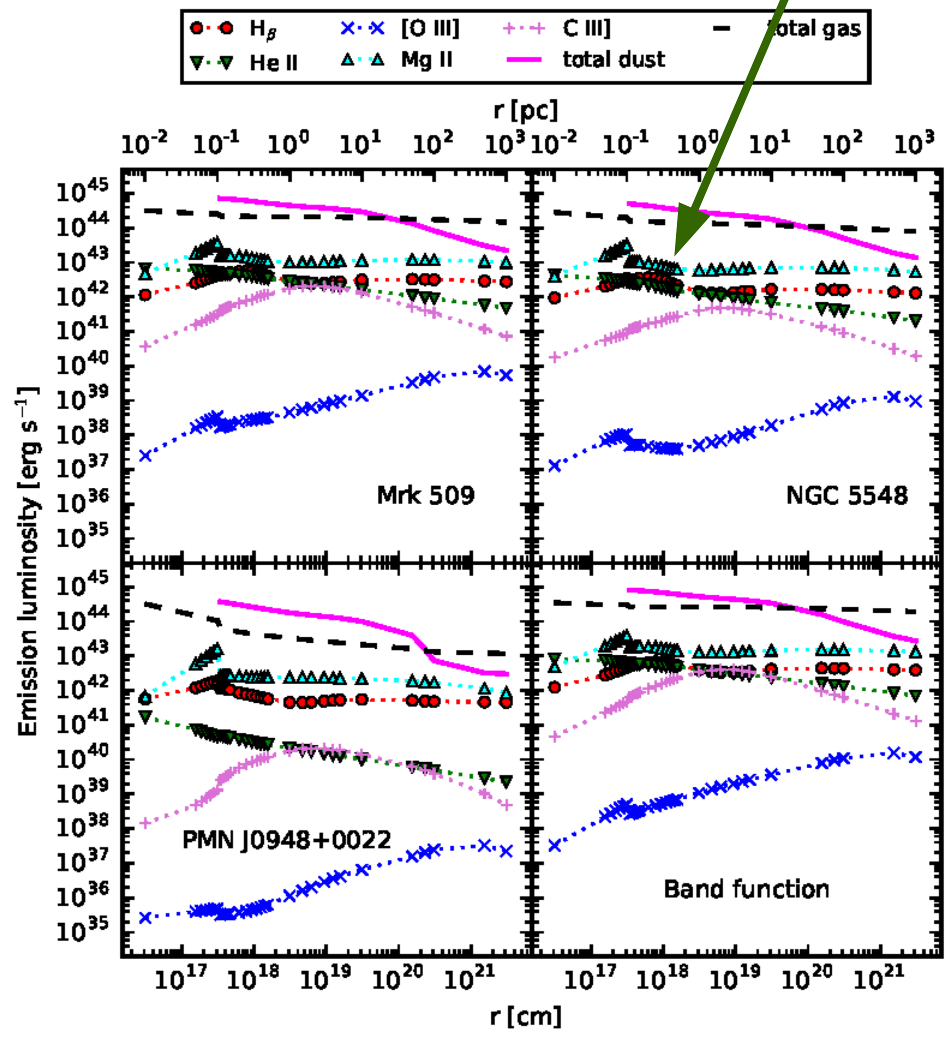

$n\ (R_{sub}) = 10^{11.5}\ cm^{-3}$

Thermal Instability in Sgr A*

Kunneriath +12, **Cold gas – 30"**

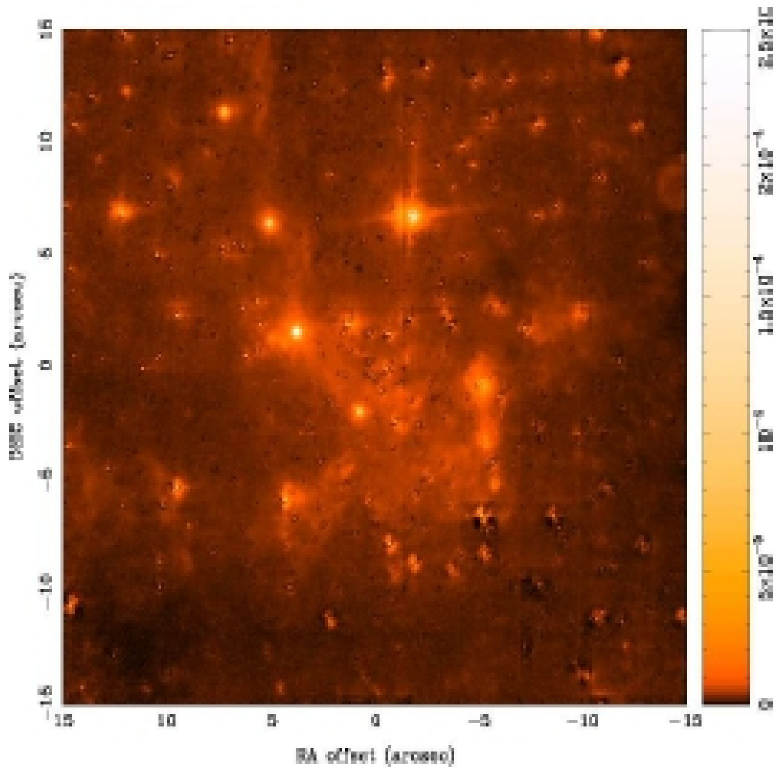

Fig. 1. Brγ image of the central 30″ mini-spiral region around Sgr A*. The colour bar indicates flux density units of Jy/pixel.

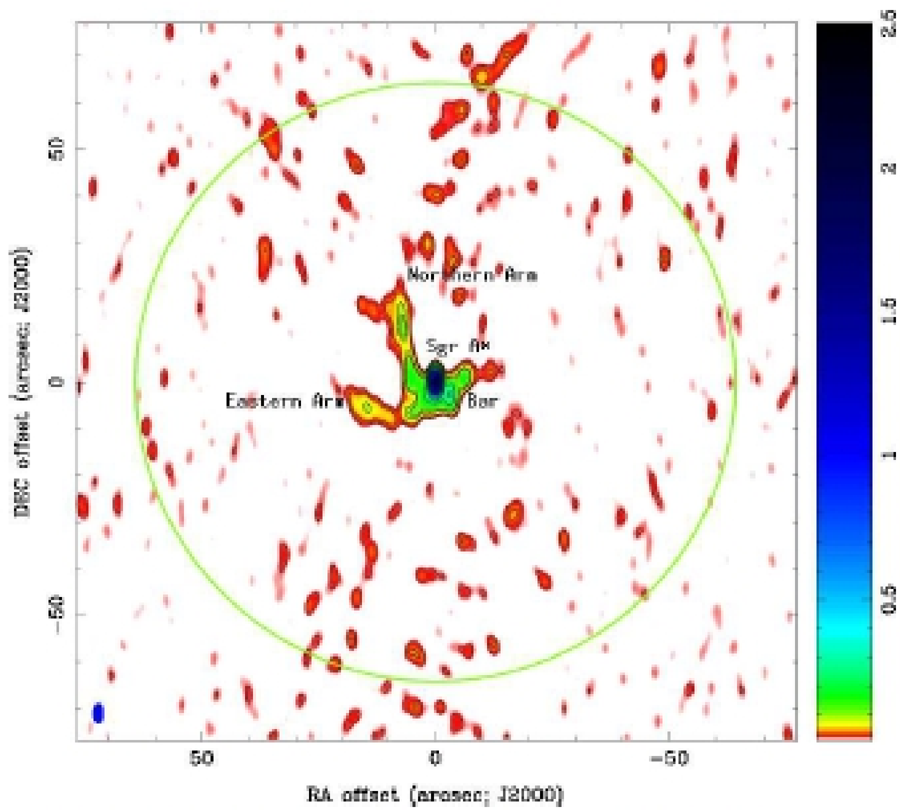

Fig. 2. Three-mm map of the mini-spiral region at resolution 2.68″ by 1.71″ (P.A=-20.7°). The green circle marks the HPBW. Contour levels are 0.02, 0.03, 0.04, 0.05, 0.1, 0.6, 0.9, 1.2, 1.5, and 2.5 Jy/beam.

Thermal Instability in Sgr A*

Kunneriath +12, **Cold gas – 30"**

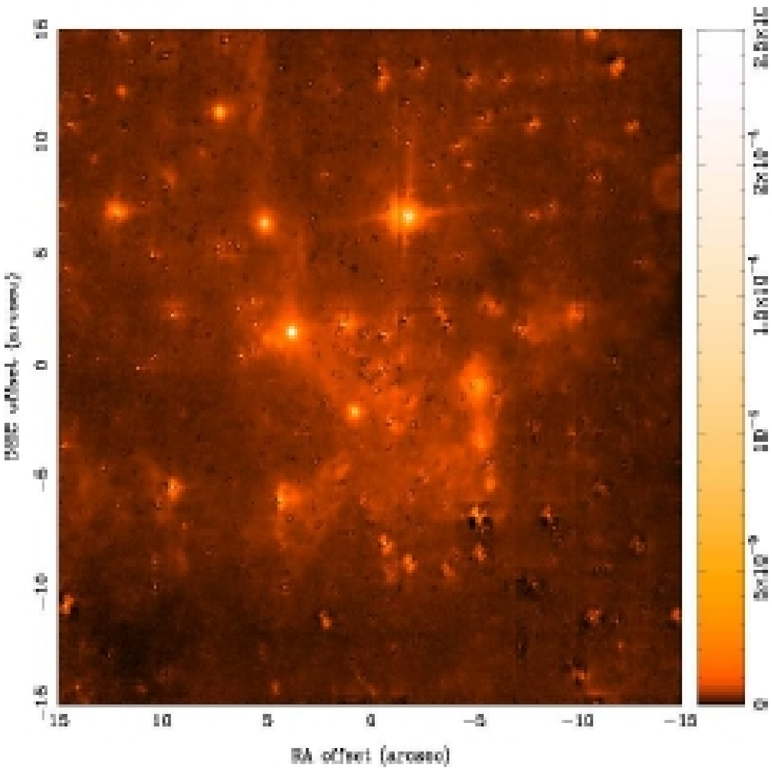

Fig. 1. Brγ image of the central 30″ mini-spiral region around Sgr A* . The colour bar indicates flux density units of Jy/pixel.

Różańska +15, **Hot gas – 17'**

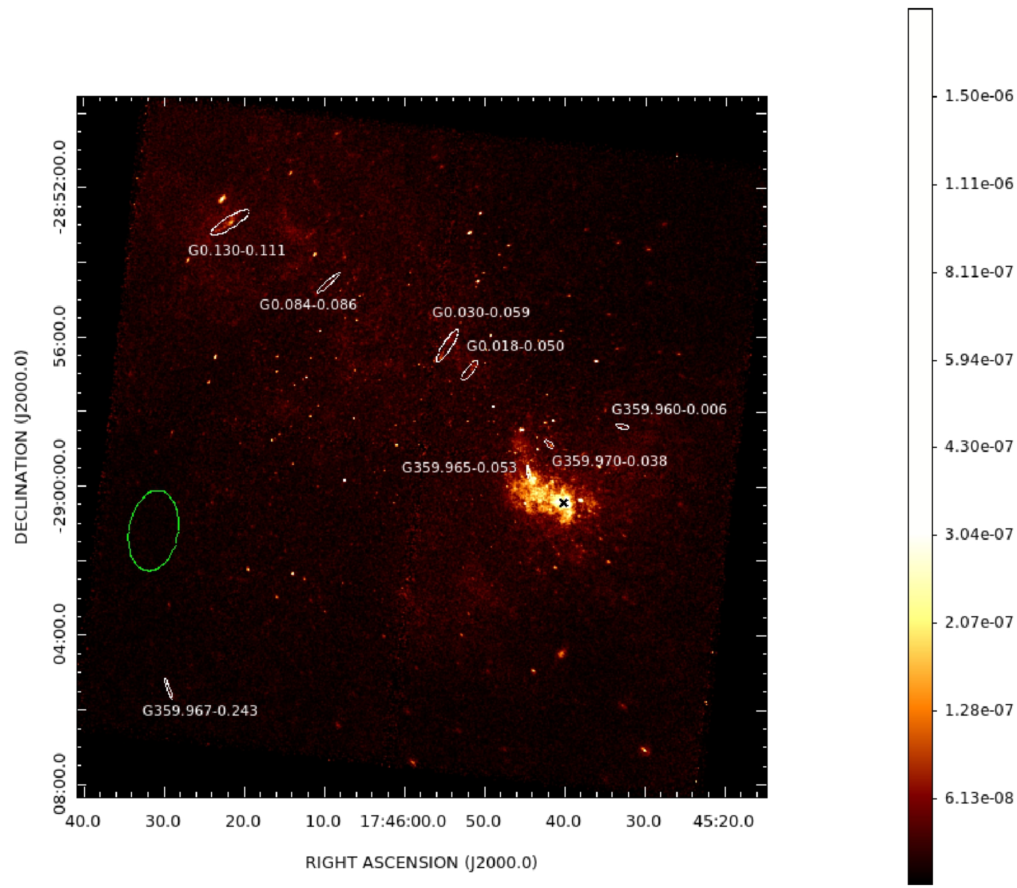

Thermal Instability in Sgr A*

Różańska +14, **For SEDs in different Sgr A* luminosity states**

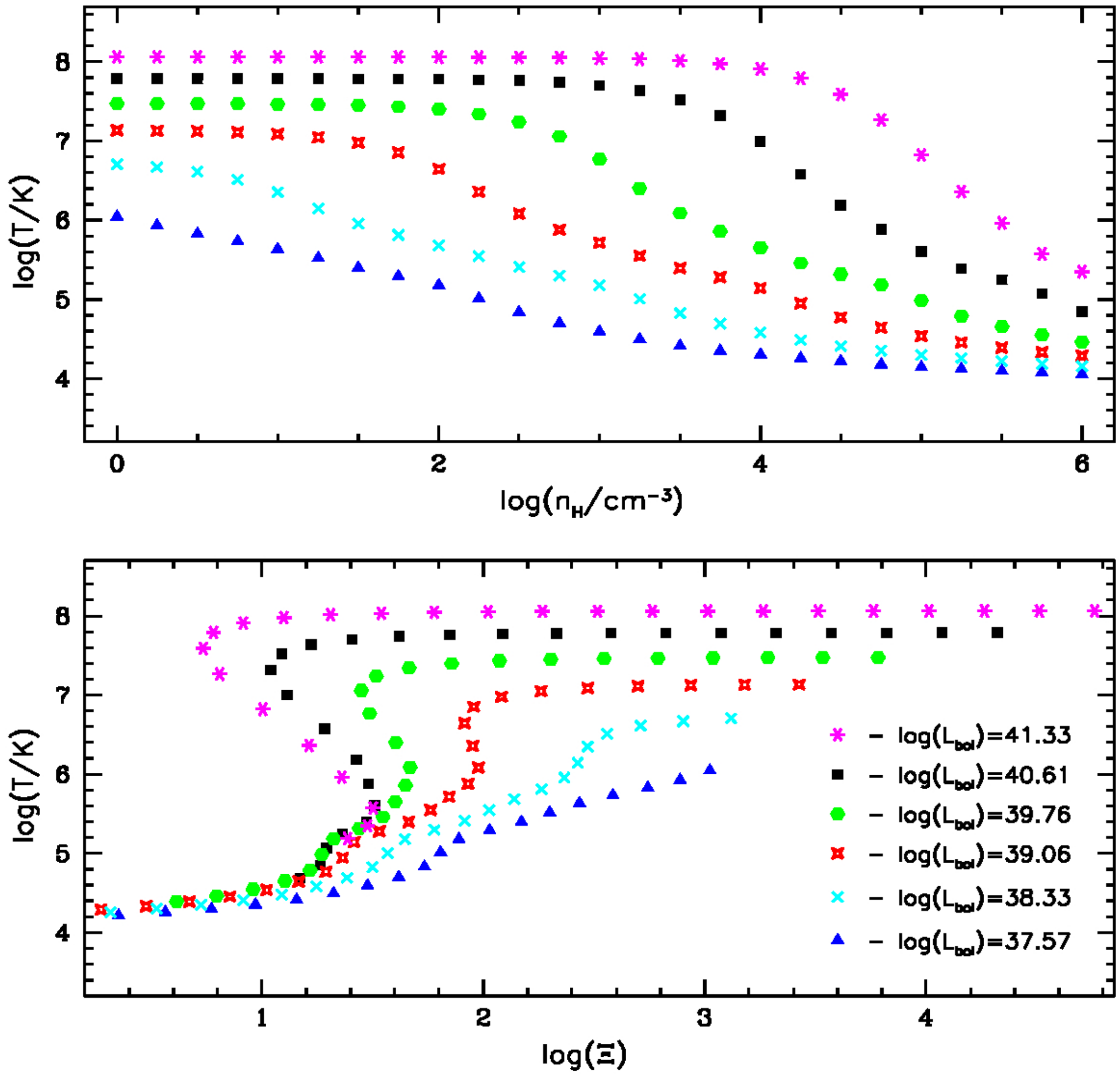

Thermal Instability in Sgr A*

Różańska +15, **Gas pressure and density radial structure from the Bondi flow fitted to the CHANDRA**

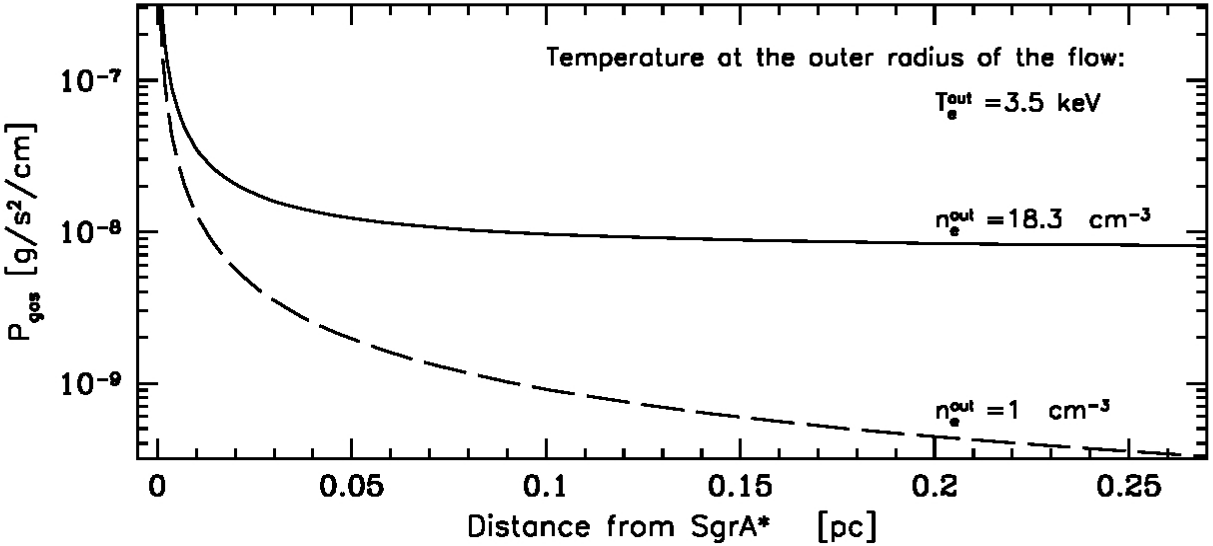

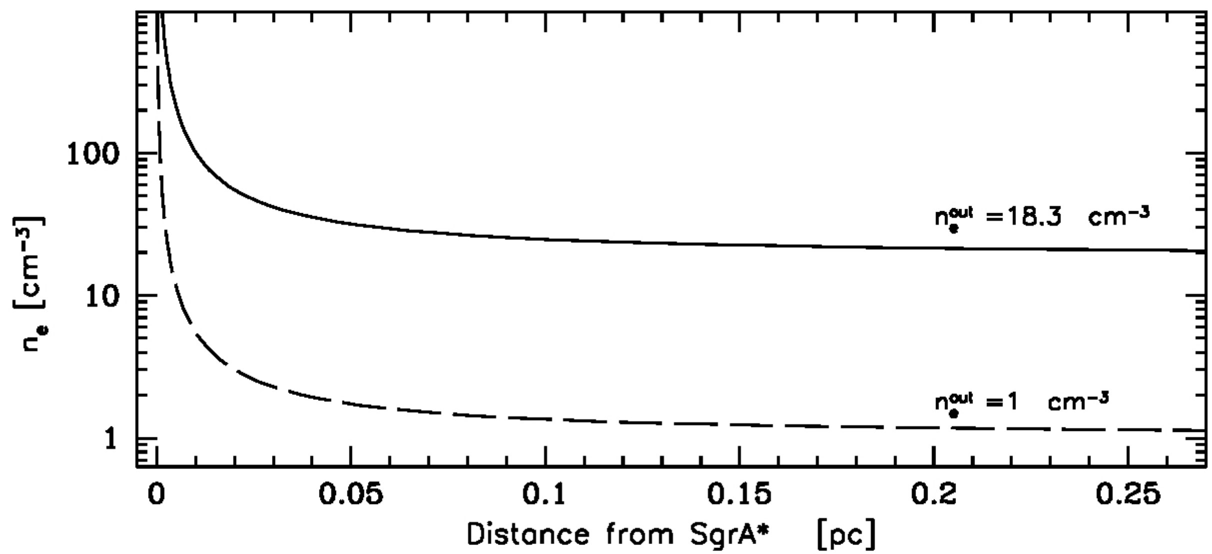

Thermal Instability in Sgr A*

Różańska +14, **For SEDs in different Sgr A* luminosity states**

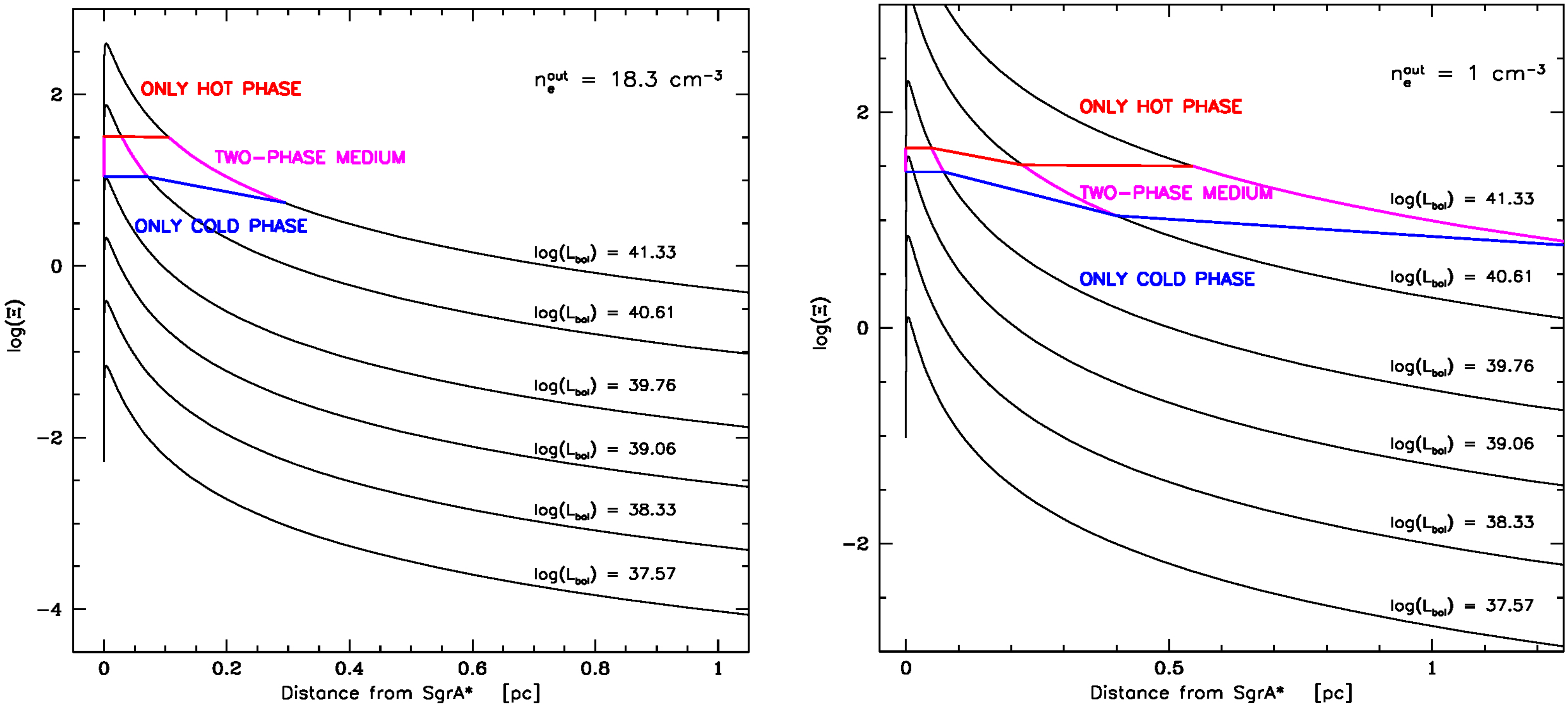

Thermal Instability in Sgr A*

Różańska +14, **For SEDs in different Sgr A* luminosity states**

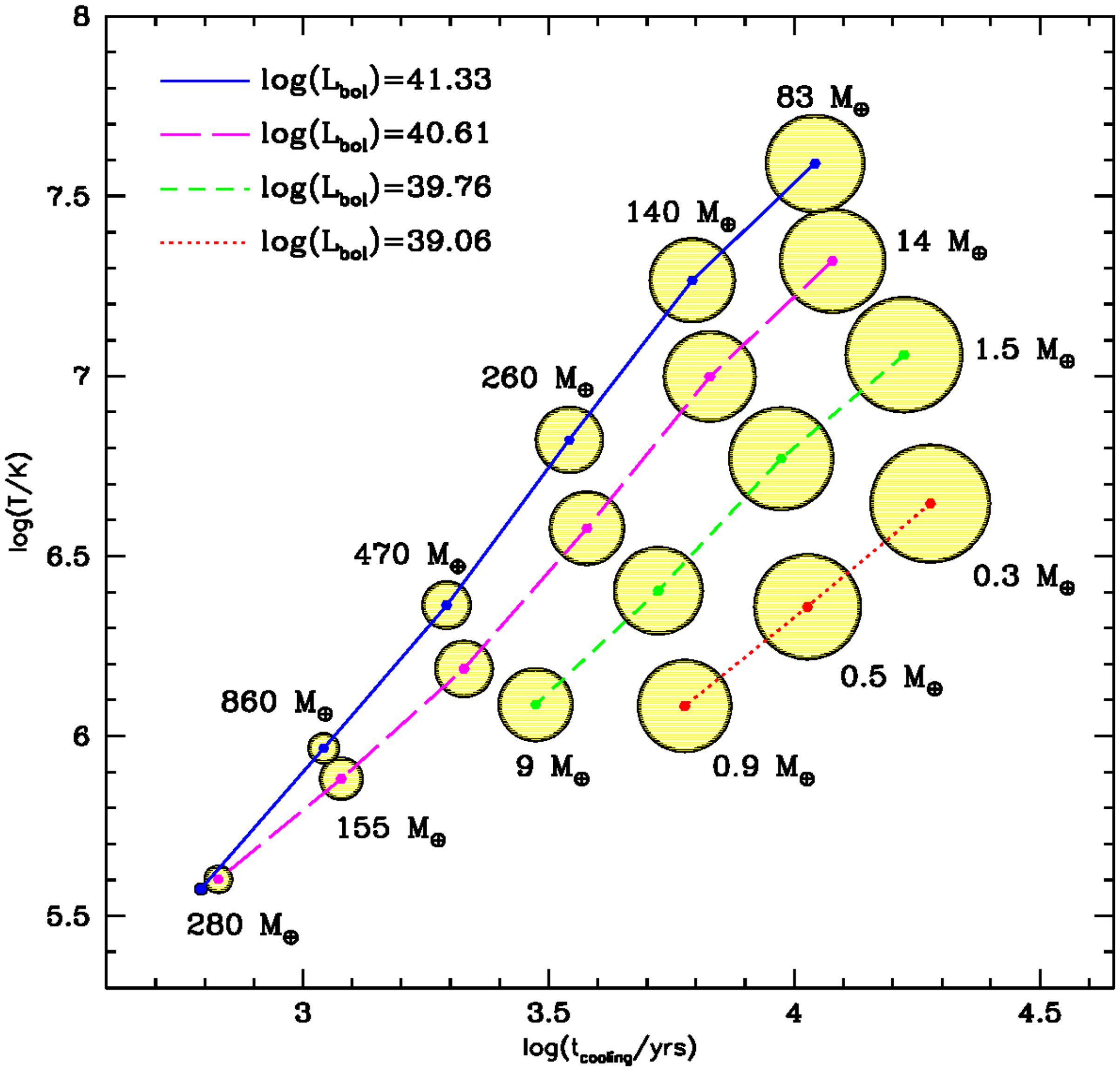

Thermal Instability in Sgr A*

Różańska +17, **For SEDs in different Sgr A* luminosity states**

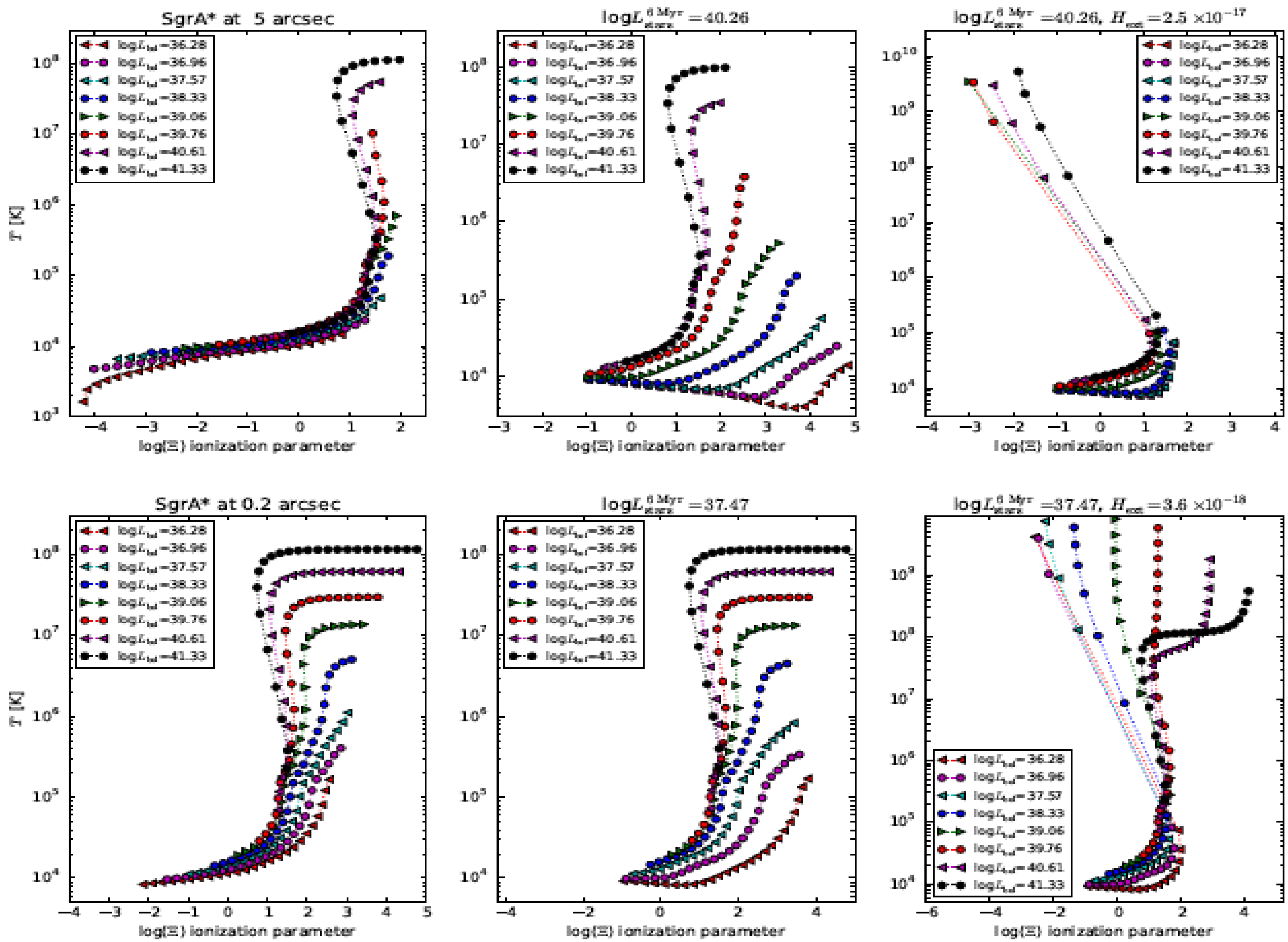

Figure 2. Solutions for S-curve of TI in the plane of temperature vs. ionization parameter, as defined in Eq. 5, for different luminosity states of the radiation: from the central source only (left panels), together with heating by stellar radiation (middle panels), and together with mechanical heating by winds (right panels). Values of central source luminosity are marked within the panels. We present results for the gas located at 5 arcsec from Sgr A* (upper row of panels) and at 0.2 arcsec (bottom row of panels). The luminosity of the NSC is always equal to $\log(L_{\rm stars}/{\rm erg\ s^{-1}}) = 40.03$, and the volume mechanical heating is $H_{\rm ext} = 2.5 \times 10^{-17}$ erg s^{-1} cm^{-3} at 5 arcsec and $H_{\rm ext} = 3.6 \times 10^{-18}$ erg s^{-1} cm^{-3} at 0.2 arcsec from Sgr A*.

Questions to the audience

- Do we observe saturated lines in X-ray domain?
- Do we derive AMD for UV absorbers?
- Are we able to distinguish between ***const. P*** and ***const. n*** models from observations?
- Are f-f winds more important than Compton winds?
- Can we distinguish volume density of the absorber?
- Can AMD indicate the wind density?

Conclusions:

- The fact that the photoionization models give the same results for broad range of densities is only valid for strong X-ray illumination, and weak optical/UV SED component.
- The radiation pressure is dominant in the vicinity of BH.
- Thermal Instability occurs only when hydrostatic equilibrium is solved.
- AMD normaliztion is higher for SED with strong X-ray component and weak optical UV component.
- For the given SED the position of the AMD drop position depends on the volume density.
- Thermal Instability may play role in shaping BH environment.
- Not in all objects, but at least in 50%